Ministry of Higher Education
And Scientific Research
University of Kerbala
College of Engineering
Mechanical Engineering Department

Investigation of thermal features of latent heat thermal energy storage with internal fins

A Thesis

Submitted to the College of Engineering / University of Kerbala in Partial Fulfillment of the Requirements for the Degree of Master of Science in Mechanical Engineering, Thermo-fluid Mechanics

By:

Hayder Abdulkhalik Azeez

(B.Sc. University of Babylon 2003)

Supervisors

Prof. Dr. Nabeel S. Dhaidan

Asst. Prof.Dr. Fadhel N. Al-Mousawi

2023 **1445**

بِسْمِ اللَّهِ الرَّحْمَٰنِ الرَّحِيمِ

﴿يَرْفَعِ اللَّهُ الَّذِينَ آمَنُوا مِنْكُمْ وَالَّذِينَ أُوتُوا الْعِلْمَ دَرَجَاتٍ وَاللَّهُ بِمَا تَعْمَلُونَ خَبِيرٌ﴾

صدق الله العلي العظيم

(سورة المجادلة، آية: 11)

Examination committee certification

We certify that we have read the thesis entitled " **Investigation of thermal features of latent heat thermal energy storage with internal fins** " and as an examination committee, we examined the thesis of the student " **Hayder Abdulkhalik Azeez** " in its content and in what is connected with it and that, in our opinion, it is adequate as a thesis for the degree of Master of Science in Mechanical Engineering.

Supervisor

Signature:
Name: **Prof. Dr. Nabeel S. Dhaidan**

Date: 22/5/ 2024

Supervisor

Signature:
Name: **Asst. Prof.Dr. Fadhel N. Al-Mousawi**

Date: 22/5/ 2024

Member

Signature:
Name: **Asst. Prof. Dr. Zaid SAttar Kareem**
Date: 22/5/ 2024

Member

Signature: Hasanain Jabbar
Name: **Dr. Hasanain Jabbar Abed Juaifer**
Date: 22/5/ 2024

Chairman

Signature:
Name: **Asst. Prof. Dr. Hayder Jabbar Kurji**
Date: 22/5/ 2024

Signature:
Name: **Asst. Prof. Dr. Hayder Jabbar Kurji**
Head of the Department of Mechanical Engineering
Date 22/5/ 2024

Signature:
Name: **Asst. Prof. Dr. Haider Nadhom Azziz**
Dean of the Engineering College
Date: 15/7/ 2024

Supervisors' Certification

We certify that this thesis entitled "**Investigation of thermal features of latent heat thermal energy storage with internal fins**" was prepared by **Hayder Abdulkhalik Azeez** under our supervision at the Mechanical Engineering Department / College of Engineering / University of Karbala, in partial fulfillment of the requirements for the degree of Master of Sciences in Mechanical Engineering thermo-fluid.

Signature:

Prof. Dr. Nabeel S. Dhaidan

Date: / / 2023

Signature:

Asst. Prof.Dr. Fadhel N. Al-Mousawi

Date: / / 2023

Linguistic certificate

I certify that the thesis entitled " **Investigation of thermal features of latent heat thermal energy storage with internal fins** " which has been submitted by **Hayder Abdulkhalik Azeez** has been proofread, and its language has been proven to meet the English style.

Signature:

Name: **Prof. Dr. Hakim S. Sultan**

Date: 29/ 11 / 2023

أ. د. حاكم سماوي الجبوري
Prof.Dr. Hakim S. S. Aljibori

Author's comment

I certify that research work entitled "**Investigation of thermal features of latent heat thermal energy storage with internal fins** " is my own work. The work has not been presented elsewhere for publication. If a material has been used from other sources, it has been properly acknowledged / referred.

Signature:

Name: Hayder Abdulkhalik Azeez

Date: / / 2023

Dedication

I Dedicate This Modest Effort:

To the benefactors of my lord and master, Imam Hussein (peace be upon him)

To my esteemed teachers ...

To my dear parents …

To my dear wife ...

To my dear children ...

To everyone who wished me well and success ...

Signature:

Hayder Abdulkhalik Azeez
Date: / / 2024

Acknowledgments

First of all, I thank God Almighty for enabling me to carry out this work, and secondly, I thank my benefactor, Imam Hussein, peace be upon him.

I extend my thanks and appreciation to all the esteemed gentlemen, starting with the thesis supervisors and the head and teachers of the Mechanical Engineering Department.

I extend my special thanks to my dear wife and children who supported me and endured various circumstances for my sake

I also extend my thanks to all of my family and friends who helped and supported me to complete this work.

Hayder, ***2024***

Abstract

The present study includes a numerical and experimental verification of the thermal properties of PCM placed in a horizontal annular latent heat thermal energy storage (LHTES) unit with the addition of internal fins. The energy storage device has a length of 500 mm consisting of a thermally insulated outer shell made of transparent plastic with a diameter of 75 mm and an inner copper tube used to transport the heat transfer fluid (water), with a diameter of 25 mm. The space between the inner tube and the outer shell is filled with a phase change material of the RT 42 paraffin wax type.

Three models of LHTES are tested and investigated: unfinned, X-shape fin distribution, and below-distribution fin. The fin/PCM mass ratio is constant for two finned storage units. The longitudinal fin has a length of 500 mm and a height of 20 mm and is attached to the internal tube of the LHTES unit. The enthalpy-porosity method was used to solve the two-dimensional numerical model of the PCM melting problem. The effect of various hot water inlet temperatures (60, 70, and 80 °C) on the melting time was investigated experimentally and numerically.

By monitoring the melting process, the results showed a significant convergence between the numerical and practical results. Natural convection and overheating dominate the melting at the top part of the unfinned storage unit, while thermal conduction with a low melting rate controls the bottom part. Inserting fin suppresses overheating in the top part and increases the melting rate at the bottom part of the thermal storage unit. Also, increasing the HTF (water) inlet temperature has a significant effect on reducing the melting time; the melting time was reduced by 31 % and 45.5 % by increasing the water inlet temperature from 60 to 70 °C, and from 60 to 80 °C, respectively. The greatest numerical and experimental reductions in charging time due to using a below-fin distribution unit compared to an unfinned unit instead are 79.31% and 77.75 %, respectively, at a water inlet temperature of 80 °C. At the same time, the numerical and experimental reductions in charging times are 79% and 78, respectively, at a water inlet temperature of 70 °C.

Table of Contents

NOMENCLATURE

Symbol	Description	Units
Cp	Specific heat	J. kg^{-1} .K^{-1}
D	Outer diameter	mm
d	Inner diameter	mm
f	Liquid fraction	
h	Average heat transfer coefficient	W m^{-2} K^{-1}
k	Thermal conductivity	W m^{-1} K^{-1}
L	Latent heat of melting	kJ kg^{-1}
Q_s	Stored thermal energy	kJ
T	Temperature	^oC
r_i	Radius of inner pipe	mm
r_o	Radius of outer cylinder	mm
g	Gravitational acceleration	m/s2
V	Velocity of liquid PCM ,	m/s
H	Total enthalpy	J/kg
ΔH	latent enthalpy	kJ.kg^{-1}
h	Sensible enthalpy	J/kg
U,V	Velocity components	
Ɵ , r	Polar coordinates, degree, and m	
t	Time	

HTF	Heat transfer fluid	
S_g	gravitational force	
S_D	Darcy term	
A_{mush}	mushy zone constant	
n	fin number	
h	fin height	mm
t	fin thickness	mm

GREEK SYMBOLS

Symbol	Description	Units
ρ	Density of PCM	Kg/m^3
μ	Dynamic viscosity	Kg/m.s
υ	Kinematics viscosity	m^2/s
α	Thermal diffusivity	m^2/s
β	Thermal expansion coefficient	1/k

SUBSCRIPTS

Symbol	Description
w	heated wall
l	liquid PCM
s	solid PCM
M	Melting
PCM	phase change material
i	initial , inner pipe
o	Outer cylinder
Ref	Reference value
avs	average solid temperature
avl	average liquid temperature

Chapter One

Introduction

CHAPTER ONE: INTRODUCTION

1.1 Overview

Fossil fuels such as oil, natural gas, and coal have been the primary sources of energy for many years. As a result of the increase in population and the increase in the consumption of energy resources in manufacturing, means of transportation, heating homes, and producing electricity, and due to the increased intensity of competition between countries of the world, especially the major industrial countries in the field of manufacturing and factories, the reasons mentioned led to a rise in global demand for oil, natural gas, and coal. As a result of the changes occurring in the climate due to pollution from carbon emissions associated with high energy consumption, as well as the global energy crisis due to the depletion of traditional energy sources, it has become necessary to reduce energy consumption and rely on environmentally friendly renewable energy sources.

1.2 Renewable energy

Renewable energy refers to energy obtained and derived from natural resources that are constantly replenished in nature and do not get depleted over time, are largely present in nature and not depletion, and are very clean as they do not cause pollution and do not cause harm to living organisms; aside from some exceptions, that's why it's called clean energy [1]. It is also possible to benefit from many renewable energy resources by using simple and inexpensive technologies, which is the opposite of non-renewable and depletion of traditional energy resources. Renewable energy includes solar, hydroelectric, wind, biomass, and wave energies.

1.3 Energy storage systems

The process of storing energy can be defined as the process of reserving energy produced for a specific time for use at another time to reduce the gap between the energy source and the energy requirement.

The device that stores energy is called an accumulator or battery. There is a gap between the source of renewable energy and the demand for it due to the absence of natural phenomena related to energy generation for a period of time throughout the day, such as solar energy generation, which exists only during the day [1], not at night, and the wind turbines, etc. It is necessary to use one type of the energy storage systems (thermal, chemical, electrical, kinetic, etc.) to continuously provide energy at the time of its interruption from its prepared source.

1.4 Thermal energy storage

The working principle of thermal energy storage systems depends on phase-change materials in which sensible and latent energies are stored Fig. (1.1). The sensible energy is stored by changing temperatures while remaining in the same phase of the material, while latent energy is stored by changing phases with temperatures remain approximately constant [2].

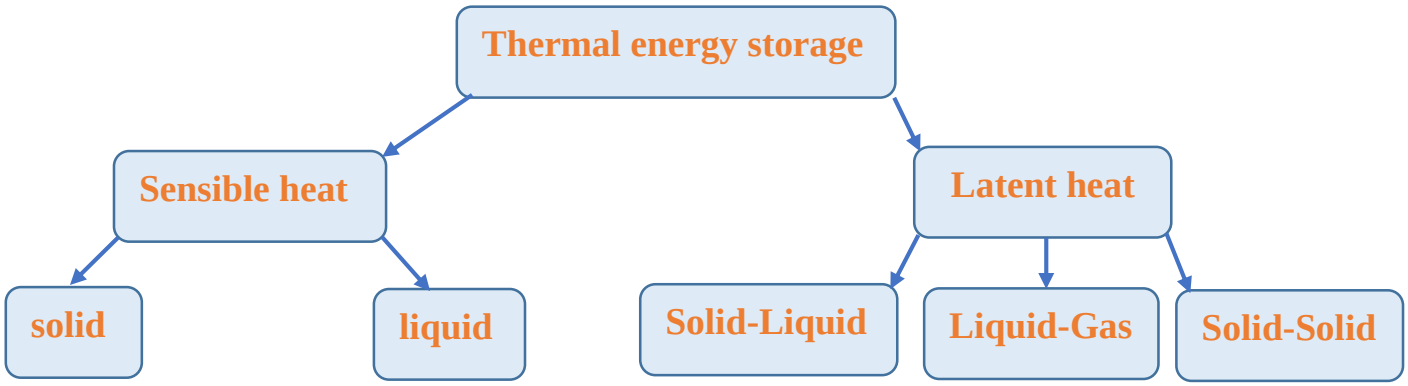

Fig. (1.1) Thermal energy storage [2]

1.5 Phase Change Materials (PCMs)

Phase Change Material (PCM) is a type of thermal energy storage material that stores and releases latent heat by changing its phase. The material can store a significant amount of thermal energy during the charging process by transforming from solid to liquid, and release the stored energy during the discharge process by transforming from liquid to solid [3].

1.5.1 Working principle of PCMs

When the temperature of the space containing PCM rises above its melting temperature, the PCM phase turns from solid to liquid, which leads to heat absorption. When the temperature of the space drops below the melting point of PCM, the phase changes from liquid to solid occurs, releasing the stored heat fig. (1.2) a, b. The sum of latent and sensible energies in the PCM results in the total stored thermal energy [3].

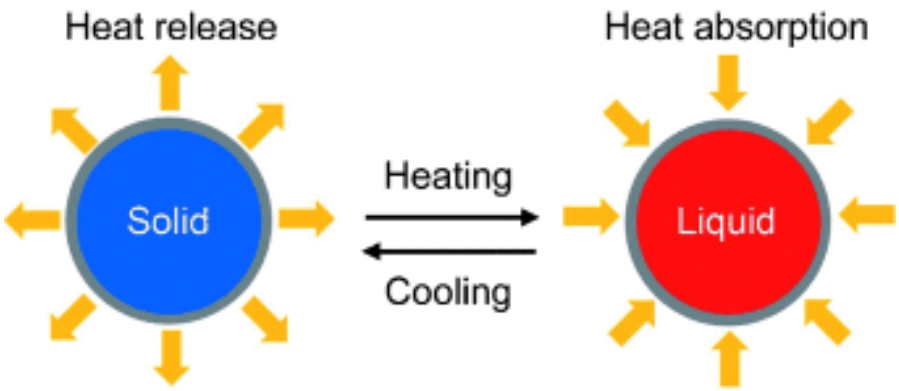

Fig (1.2) (a) phase change process [3]

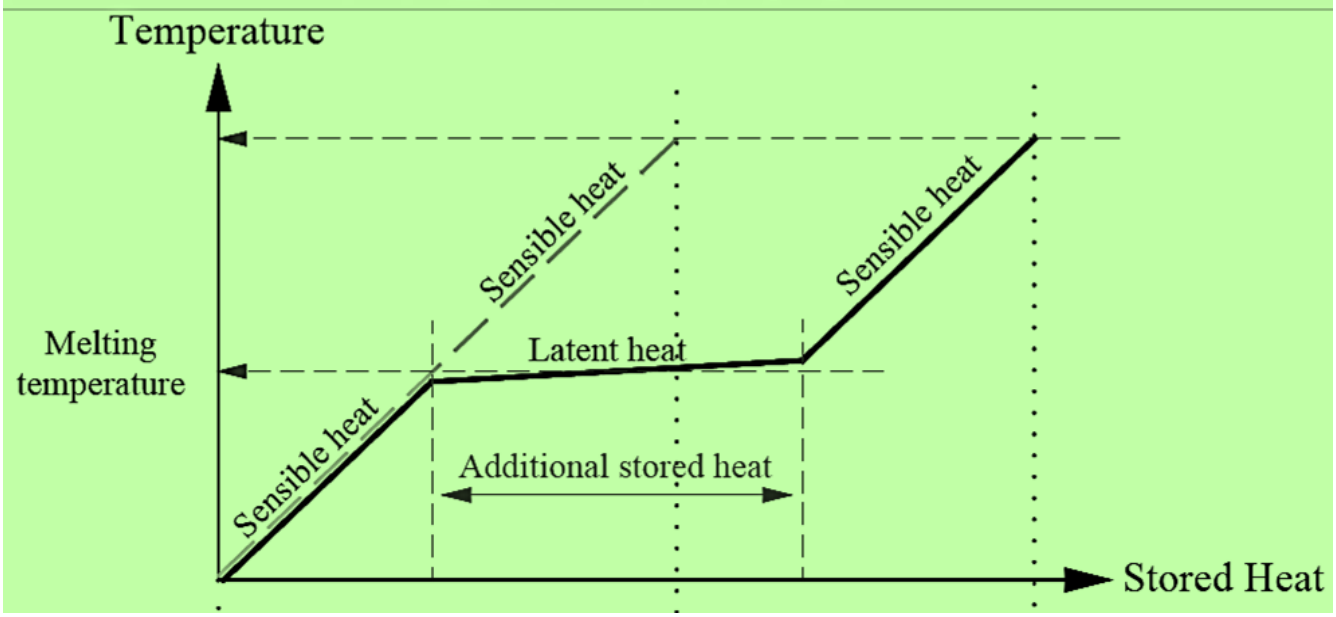

Fig. (1.2) (b) Heat stored in PCM [3]

1.5.2 PCMs classification

Fig. (1.3) shown the types into which PCM is classified.

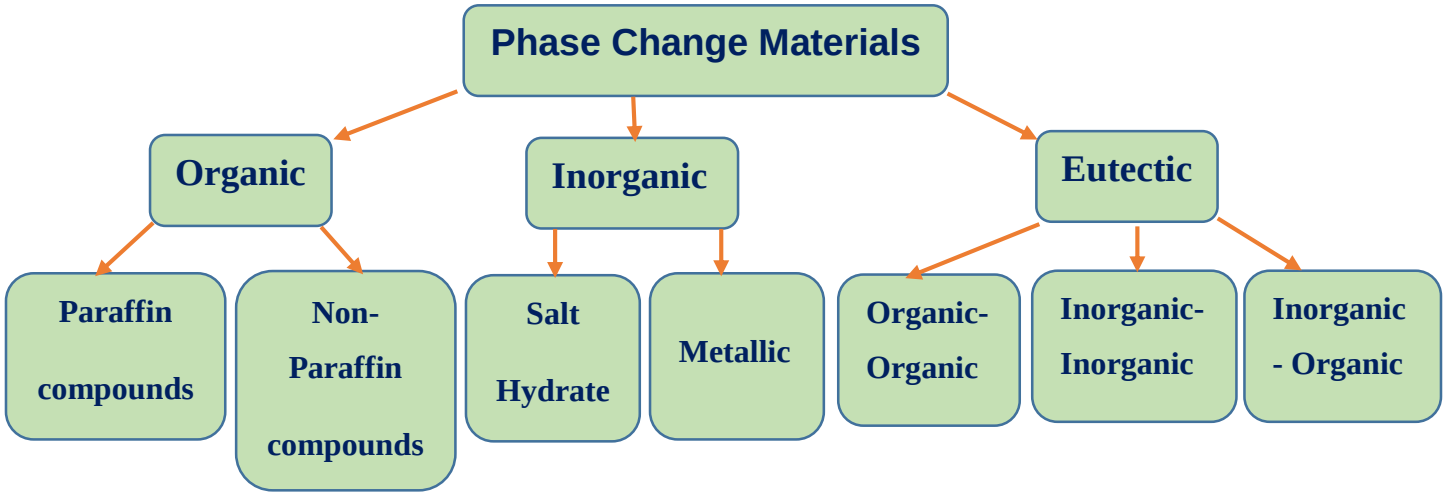

Fig (1.3) PCM classification [2]

1.5.3 PCMs Properties [2], [4]

The following properties must be available in the PCM in order to benefit from it in various applications:

1- Thermal properties:

- The thermal conductivity of the material must be acceptable
- The melting latent heat must be high
- The specific heat must be high

2- Physical properties

- High energy density per unit volume
- Small volume changes on phase change

3- Chemical properties

- Chemical stability
- Non- poisonous
- Non-combustible
- Non-explosive
- Non-corrosive

4- Kinetic properties

PCMs should have:

- High nucleation rate
- High rate of crystal growth

5- Economic properties

- Easy to get

- The price of the material is cheap

1.5.4 PCMs applications:

PCM is used in a various field, the most important of which are [4]:

- Building and Space Loads (Heat Capture), low thermal conductivity is required

- Electronic cooling, high thermal conductivity is required

- Solar Energy Storage, high thermal conductivity is required

- Commercial refrigeration and absorption cooling systems

- Textile, medical applications, etc.

Figure (1.4) illustrates some PCM applications.

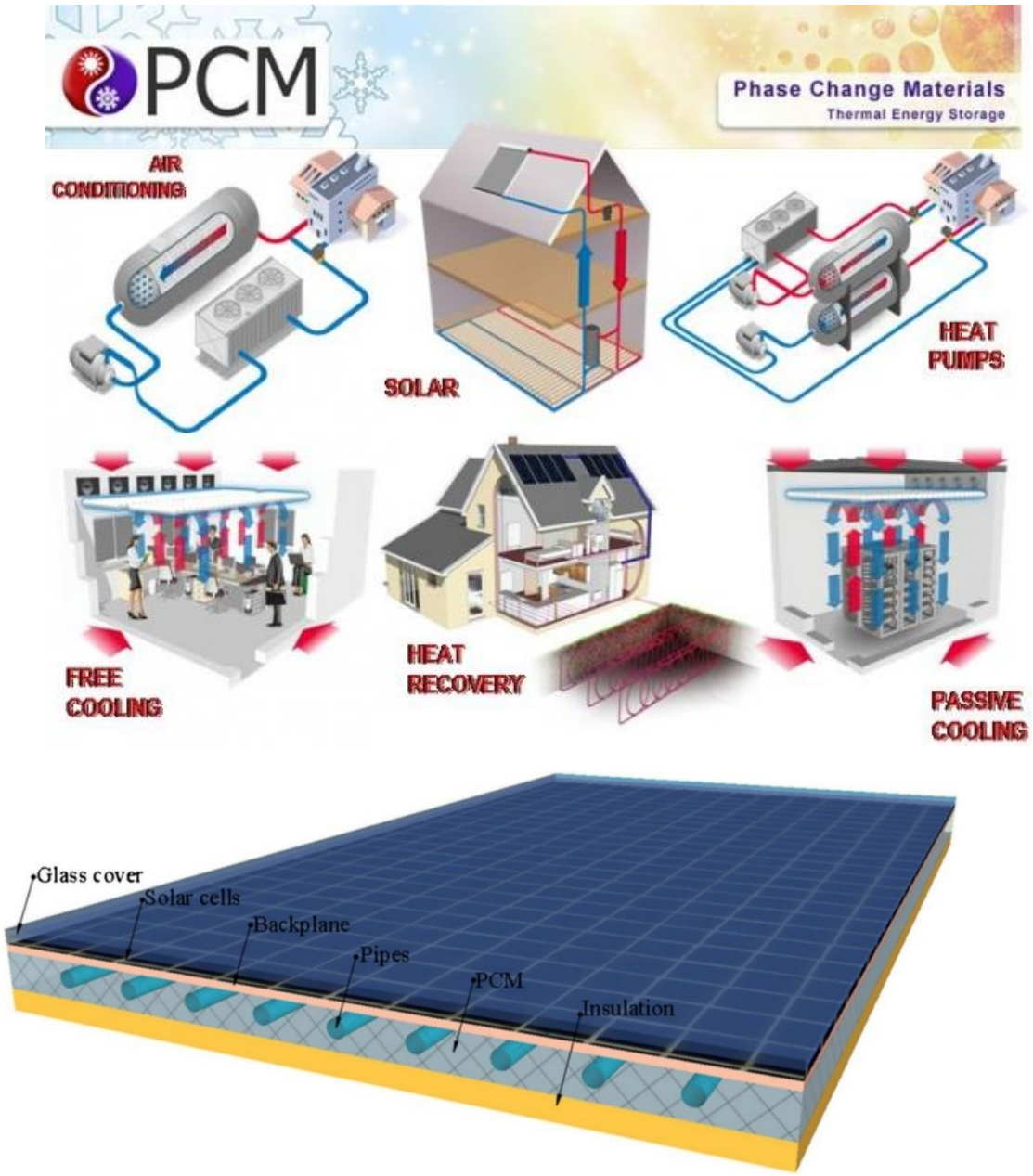

Fig. (1.4). Various applications of PCM [4]

1.6 The melting of (PCM) without fins

By studying the process of melting PCM in horizontal latent heat thermal energy storage devices without the use of fins, it is observed that natural convection controls the melting in the upper part of the heat exchanger. As a result of the low thermal conductivity of PCM, the rate of melting is high at the upper part (overheating), associated with a low melting rate in the lower part, as depicted in Fig. (1.5). The red area represents the amount of molten PCM. In contrast, the blue area represents the amount of solid PCM.

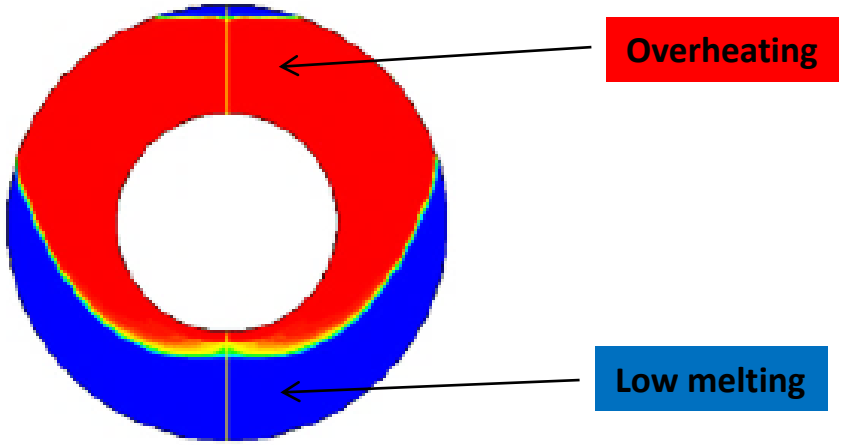

Fig. (1.5) PCM melting in without fins cavity [3]

To address the problem of low thermal conductivity of PCM and enhanced the heat transfer rate to the PCM, the following methods were used fig. (1.6):

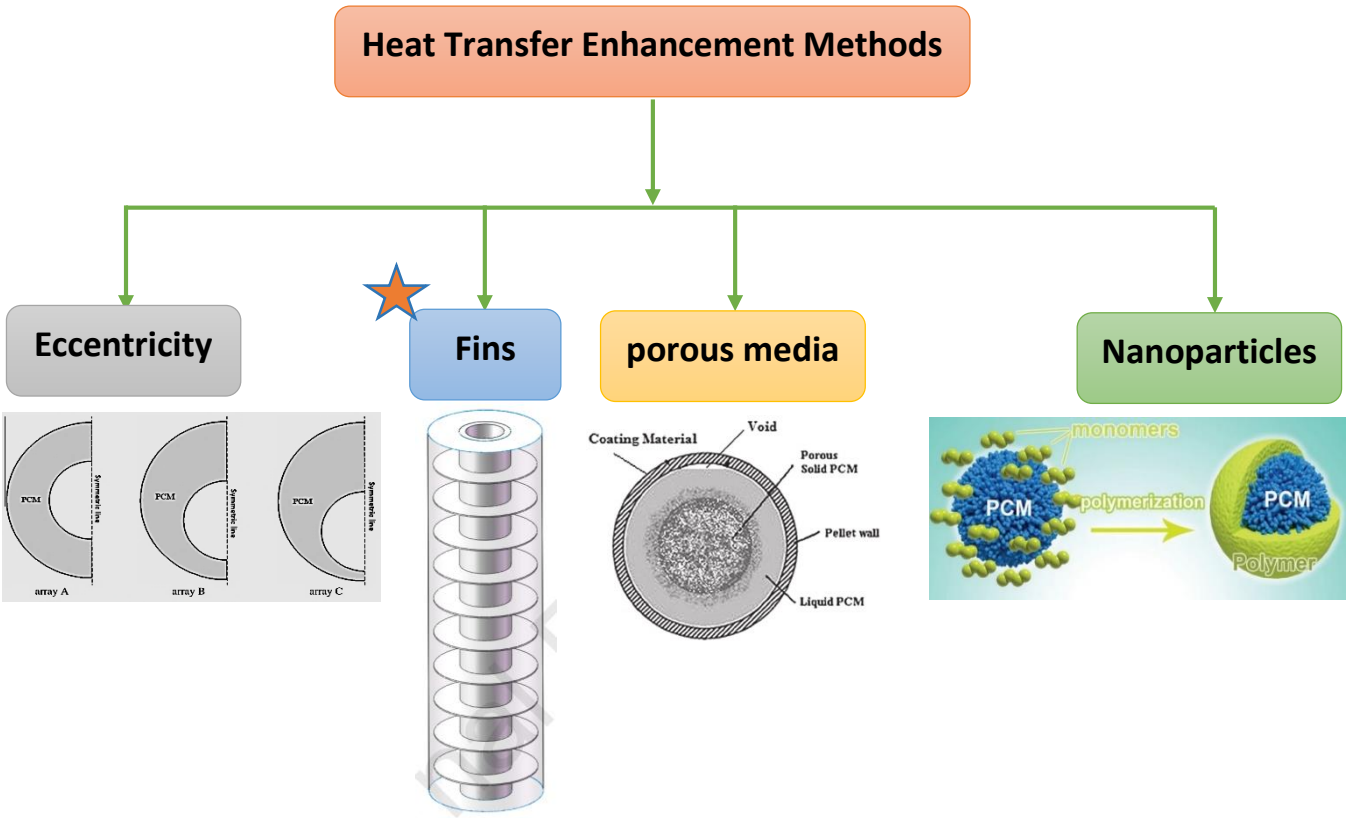

Fig. (1.6) melting enhancement methods

In the current study, fins were added to the latent heat energy storage system to improve heat transfer due to the low thermal conductivity of PCM.

1.7 The objectives of the present study

The inherent PCM overheating in the top region of the container and the low melting rate of PCM in the lower part of the container can be mitigated by inserting fins within the latent heat storage unit. The present study aims to investigate experimentally and numerically the thermal performance of PCM inside a finned thermal storage unit. The unit consists of an outer insulated shell and an inner pipe where HTF flows. The effect of flowing HTF is considered. Also, the comparison between the thermal characteristics of finned and unfinned thermal storage units is performed.

Chapter Two

Literature Review

Chapter Two: Literature Review

This chapter provides a comprehensive review of the previous research associated with the melting behavior of phase-change materials in an annular LHTES heat exchanger without fins and with different shapes of fins.

2.1 PCM melting in (LHTES) unit without fins

This section addresses previous studies by researchers on melting PCM in horizontal and vertical latent heat thermal energy storage devices without using fins. It discusses the most important results obtained by the researchers.

2.1.1 Melting of PCM in horizontal LHTES

The annular heat exchangers were positioned horizontally. In common, the melting of PCM occurs due to the heat supplied by the hot HTF passing through the inside tube.

Dutta et al. [5] performed a numerical and experimental investigation on the performance of (LHTES) system during the PCM melting processes. Paraffin wax was used as a PCM material, and the water was used as a HTF. With the application of different heat fluxes, it was concluded that there is agreement between numerical and experimental results, which showed that the natural convection controlled the melting operation. There was a significant effect of the angle of inclination and eccentricity on the PCM melting.

Adine and El Qarnia [6] numerically studied the thermal performance of (LHTES) using two PCMs with various melting temperatures. It was found that there is a significant effect of a set of parameters, which are the (HTF) entrance temperature, the mass flow rate of HTF, and the length of the storage unit. The efficiency of the heat exchanger is higher as the HTF inlet temperature increases.

Darzi et al. [7] achieved numerical research on the properties of melting PCM in horizontal LHTES units with concentric and eccentric arrays of inner tubes. Natural convection controls the melting in the top part, while conduction controls the melting in the lower part. The researchers found that increasing the convection area by using the eccentric case caused an increase in the rate of melting.

In a study conducted by Hosseini et al. [8], numerically and experimentally the examined impact of natural convection on the melting process of PCM within a horizontal shell-and-tube heat exchanger. Also, the impact of the HTF entrance temperature on the melting time was investigated. It was concluded that raising the temperature of the HTF to 80 degrees Celsius led to a reduction in the melting time by 37%.

Another study by Wang et al. [9] conducted a numerical analysis to investigate the effects of HTF's flow rate and inlet temperatures on the PCM melting process placed inside a horizontal LHTES unit. The results indicated that natural convection is the main factor controlling melting, and the HTF entrance temperature significantly impacts the time specified to finish melting. As the water inlet temperature raised, the stored thermal energy increased, and the melting time decreased. Also, the mass flow rate greatly impacted the melting time while it had a low impact on the stored thermal energy.

Avci and Yazici [10] completed an experimental study of the thermal properties of a PCM material placed inside a horizontal annular cavity of the LHTES system using paraffin as a material of PCM and distilled water as HTF. Melting of PCM occurred due to natural convection, where the molten material raised to the top due to its melting, leading to the melting of the rest of the solid material. The results indicated that the natural convection controlled the PCM melting process, and the HTF inlet temperature had a main role in improving the melting process and reducing the time required to complete it.

2.1.2 Melting of PCM in vertical LHTES

The melting of (PCM) inside vertical cylinders occurs due to the heat supplied from hot water passing through the inside tube.

Akgun et al. [11] conducted an experimental study to examine the melting and solidification of PCM, namely paraffin (P1), placed in vertical shell-and-tube LHTES. When the HTF circulates, which is water in this study, PCM begins to melt. It was observed that improving heat transfer by tilting the outer shell of the heat exchanger by 5 degrees. In addition, increasing the water entrance temperature caused a reduction in the duration required for PCM melting. To reduce energy consumption, it was suggested to use a low mass flow rate of water.

Shmueli et al. [12] verified numerically and experimentally the PCM melting within a vertical LHTES unit and its thermal behaviour. They found that thermal conduction is the main heat transfer mechanism that affected the melting process at the beginning of melting. As the process progresses, natural convection is the main factor through the high-temperature liquid PCM melting the solid PCM through convection.

Longeon et al. [13] did a numerical and experimental study to inspect the influence of the heat transfer mechanism and injection side on the melting and solidification of paraffin RT35 inside the vertical shell and tube (LHTES) system. The impact of natural convection and the HTF flow direction on the melting process were investigated. It was concluded that natural convection controls melting. Moreover, it was recommended that the direction of water flow be from the top in the case of melting and from the bottom in the case of solidification.

Wang et al. [14] experimentally studied the thermal behaviour of charging and discharging of the phase change material (erythritol) inside a vertical LFTES unit which used the air as a HTF. The results indicated that natural convection plays an essential role in melting by transferring heat from the liquid to the solid region. In addition, raising the

HTF inlet's temperature and mass flow rate improved heat transfer and decreased the melting duration.

Seddegh et al. [15] verified experimentally and numerically the mechanism of heat transfer of charging and discharging of PCM in PCM in a vertical (LHTES) unit. It was concluded that natural convection is controlling the melting process. The molten PCM material with high temperature activates natural convection's role to reach the solid PCM's upper side and melt it.

2.2 PCM melting in finned annular (LHTES) unit

Researchers' previous studies on the melting of PCM in horizontal and vertical latent heat thermal energy storage devices using fins will be addressed, and the researchers will discuss the most important results.

2.2.1 Horizontal finned thermal energy storage units

The PCM melting behavior within a horizontal finned LHTES unit consisting of a shell and tube is reviewed. The influence of geometrical and configuration of various fin types on the melting process was considered.

Agyenim and Hewitt [16] presented an experimental investigation to estimate the heat transfer properties of RT58 inside a horizontal cylinder, including longitudinal fins. It was inferred that using enhanced heat transfer processes, including the application of fins, significantly reduced the storage size by around 30%. Also, increasing the water inlet temperature produced more thermal energy stored in the PCM, which can be utilized later in the discharge process.

Mat et al. [17] verified numerically the thermal properties of an RT82-PCM melting inside a triple tube type heat exchanger (**Fig. (2.1)**). The melting was carried out using three different methods for heating the PCM, including heating from the inner tube,

heating from the outer tube, and heating from both tubes together. Several methods were analyzed and compared to enhance heat transmission between its source and the PCM using fins of three types, internal, external, and internal-external, together (**Fig. (2.1)**). Also, the influence of various fin heights on the enhancement strategies was considered. The obtained results indicated that the use of internal-external fins resulted in a reduction of melting rate by 43.3% compared to the without fins state.

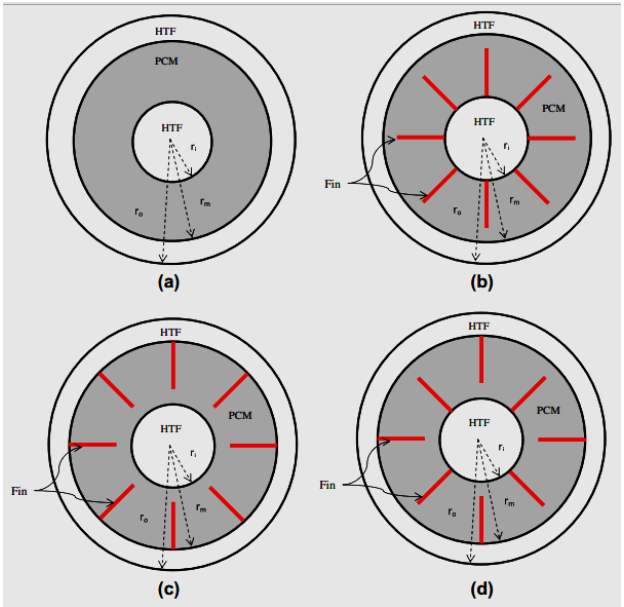

Fig. (2.1). The configuration of (a) unfinned TTHX, (b) TTHX with internal-tube fins, (c) TTHX with external-tube fin, (d) TTHX with internal – external fins (Mat et al. [17])

Al-Abidi et al. [18] experimentally investigated the melting and solidification of PCM placed inside a horizontal heat exchanger consisting of triple tubes with internal and external fins. The temperature distribution was studied in this experimental investigation, in addition to studying the impact of different factors on melting, including the temperature of the inlet water, its mass flow rate, and the use of fins. The researchers concluded that adding fins to the system accelerates the melting of the PCM as a result of the enhancement of heat transported within the PCM.

Li and Wu [19] numerically analyzed the thermal properties of charging and discharging NaNO3 PCM and NaNO3/expanded graphite composite inside a horizontal finned annular LHTES device. The inner tube was equipped with longitudinal fins fixed. The predicted results demonstrated that the use of longitudinal fins and composite led to a reduction in the duration of melting by 14%.

Wang et al. [20] presented a numerical study to investigate the thermal characteristics of PCM melting inside a horizontal LHTES device in the existence of longitudinal internal fins. The impact of some fin parameters on the melting process was studied, including height, ratio of fin, and angle between fins (Fig. 2.2). The result showed that using fins with a low fin ratio led to a decrease in melting time. In addition, the angle between the fins had a small effect on the melting. Also, making the angle between adjacent fins between 60 and 90 degrees reduced melting duration by 49.1% for full-scale fins.

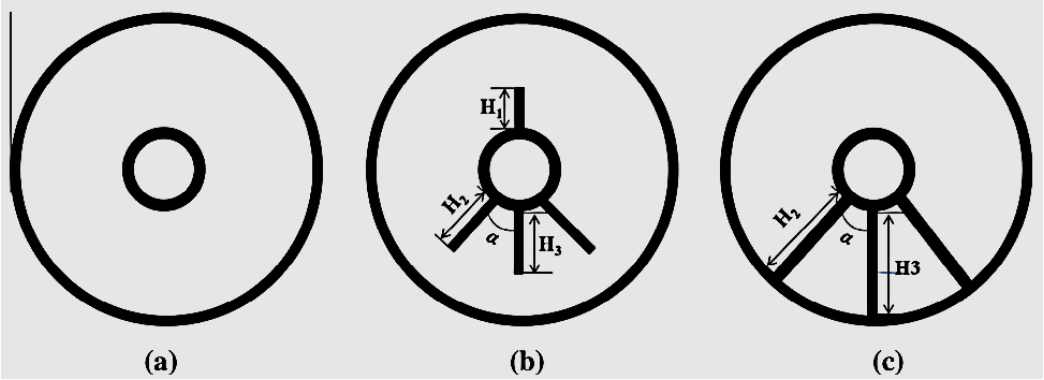

Fig. (2.2). Schematic of the sleeve-tube LTES units (a) no fin; (b) four half-scale fins; (c) three full-scale fins (Wang et al. [20]).

Yuan et al. [21] investigated numerically and experimentally the thermal properties of PCM melting inside a finned horizontal annular container of a LHTES device. The fins were fixed on the inner tube of the device and at different installation angles (0, 30, 45, 60, and 90 degrees). The PCM melting process was tested by choosing three temperatures for the inner tube (60, 70, and 80) degrees Celsius. It was discovered that, although the existence of fins hindered the natural convection, it accelerated the melting of PCM as a result of the increased heat exchanged. Also, the rate of melting was greater when the fins' installation angle was 0 (**Fig. (2.3)**), followed by when the installation angle was 30. However, raising the angle above 45 degrees did not have an important impact on the rate of melting.

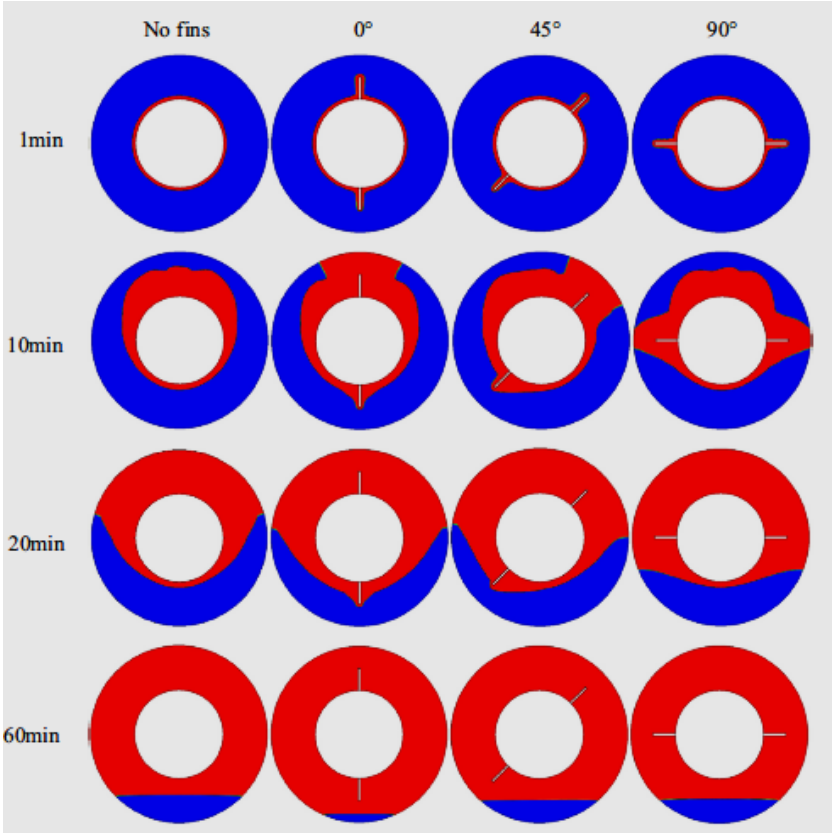

Fig. (2.3). Melting behaviour of finned and unfinned heat exchangers at different times (Yuan et al. [21]).

The melting and solidification of PCM in various inner tube configurations of horizontal annular cavities was numerically investigated by Darzi et al. [22]. The considered configurations of the inner tube are circular, vertical-oriented elliptical, horizontal-oriented elliptical, and finned circular, as described in **Fig. (2.4)**. The nanoparticle dispersion within PCM was also examined. The predictions proved that adding fins enhanced the melting and solidification process. However, the enhancement in solidification was more than that in the melting process.

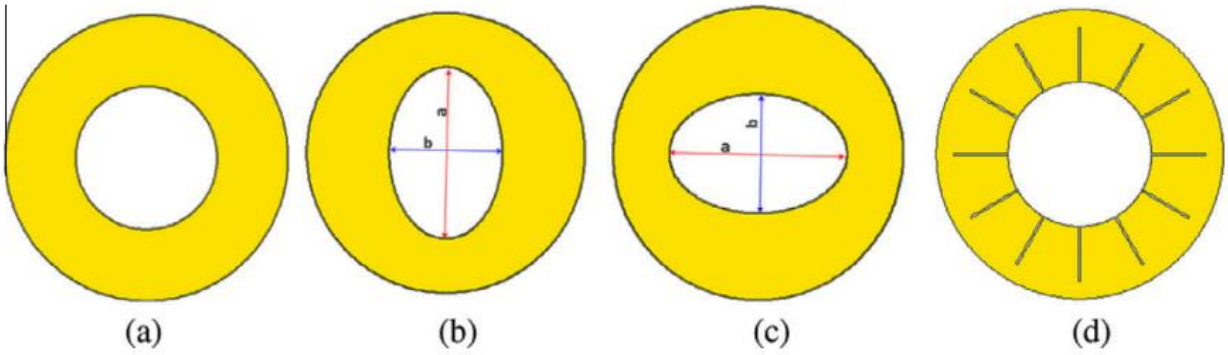

Fig. (2.4). Schematic of computational domain (a) circular tube, (b) vertical-oriented elliptical tube, (c) horizontal-oriented elliptical tube and (d) finned circular tube (Darzi et al. [22]).

Wang et al. [23] conducted a numerical study to examine the influences of various parameters on the horizontal radial-finned LHTES unit (**Fig. (2.5)**). It was found that both the energy efficiency percentage and the rate of heat storage were not significantly impacted by both the height and thickness of the fin when the space between fins is over four times the inner tube radius. Reducing fin pitch enhanced performance, particularly when accompanied by increased fin height and width.

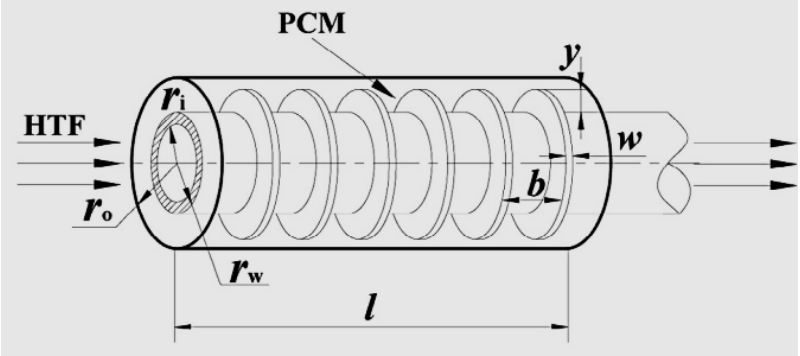

Fig. (2.5). Schematic of the finned tube phase change heat storage unit internal cross-sectional view (Wang et al. [23]).

Cao et al. [24] numerically investigated the PCM melting in a horizontal finned annular storage unit. The impact of varying longitudinal fin numbers (n = 4, 6, 8, 10, and 12), the shape and size of the fins, and the wall temperature on the thermal performances were researched. They concluded that the thermal properties of PCM were affected by several factors, including the number of fins, their shape and size, and the results obtained were compared with without fins state. The results also demonstrated that using fins significantly improved PCM's melting rate. The optimal number of fins was 10 fins for study conditions.

Mahdi et al. [25] numerically proved that utilizing an uncommon fin configuration in the triplex-tube heat exchanger (**Fig. (2.6)**) achieved a better PCM melting rate than nanoparticle dispersion. It was inferred that the most efficient and quickest melting of PCM might be obtained by inserting long fins in the bottom half and comparatively shorter fins in the top part of the LHTES unit.

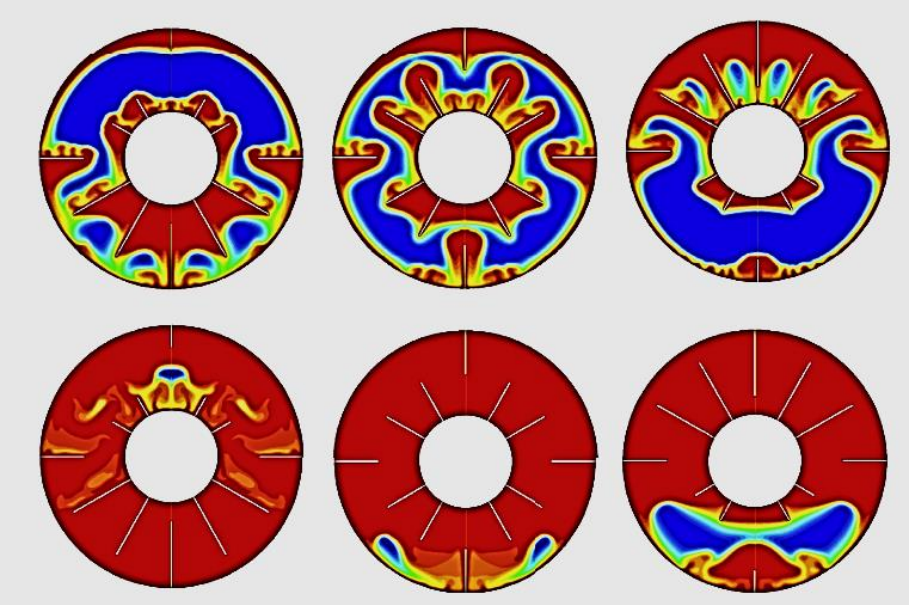

Fig. (2.6). Melting characteristics of different fin distributions (Mahdi et al. [25]).

Deng et al. [26] numerically examined the melting behaviour of PCM inside a horizontal finned heat exchanger. The position of the double fins was in the lower section, and the variation in angle between them was compared with the conventional configuration (**Fig. (2.7)**), which included one fin positioned at the upper part and the other at the bottom. It was found that raising the height of the fins while making the angle between the two fins at 120 degrees caused a decrease in melting duration by 53.1%.

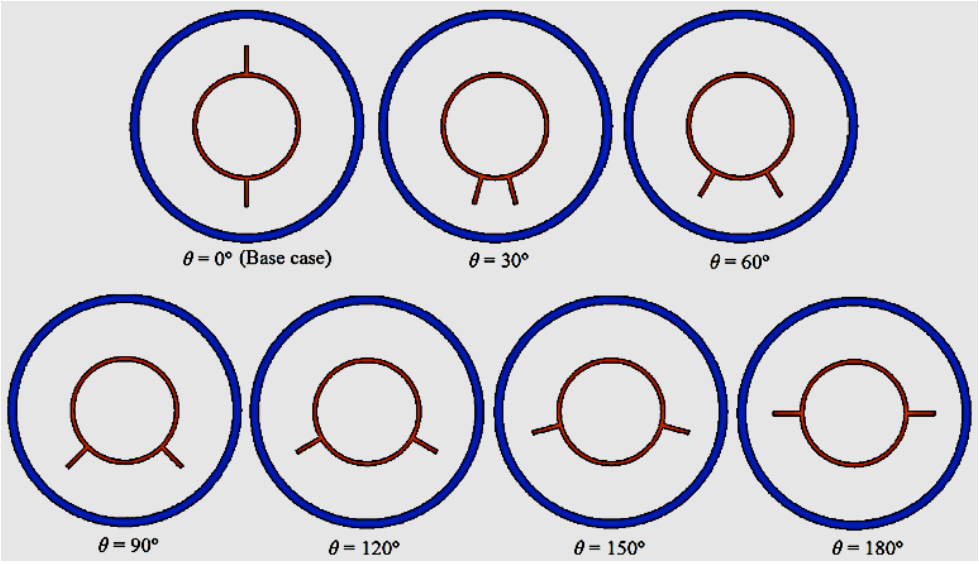

Fig. (2.7). Physical configurations of all cases (Deng et al. [26]).

Abdulateef et al. [27] achieved a numerical investigation to explore the effect of adding fins-nanoparticles on the charging and discharging triplex-tube heat exchanger. It was deduced that the external triangular fins-nanoparticle model, consisting of eight fins with a height of 141 mm and a ratio of aspect of 18% (**Fig. (2.8)**), had the optimum effectiveness that reduced the melting and solidification periods of PCM. Furthermore, a strong correlation had been shown between the numerical findings and the experimental data.

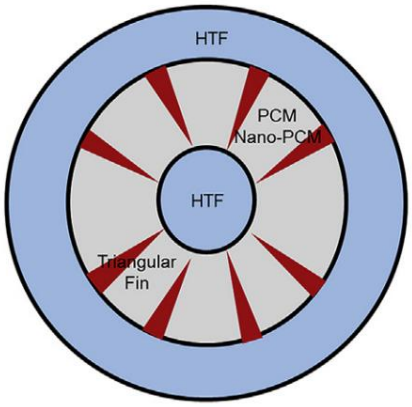

Fig. (2.8). Model of the TTHX with external triangular fins (Abdulateef et al. [27])

Khan and Khan [28] used a computational model to explore the impact of fin position on the melting performance in a horizontal (LHTES) unit. Five various angular directions of the fins, ranging from 0 degrees to 90 degrees, were examined. When the angle θ is equal to 90 degrees, it resulted in a ⅄-fin configuration; however, when θ is equal to 30 degrees, it generated a Y-fin configuration (**Fig. (2.9)**). The rate of melting of the Y-fins configuration was higher than that of ⅄-fins arrangement. The high fin height-to-thickness ratio greatly enhanced the melting performance.

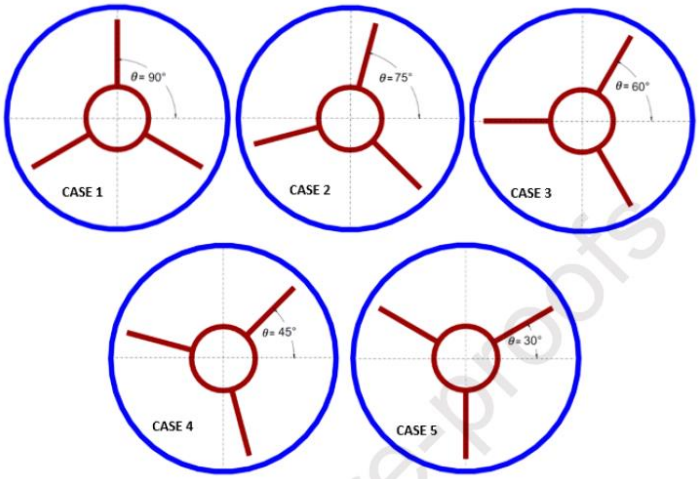

Fig. (2.9). Configurations based on topologies of fins (Khan and Khan [28]).

Yu et al. [29] conducted a numerical test on a horizontal LHTES system to assess the impact of longitudinal fins' varying thicknesses and angles on melting. The use of graded fins with varying angles and thicknesses had been shown to enhance thermal performance and reduced the melting period of PCM. A suitable arrangement of fins involved a gradual variation in thickness and angles, which mean the fins should be thinner in the upper section and thicker in the bottom half. It was found that the optimal angle and thickness were 14.96° and 2.846 mm, respectively, led to a decrease in the melting time by 30.5%.

Li et al. [30] numerically analyzed the melting inside a horizontal latent heat storage device equipped with longitudinal fins. Four different fin models were designed to improve the PCM melting process. These models involved changing the fins' height and thickness. The performance of these modified fin models was then compared to a standard case where fin length and thickness remained unchanged. The prediction showed that decreasing the length and thickness of the top fins while raising the thickness and height of the bottom fins led to a reduction in melting time of 47.1%. Furthermore, using the longest and the thickest bottom fins model decreased the melting time by 54.1%.

Al-Mudhafar et al. [31] used a numerical code to evaluate the impact of fins configuration on the PCM charging in an annular thermal storage unit. The effect of six longitudinal fins in several different shapes on improving the device's performance was studied: traditional longitudinal fins, T-shaped fins, and tree-shaped fins (**Fig. (2.10)**), and the results for the three shapes were compared with without fins case. It was concluded that adding T-shaped fins caused a rise in the rate of melting compared to longitudinal and tree fins and that the melting duration was decreased by 33 % compared to traditional longitudinal fins.

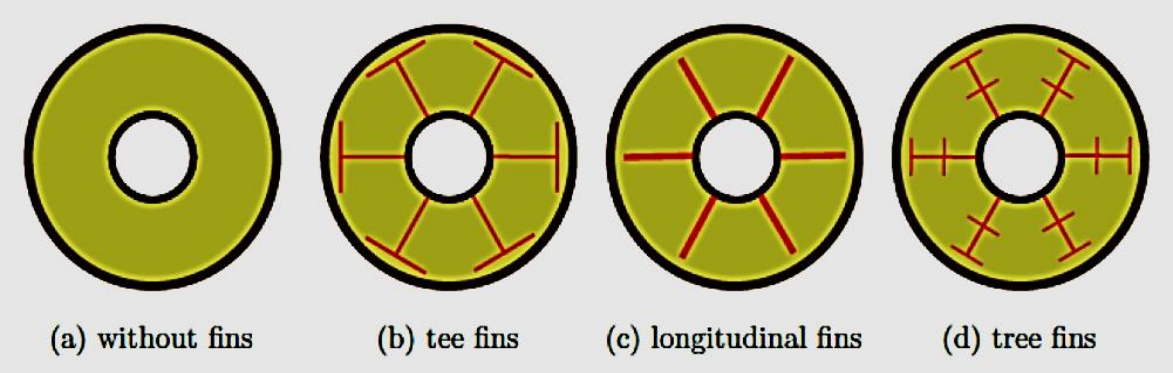

Fig. (2.10). The computational domains for the various heat exchangers with different fin configurations: (a) without fins, (b) tee fins, (c) longitudinal fins and (d) tree fins (Al-Mudhafar et al. [31]).

Zhang et al. [32] investigated the topology-optimization method to evaluate the effect of fins on the melting performance experimentally and numerically. The findings revealed that topology-optimized structure fins (**Fig. (2.11)**) reduced the melting period eight times that of longitudinal fins. The melting time was reduced by 40% using topology-optimized fins compared to longitudinal fins.

The summary of studies related to PCM melting in horizontal finned LHTES is listed in **Table 2.1**.

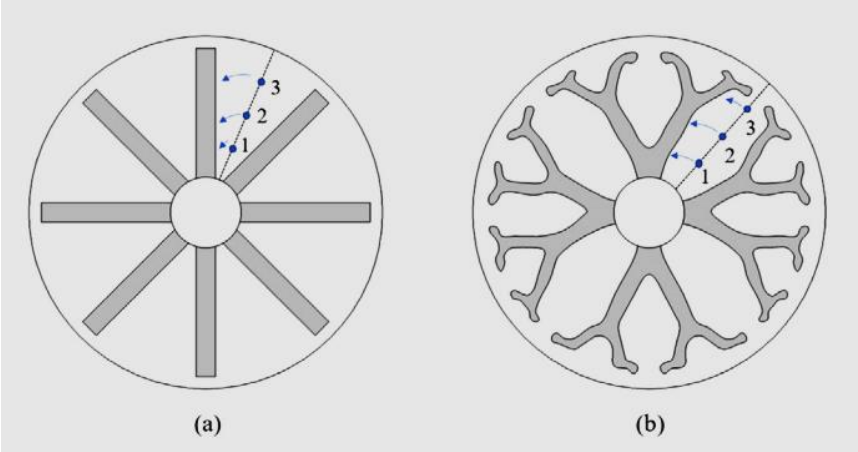

Fig. (2.11). (a) longitudinal fins (b) topology-optimized fins (Zhang et al. [32]).

Table 2.1. Summary of the research conducted on the horizontal (LHTESS) with the addition of fin-assisted processes.

Authors (Year)	**Dimensions of the Annular Container (d, D and L)**	**PCM; T_m; k and λ**	**Study Types**	**Fin specifications**	**Highlighted Results/Findings**
Agyenim and Hewitt (2010)	d= 65 mm D = 375 mm L= 1200 mm	RT58 T_m= 48-62 °C k = 0.2 W/m.K λ = 181 kJ.kg^{-1}	Experimental	Longitudinal fins: t=1 mm h=120 mm n = 8	- Using fins resulted in a significant reduction of the storage capacity by around 30% - increasing the water inlet temperature produced more thermal energy stored in the PCM
Mat et al. (2013)	d=50.8 mm D1= 150 mm D2= 200 mm	RT82 T_m= 77- 85 °C k= 0.2 W/m.K λ = 176 kJ.kg^{-1}	Numerical	Three configurations of longitudinal fins; t=1 mm h=42 mm n= 8	The use of an internal-external fin reduced melting duration by 43.3% compared to the absence of fins.
Al-Abidi et al. (2014)	d=50.8 mm D_1 =150mm D_2=200mm L= 500 mm	RT 82 T_m= 82 °C k= 0.2 W/m.K λ = 176 kJ.kg^{-1}	Experimental	Internal and external longitudinal fins n =8 t=1 mm h= 42 mm	The use of fins assisted PCM melting.
Li and Wu. (2015)	D =4 d mm L=100 d mm	Pure NaNO3 T_m= 33 °C k= 0.5 W/m.K	Numerical	Longitudinal fins, n = 6	Adding longitudinal fins reduced melting time by 14 % of a composite of

		λ = 173.3 $kJ.kg^{-1}$ Composite of $NaNO_3$/expanded graphite T_m= 33 °C k= 10 W/m.K λ = 155.97 $kJ.kg^{-1}$		t=(D-d)/2 mm h= 2.5 d mm	$NaNO_3$/expanded graphite.
Wang et al. (2016)	d=50 mm D=146.4mm	T_m= 121 °C k= 0.326 W/m.K λ= N/A	Numerical	Two types of longitudinal fins: full-scale fins n = 3 t=1 mm H2 = H3 = 46.2 mm half- scale fins n = 4 t=1 mm H1 + H3 = 2-H2 = 69.3 mm	Using optimal full-scale fins with an angle range of 60 to 90 degrees resulted in a significant reduction of 49.1% in the melting duration.
Yuan et al. (2016)	d=40 mm D = 80 mm	Lauric acid T_m= 44.22 °C k= 0.147 W/m.K λ = 173.8 $kJ.kg^{-1}$	Experimental and numerical	Longitudinal fins: t=1 mm h=10 mm n = 2	The highest melting rate was associated with a fin installation angle of 0 degrees. Increasing the fin installation angle beyond 45 degrees did not affect the charging rate.
Darzi et al. (2016)	d=40 mm D = 80 mm	N-eicosane T_m = 35 - 37 °C	Numerical	Longitudinal fins: t=1 mm	Inserting fins enhanced the charging and discharging rates.

		k = 0.15-0.24 W/m.K λ =247.6 kJ.kg^{-1}		h=15 mm n=4,10,15,20	
Wang et al. (2016)	d=127 mm D = 258 mm	N-Octadecane T_m= 27 °C k = 0.15 - 0.36 W/m.K λ = 243.5 kJ.kg^{-1}	Numerical	Circular fins: n = 6 h=30 mm t=10 mm	The fin pitch must be low in order to give better performance.
Cao et al. (2017)	d=40 mm D = 80 mm L= 500 mm	lauric acid T_m= 44.22 °C k= 0.147 W/m.K λ = 173.8 kJ.kg^{-1}	Numerical	Longitudinal fins: t=1 mm h=10 mm n = 4, 6, 8, 10, and 12	The addition of fins shortened the melting time The melting rate decreased if the number of fins exceeded its optimal value.
Mahdi et al. (2018)	d=50.8 mm D_1 =150 mm D_2 =200 mm L= 500 mm	RT82 T_m= 77- 85 °C k= 0.2 W/m.K λ = 176 kJ.kg^{-1}	Numerical	Longitudinal fins of different sizes in the upper and lower halves	The use of long fins in the lower region and considerably shorter fins in the upper region accelerated the melting.
Deng et al. (2019)	d=23 mm D =50 mm	Lauric acid T_m= 43-48 °C k= 0.174 W/m.K λ=187.21 kJ.kg^{-1}	Numerical	Longitudinal fins with different angles and length n =2 t=1 mm h=6.25,9.375, 12.5 mm	Melting time can be reduced by using the longer lower double fin. The optimum angle between fins is 120°.

Abdulateef et al. (2019)	d=76.2 mm D1= 381 mm D2= 500 mm	RT82 T_m= 77-85 °C k= 0.2 W/m.K $\lambda = 176\ kJ.kg^{-1}$	Numerical	External triangular fins: aspect ratio (18%) h=141 mm n= 8	The use of external triangular fins successfully decreased the melting and solidification times.
Khan and Khan. (2020)	d=35 mm D = 121 mm L= 400 mm	Stearic Acid T_m= 54-64 °C k= 0.29 W/m.K $\lambda = 186.5\ kJ.kg^{-1}$	Experimental and numerical	Longitudinal fins: t=3 mm h=36 mm n= 3	The Y-fins structure, when compared to the ⅄-fin configuration, resulted in a 50.7% lessening in melting duration and increased total energy capacity by 10%
Yu et al. (2020)	d=90 mm D =300 mm	RT58 T_m= 48-62 °C k= 0.2 W/m.K $\lambda = 181\ kJ.kg^{-1}$	Numerical	Longitudinal fins with different thickness and angles n =8 h= 103 mm	The optimum values of gradients in fin central angle and fin thickness were 14.96° and 2.846 mm, respectively.
Li et al. (2021)	d=50 mm D = 150 mm L= 300 mm	(RT52) T_m= 51 °C k= 0.2 W/m.K λ=156.82 $kJ.kg^{-1}$	Numerical	longitudinal fins with different fin models n =8	Decreasing the thickness and height of the top fins, coupled with an increase in the length and thickness of the bottom fins, decreased the charging time.
Al-Mudhafar et al. (2021)	d=5.08 cm D = 15 cm L= 42 cm	(RT82) T_m= 77–85 °C k= 0.2 W/m.K $\lambda = 176\ kJ.kg^{-1}$	Numerical	Tee-fin shape n = 6 t=1 mm Tree- fins shape	The melting rate of the tee fins heat exchanger was higher than that of longitudinal and tree fins.

				n = 6 t=1 mm	
Zhang et al. (2021)	d= 60 mm D = 300 mm	T_m= 13-17 °C k= 0.18 W/m.K λ = 132.7 kJ.kg^{-1}	Experimental	Longitudinal topology-optimized fins: n = 8	Using topology-optimized fins reduced melting time by 40% compared to using longitudinal fins.

d, D and L are the tube's inside diameter, the shell's inside diameter and the container's length, respectively.

T_m; k and λ are melting temperature, thermal conductivity and latent heat of PCM, respectively.

n, h, t = fin number, fin height, and fin thickness, respectively.

2.2.2 Vertical finned thermal energy storage units

The LHTES unit is positioned vertically, where the fins are inserted into the energy storage unit to increase the heat exchange between the heat source and PCM.

Rathod and Banerjee [33] conducted an experimental analysis to investigate the impact of using three longitudinal fins fixed on the inner tube of a vertical LHTES unit. A decrease in melting duration was found by 12.5% and 24.5% when fins were used, corresponding to fluid input temperatures of 80 °C and 85 °C, respectively.

Sciacovelli et al. [34] introduced the concept of using tree-shaped fins to improve the efficiency of the shell-and-tube storage system. Two different fin designs were considered: a single bifurcated arrangement and a dual bifurcated one (**Fig. (2.12)**). The predictions revealed that, for shorter working durations, fins with a Y-shaped configuration with wider angles between their branches seemed more favorable. In contrast, using smaller angles for long operational durations was important. Furthermore, the utilization of this particular configuration of fins resulted in a notable enhancement in system efficiency, with a substantial rise of 24%.

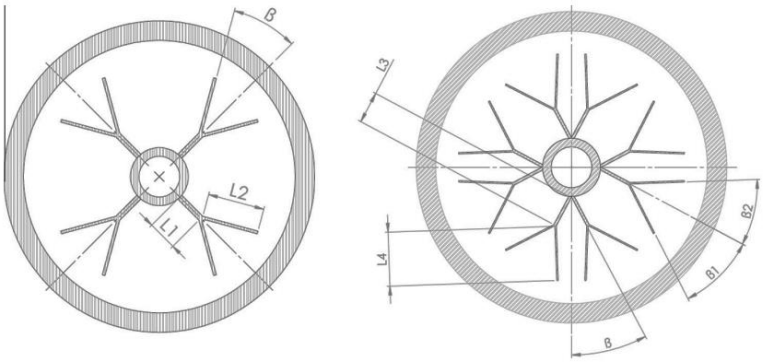

Fig. (2.12). Fin configurations. (Left) Single bifurcation. (Right) Double bifurcation (Sciacovelli et al. [34]).

Yang et al. [35] investigated numerically the melting performance in a shell-and-tube (LHTES) unit supplied with a non-uniform distribution of annular fins. The influences of the fins' number, height, and thickness on the melting were examined. The simulation indicated that using annular fins led to a reduction rate of 65% from the time of melting.

Rozenfeld et al. [36] experimentally and numerically investigated the thermal behavior of fin-assisted melting in vertical annular storage units. A helical fin is connected to the inner tube that carries the (HTF) (**Fig. (2.13)**). The researchers concluded that the proposed model has many advantages, including improving melting, avoiding increased pressure during melting and solidification, and ease of filling, unloading, and maintaining the system. Also, a very good agreement is observed between numerical and experimental findings.

Fig. (2.13). The process of melting (charging) in a helical-fin laboratory prototype (Rozenfeld et al. [36]).

Latent heat storage (LHS) finned units were experimentally studied by Khan and Khan [37]. The unit was a heat exchanger made of shells and tubes supported with longitudinal fins. Since natural convection serves the quick melting of PCM, it was decided that vertical longitudinal fins would be the best choice. The use of fins improved the thermal efficiency of the LHS unit, and the melting interval of PCM was decreased.

Pu et al. [38] numerically tested the thermal efficiency of PCM melting that was used as a heat storage material in a vertical thermal energy storage device under the effect of adding several arrangements of fins. These arrangements were the bottom fins, top fins, middle fins, and arithmetic fins (**Fig. (2.14)**). The effect of some parameters on the melting operation was also studied, such as the length and number of fins and the distance between one fin and another. The computational findings revealed that the shortest melting time was when using arithmetic fins, with a time reduction rate of 49.9%, followed by the middle fins with a reduction rate of 46.9%, the lower fins with a reduction rate of 38.9%, and the upper fins with a reduction rate of 13.9%, all in comparison to the case without any fins.

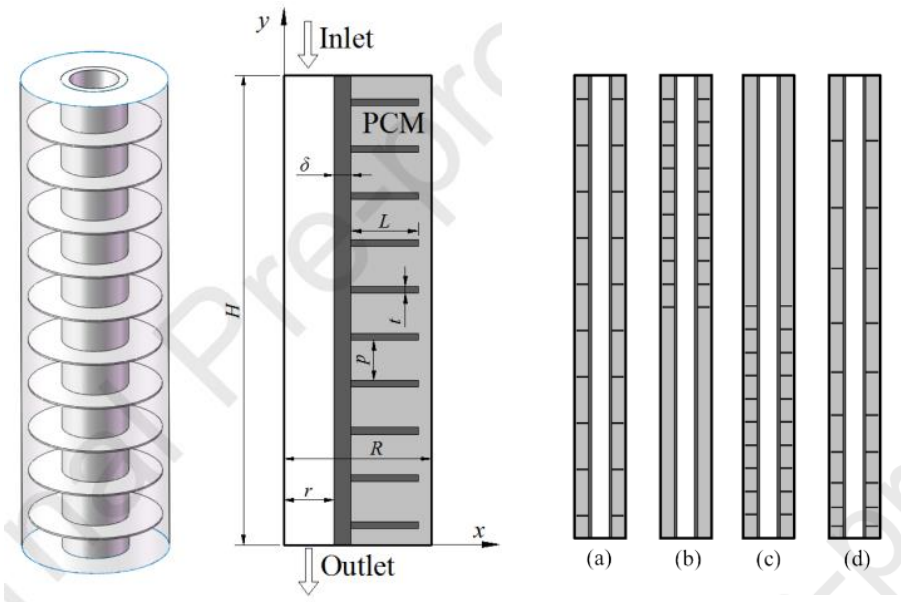

Fig. (2.14). Different fin arrangements of vertical finned LHTES: (a) middle fins, (b) upper fins, (c) lower fins, (d) arithmetic fins (Pu et al. [38]).

Yagci et al. [39] achieved an experimental investigation of the charging/discharging of PCM in a vertical annular heat exchanger consisting of a shell and a tube. It was explored various surface arrangements of the heat transfer tube, including both without fins tubes and finned tubes, with the aim of optimizing the thermal performance of the overall system. Additionally, examined various fin geometries with different ratios of top edge height to lower edge height (**Fig. (2.15)**), specifically considering three values of w_1/w_2 (1, 1/3, and 0). The experimental outcomes indicated that using a fin with the inner tube enhanced the melting in the lower region, where natural convection was limited. Additionally, selecting a certain ratio of fin edge heights (w_1/w_2) within the range of 0.1 to 0.3 produced a reduction in melting time by 62% and 58%, respectively, in comparison to a model without fins.

.

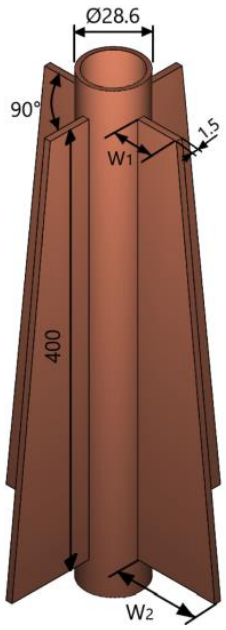

Fig. (2.15). Geometric characteristics of the heat transfer tube (Yagci et al. [39]).

Yang et al. [40] conducted a numerical and experimental study on the thermal properties of PCM inside a vertical LHTES device. The study aimed to assess the influence of the space between fins and fins position on the melting of PCM. Based on

their results, compared to the basic configuration where the annular fins were evenly spaced, the researchers found that the overall melting period was reduced by 62.8% when using unevenly spaced fins. Furthermore, the use of unevenly spaced annular fins resulted in a 4.7% improvement in the homogeneity of the melting rate. Furthermore, the use of unevenly spaced annular fins resulted in a 4.7% improvement in the homogeneity of the melting rate. Among the several cases considered, case (c) (**Fig. (2.16)**) demonstrated the most ideal performance.

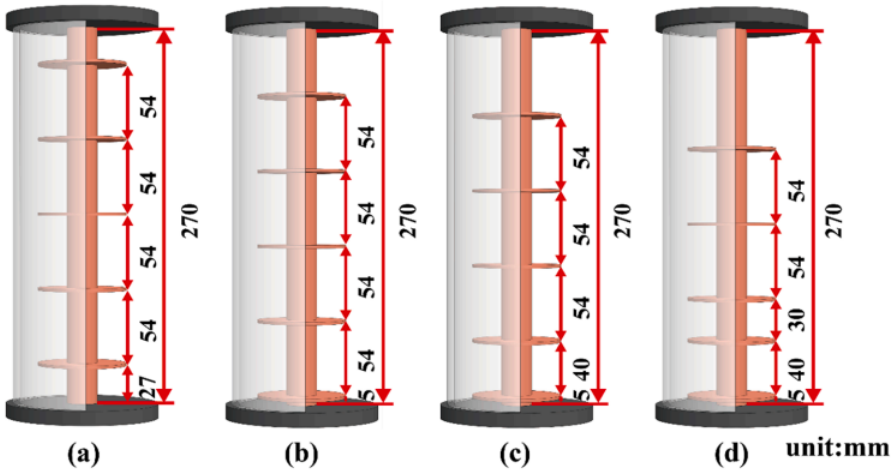

Fig. (2.16). Four representative TES units with annular fins: (a)-(c) uniform pitch; (b)-(d) non-uniform pitch (Yang et al. [40]).

Elmaazouzi et al. [41] studied numerically the impact of adding annular fins to the LHTES devices. Also, the effect of increasing the length of the fins on the melting period was examined. The predicted results showed that the duration required for melting decreased by extending the length of the fins. Among the many fin designs examined, case 5, characterized by a fin height of 14 mm, was the most favourable as the melting time decreased by 50.64%. The same authors [42] simulated the impact of the insertion of annular fins on the melting process of (PCM) inside a vertically LHTES unit. The simulation results revealed that the addition of annular fins significantly impacted the

charging time. Moreover, it was noted that as the fins number increased, the performance of the (LHTES) system improved, leading to decreased charging time.

Gürtürk and Kok [43] conducted both experimental and computational investigations to examine the influence of heat transfer fin surface areas on the charging process of PCM used in LHTES units. It was concluded that increasing the surface area alone did not consistently provide better results. Instead, the specific design of the fins significantly influenced the melting process even though the surface area of the fins in design (1) is considerably larger than that of designs (4 and 5) (**Fig. (2.17)**). Design (1) significantly lessens the duration required for the melting process, with a reduction of 60%., whereas designs (4 and 5) achieved a 65% reduction.

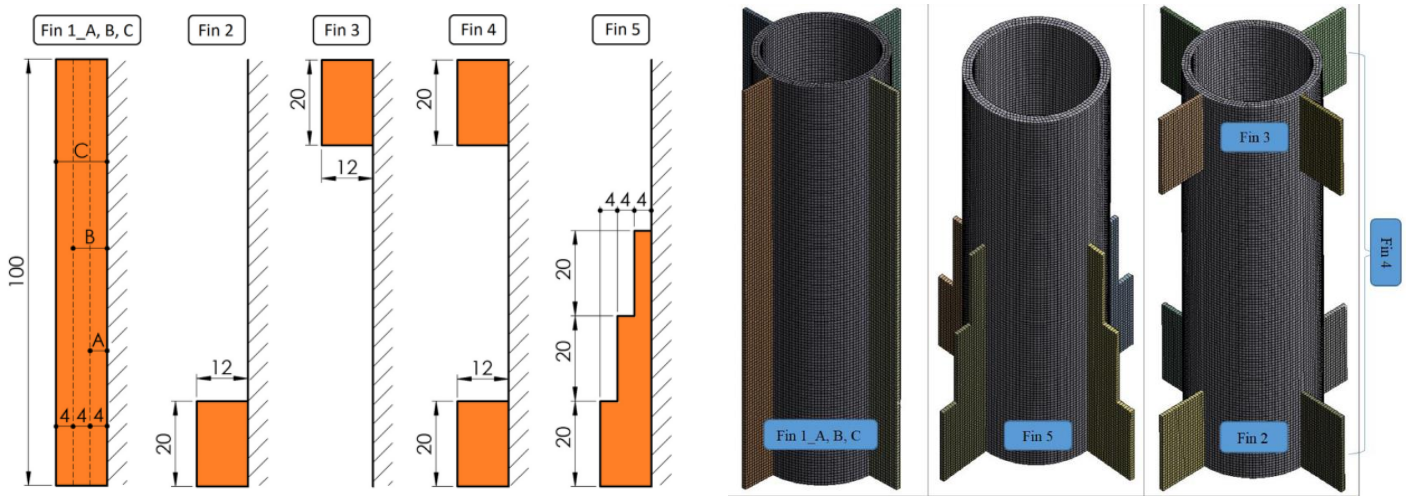

Fig. (2.17). Designs of all fins structures (Gürtürk and Kok [43]).

Mehta et al. [44] performed an experimental analysis to determine the effect of spiral fins on the charging behaviour of PCM in a vertical storage unit. It was reported that the use of spiral fins caused a decrease in the charging period by 41.48%.

Tiari et al. [45] numerically assessed the insertion of uniform and non-uniform annular fins on the performance of (LHTES) system through the melting and

solidification processes. The size of fins remained constant across all the cases studied. The fins were then divided into two groups: 10 fins of 1.587 thickness and 20 fins of 0.794 mm thickness (**Fig. (2.18)**). Subsequently, the two types mentioned were further classified into uniform and varying fin heights. It was discovered that using a fin configuration consisting of twenty fins of varying heights, with longer fins positioned at the bottom of the unit, led to a significant reduction in melting duration by 73.7%.

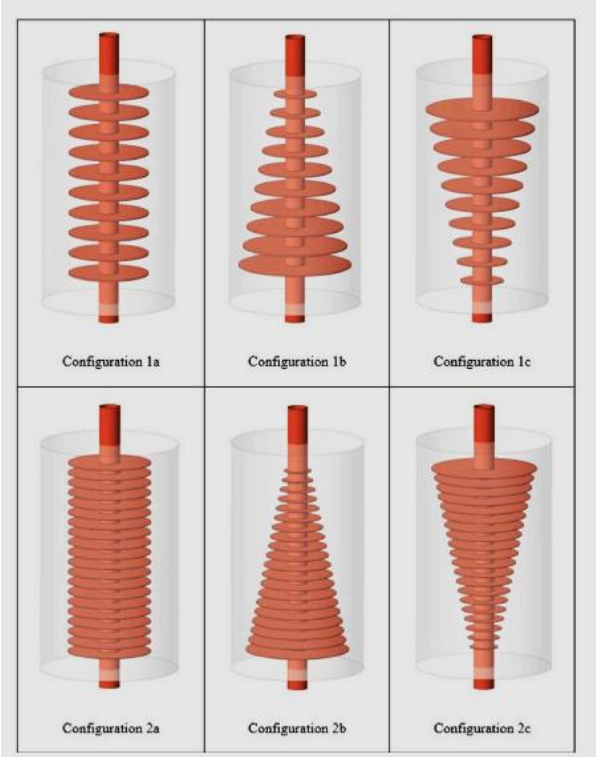

Fig. (2.18). Physical models of the six configurations that include fins, 1 represents 10 fins, 2 represents 20 fins, and configuration style is denoted by a, b, and c (Tiari et al. [45]).

Zhu et al. [46] numerically examined the melting and solidification properties of RT35 PCM confined inside a shell-and-tube finned vertical heat exchanger. It was concluded that the proposed initial improved design had the potential to enhance the rate of melting. Additionally, a partition strategy for quadratic optimization gave an additional improvement in the thermal achievement. The optimization of the seventh example (**Fig.**

(2.19)), which involves the elongation of the bottom fins, leads to a decrease in the duration of melting and an improvement in heat transfer.

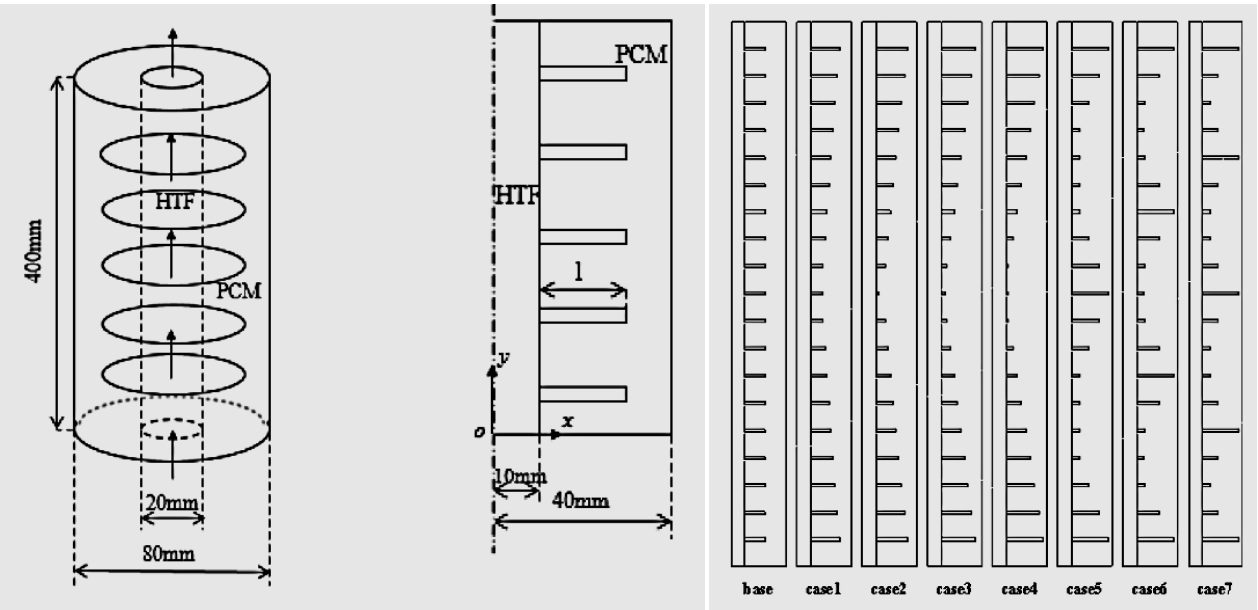

Fig. (2.19). Structures of all cases (Zhu et al. [46]).

Lu et al. [47] conducted experiments to inspect the thermal performance of a vertical multi-tube and shell (LHTES) unit with a spiral-finned tube. It was demonstrated that adding spiral fins enhanced the thermal efficiency in both energy storage and release processes. This design led to an increase in the total heat transfer coefficient of PCM by 49.21 %, and this increase led to a significant reduction in melting time.

He et al. [48] experimentally examined the thermal properties of PCM melting in a LHTES device that contains two types of fins: non-perforated solid helical fins (SHF) and perforated helical fins (PHF). It was observed that both kinds of helical fins showed better thermal performance. However, the perforated helical fins provided greater thermal performance compared to the non-perforated helical fins.

The summary of studies related to PCM melting in vertical finned LHTES is listed in **Table 2.2**.

Table 2.2. Summary of the studies on the PCM melting in vertical (LHTESS) with the addition of fin.

Authors (Year)	**Dimensions of the Annular Container (d, D and L)**	**PCM; T_m; k and λ**	**Study Types**	**Fin parameters**	**Highlighted Results/Findings**
Rathod and Banerjee (2014)	d= 33 mm D= 128 mm L= 1000 mm	Stearic Acid T_m= 55-64 °C k= 0.29 W/m.K λ =186.5 kJ.kg^{-1}	Experimental	longitudinal fins: n = 3 t= 3 mm h= 30 mm	Inserting fins reduced melting duration by 12.5% and 24.5% for fluid input temperatures of 80 °C and 85 °C, respectively.
Sciacovelli et al. (2014)	d=21 mm D= 115 mm L= 400 mm	Paraffin wax T_m= 55-60 °C k= 0.2 W/m.K λ=230 kJ.kg^{-1}	Numerical	Tree longitudinal fins: n = 4, and 8	Using tree fins increased the system efficiency by 24 %.
Yang et al. (2017)	d=15 mm D = 44 mm L= 400 mm	RT35 T_m= 28-40 ° C k= 0.2 W/m.K λ = 157 kJ.kg^{-1}	Numerical	annular fins n = 31	Using annular fins led to a reduction rate of 65% from the time of melting.
Rozenfeld et al. (2017)	d=12 mm D= 44 mm L= 218 mm	Lauric acid T_m= 36-44 °C k= 0.147 W/m.K λ =173.8 kJ.kg^{-1}	Experimental	Helical fins: n = 1 t= 3 mm h= 15.5 mm	Using helical fins improving melting, avoiding increased pressure during melting and solidification, and ease of filling, unloading, and maintaining the system.
Khan and Khan (2017)	d=22 mm D= 450 mm L= 385 mm	RT 44 T_m= 41-44 °C k=0.2 W/m.K λ =255 kJ.kg^{-1}	Experimental	longitudinal fins: n = 4 t= 1.5 mm	Using longitudinal fins reduced PCM melting duration and enhanced

				h= 40 mm	the (LHTES) device's thermal efficiency.
Pu et al. (2019)	d=15 mm D= 44 mm L= 400 mm	RT35 T_m= 29-35 °C k=0.2 W/m.K λ =157 kJ.kg^{-1}	Numerical	Radial fins: n= 8,10,14, 24 t= 1 mm h=5,7.7,10, 11.8 mm	Arithmetic fins resulted in a notable reduction in melting time by 49.9% in comparison with the absence of fins.
Yagci et al. (2019)	d=28.6 mm D= 110 mm L= 400 mm	Paraffin wax T_m= 50-58 °C k= 0.2 W/m.K λ=140.3 kJ.kg^{-1}	Experimental	longitudinal fins with different edge ratios: n = 4 t= 1.5 mm	When the ratio of fin edge lengths (w1/w2) is chosen to be in the range of 0 to 1/3, the melting time decreased by 62% and 58%, respectively.
Yang et al. (2020)	d=20mm D= 90 mm L= 270 mm	Paraffin Tm=50-55 ° C k= 0.2 W/m.K λ=102.1 kJ.kg-1	Experimental and numerical	annular fins n = 5 t=2 mm l=54 mm h= 21 mm	The overall melting period was reduced by 62.8% by using unevenly spaced fins compared with utilization of uniform fins.
Elmaazouzi et al. (2020)	d= 24 mm D = 58 mm L= 300 mm	NaNO3–NaOH (86–14) T_m= 250 °C k= 0.6 - 0.66 W/m.K λ= 160 kJ.kg^{-1}	Numerical	annular fins with six different geometries n =99 t=1 mm	The reduction of melting time may be obtained by extending the height of the fins. In the ideal case, where the fin height is 14 mm, the melting time is decreased by 50.64%.
Elmaazouzi et al. (2020)	d=20 mm D = 54 mm L= 300 mm	(NaNO2-NaNO3) T_m= 233 °C	Numerical	annular fins n =10,30,50 t=2 mm	The addition of fins to the thermal storage system resulted in

		k= 0.54 - 0.59 W W/m.K λ = 163 kJ.kg^{-1}		h= 14 mm $l_{(10)}$ = 28 mm $l_{(30)}$= 8 mm $l_{(50)}$=4 mm l: distance between fins	improved performance and a decrease in melting time.
Gürtürk and Kok (2020)	d=12 mm D= 45 mm L= 100 mm	RT 55 T_m= 51-57 °C k= 0.2 W/m.K λ =172 kJ.kg^{-1}	Experimental and Numerical	Various longitudinal fins: n = 2,4,8 t= 1 mm h= 12 mm	The factor affecting melting was the fin design and only sometimes surface area.
Mehta et al. (2020)	d= 30 mm D= 88 mm L= 600 mm	Stearic Acid T_m= 55-56 °C k= 0.172 - 0.3 W/m.K λ = 196.1 kJ.kg^{-1}	Experimental	Spiral fins: n = 1 t= 2.5 mm h= 20 mm	Using spiral fins reduced melting time by 41.48 %.
Tiari et al. (2021)	d= 25.4 mm D= 177.8 mm L= 304.8 mm	RT55 T_m= 51-57 ° C k= 0.2 W/m.K λ = 172 kJ.kg^{-1}	Numerical	Two categories of annular fins: 1- n = 10 t= 0.794 mm h=4 cm 2- n = 20 t=0.794 mm h=4 cm	The maximum reduction in the charging time was achieved using 20 fins of varying lengths, with longer fins positioned at the bottom of the inner tube.
Zhu et al. (2021)	d=20 mm D =80 mm	RT35 T_m= 29-36 °C	Numerical	Annular fins n = 19	Increasing the length of the bottom fins

	L= 400 mm	k= 0.2 W/m.K λ = 170 kJ.kg^{-1}		t=2 mm h= 15 mm l= 20 mm	decreased melting time and increased heat transferred.
Lu et al. (2021)	d=16 mm D= 300 mm L= 300 mm	paraffin wax T_m= 52-56 °C k= 0.21 W/m.K λ =185.7 kJ.kg^{-1}	Experimental	Spiral fins: t= 0.3 mm h= 7.5 mm	Using spiral-finned tubes led to high thermal performance and reduced melting time.
He et al. (2023)	d= 15 mm D= 110 mm L= 500 mm	RT 55 T_m= 51-57 °C k= 0.2 W/m.K λ =172 kJ.kg^{-1}	Experimental	helical fins: n = 12 t= 3 mm h= 42.5 mm	Perforated helical fins gave a higher thermal performance.

2.3 Aims and scope of present study

In this study, the thermal characteristics of PCM inside a horizontal heat exchanger are investigated numerically and experimentally for three cases of the heat exchanger: without fins, X-shaped fins, and below fins. The present study aims to:

- Investigating numerically and experimentally the thermal performance of the phase change material PCM inside a heat exchanger without fins and finned heat exchangers.
- Comparing the finned and unfinned heat exchangers performance.
- Evaluating the impact of operational conditions on thermal performance.

The ANSYS FLUENT 17.2 software package was used to simulate the PCM melting. The experimental work included manufacturing the device used, installing measurement systems, and conducting practical experiments for different geometrical and operating conditions.

2.4 Summary

By reviewing many researches that studied the melting of PCM in annular latent heat thermal energy storage devices without the use of fins, it was found that the higher effect of natural convection and overheating at the upper part of the heat exchanger and the conduction dominated the lower part. Also, the inlet temperature of the heat transfer fluid (HTF) significantly affected the melting process. Inserting the fins mitigates the issues and improves the melting process. The present work will investigate the effect of inserting uniform and nonuniform distributions of longitudinal fins.

CHAPTER THREE

NUMERICAL STUDY

CHAPTER THREE: NUMERICAL STUDY

In the current work, the physical and numerical descriptions of PCM melting within the finned annular cavity of heat exchanger is performed. For the sake of comparison, the PCM melting within the unfinned heat exchanger is also simulated.

3.1 Physical Model

The description of the physical domain that involves (PCM) placed inside the annular cylinder of a horizontally oriented heat exchanger is introduced in **Fig. (3.1)**. The PCM heat exchanger consists of double-concentric pipes. The thermally-insulated acrylic outer shell has an inner diameter of 75 mm and a wall thickness of 2.5 mm. The inner pipe is made of copper with an inner diameter of 25 mm with a wall thickness of 0.9 mm. Three different configurations exist for the inner copper pipe: (without fins, four longitudinal X-shape fins, four longitudinal fins positioned below the pipe). The heat exchanger has a length of 500 mm. The PCM (RT-42 Rubitherm) is used to entirely fill the annular space between two pipes with a melting range of 38 to 42 °C. A list of the employed PCM's thermophysical characteristics is presented in **Table (3.1)**. The storage cell's heat source is a hot water HTF that flows through the inner pipe. The melting inside the horizontal annular heat exchanger is characterized by a 2-D radial and angular coordinates (r, θ). The initial temperature of the PCM is T_{ini} when it is in the solid state. The heat transfer fluid enters the system at a temperature T_w and a constant velocity U_{in}, and exists at atmospheric pressure. All walls are designed to be non-slip. Three configurations of HE are considered, namely, unfinned HE, X-shape finned HE, and below-fin HE, as described in **Fig. (3.2)**. The four-longitudinal fins have the geometrical parameters of 500 mm, 20 mm, and 1 mm of length, width, and thickness, respectively.

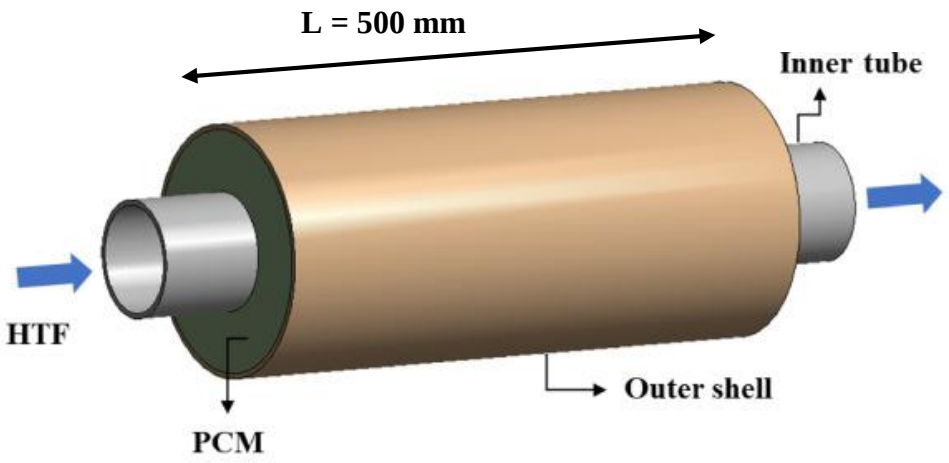

Fig. (3.1). The double-concentric pipes heat exchanger

Table (3.1) Physical and thermal properties of the PCM [49], appendix(A).

Coefficient of thermal expansion, β	**0.0008 1/k**
Density, ρ	**880 kg/m^3 (solid)** **760 kg/m^3 (liquid)**
Dynamic viscosity , μ	**0.02728 kg/m s**
Liquidus Temperature, T_l	**43 °C**
Melting latent heat of, ΔH	**165 kJ.kg^{-1}**
Solidus Temperature ,T_s	**38 °C**
Specific heat capacity, Cp	**2 kJ/kg K**
Thermal conductivity, k	**0.2 W/m^2°K**

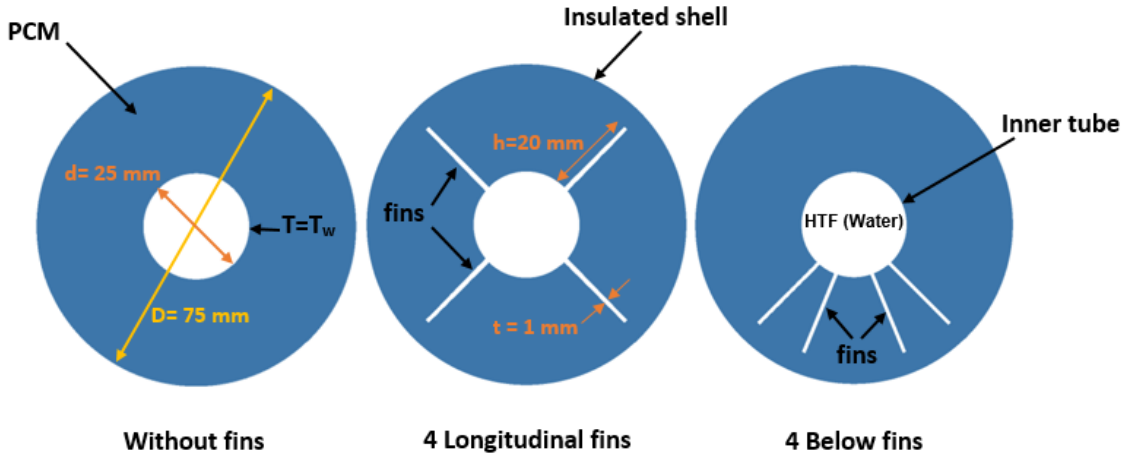

Fig. (3.2) Configurations of the heat exchangers.

3.2 Problem formulation

PCM melting inside cavities is a transient, nonlinear problem with movable melting front and boundaries. The required assumption and the governing equations are described.

3.2.1 The assumptions of the model

To reduce the complexity of the melting problem, a set of assumptions has been made as follows [3]:

1- Two-dimensional and axisymmetric model.

2- The space between inner and outer tube fully filled with PCM.

3- PCM thermophysical properties remain constant

4- Laminar, non-Newtonian, and incompressible flow is assumed for the PCM in liquid state.

5- Solid PCM sinking due to gravity is ignored.

6- During the phase change process, the PCM's volume change is not considered.

7- Because of neglecting the HTF temperature change between inlet and outlet, the surface temperature of the inner tube is constant as a boundary condition

8- There is no heat gained or lost.

3.2.2 The Governing Equations

To analyze PCM melting in a concentric annular cell, the following continuity, momentum, and energy equations are used [3]:

$$\frac{\partial \rho}{\partial t} + \nabla . (\rho V) = 0 \qquad \ldots\ldots (3\text{-}1)$$

$$\frac{\partial (\rho V)}{\partial t} + \nabla . (\rho V V) = \mu \nabla^2 V - \nabla P + S_u \qquad \ldots\ldots (3\text{-}2)$$

$$\frac{\partial}{\partial t}(\rho H) + \nabla . (\rho V H) = \nabla . (K \nabla T) \qquad \ldots\ldots (3\text{-}3)$$

Where ρ, μ, and k represent the density, viscosity, and thermal conductivity of phase change material (PCM), respectively.

The body force component in the momentum equation may be approximated using the Boussinesq approximation, which relies on a reference density (ρ_{ref}), temperature (T_{ref}), and thermal expansion coefficient (β).

Where $S_u = S_D + S_g$ …. (3-3a)

And $S_g = \rho_{ref} g \beta (T - T_{ref})$ …. (3-3b)

Also $\beta = -\frac{1}{\rho}\left(\frac{\partial \rho}{\partial T}\right)P$ ….. (3-3c)

$S_D = \frac{(1-f)^2}{f^3+\varepsilon} V A_{mush}$ …… (3-3d)

Where S_g represents the body force of buoyancy due to the density variation initiated from the temperature difference, and S_D represents the Darcy term essential method for dealing with the mushy zone.

In order to avoid a case of division by zero, a constant denoted as ε is used as a small number of 0.001. Also, the mushy zone constant A_{mush} is a constant quantity that varies from 10^4 to 10^7 and relates to the melting front's shape.

3.2.3 The enthalpy–porosity method

The enthalpy-porosity technique was used as a means to deal with the issue of PCM melting. This methodology is predicated on the ratio between the volume of the PCM liquid and the overall volume of the PCM. The computational division of the storage unit domain will include categorizing it into three distinct zones: solid, liquid, and mushy. The partly solidified zone, known as the mushy region, is considered a porous medium in the context of the enthalpy-porosity approach. The porosity (or liquid fraction) of each cell is assigned a number that is equivalent to its liquid component. In contrast, the porosity of the liquid zone is 1, while it varies between 0 and 1 for the mushy zone. The liquid fraction is computed as:

$$f = \begin{cases} 0 & if\ T \le T_s \\ \frac{T-T_s}{T_l-T_s} & if\ T_s \le T \le T_l \\ 1 & if\ T \ge T_l \end{cases} \quad \text{..... (3-4)}$$

where T_S and T_l are the solid and liquid phase transition temperatures of PCM. T refers to the temperature in this region.

The overall enthalpy H may be expressed as the summation of the sensitive enthalpy h and the latent enthalpy ΔH, as explained by the equation. (3-5).

$H = h + \Delta H$ …. (3-5)

Where,

$$h = h_{ref} + \int_{T_{ref}}^{T} C_p \, dT \quad \text{…. (3-6)}$$

$\Delta H = f L$ …. (3-7)

h_{ref} refers to the PCM sensible enthalpy at T_{ref}, C_p to PCM specific heat at constant pressure, and L to latent heat of PCM.

3.2.4 Initial and Boundary Conditions

The temperature of the inner tube's wall remains relatively constant, while the outer tube and the ends of the heat exchanger are thermally insulated. Furthermore, the heat transfer fluid (water) is pumped into the inner tube at different temperatures. As shown in the figure (3.1), The domain's boundary conditions as follow:

At time t=0, PCM and water temperatures = T_{ini}.

At time t > 0

$$\boldsymbol{U|_{r=r_i} = V = 0} \quad \text{…. (3.9)}$$

$$T|_{r=r_i} = T_w \quad \text{.... (3.10)}$$

$$U|_{r=r_o} = V = 0 \quad \text{.... (3.11)}$$

$$\left.\frac{\partial T}{\partial r}\right|_{r=r_o} = 0 \quad \text{.... (3.12)}$$

Where the radii r_i and r_o are illustrate in figure (3.3).

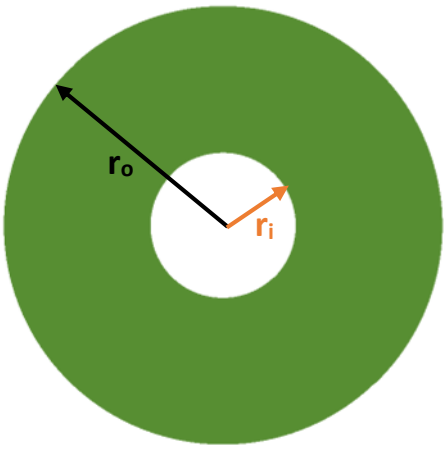

Figure (3.3). Annular PCM cavity.

3.3 Computational model

The simulation of melting process of the phase change material (PCM) in an annular heat exchanger was conducted using ANSYS Fluent 17.2 software. The computational method is shown by a diagram as presented in Figure (3.4).

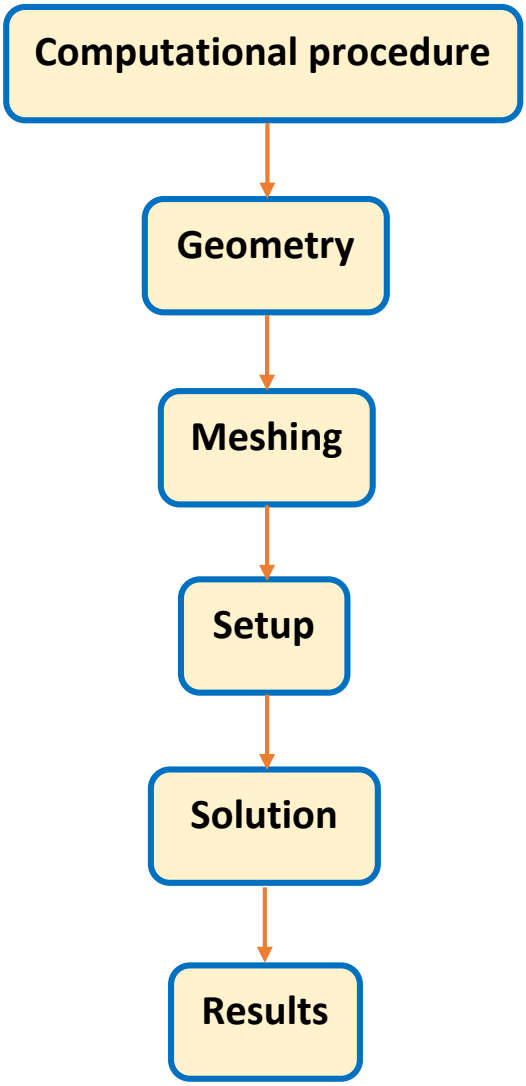

Fig. (3.4). diagram for computational steps.

➢ Geometry

In this study, a two-dimensional model is considered when designing the geometry for the numerical solution. The system includes two separate domains, namely the phase change material (PCM) located inside the annular chamber of the heat exchanger and the flow of water via the inner copper tube. The heat exchanger model that includes the above-mentioned domains for the three cases without fins, X-shape fins and below fins is designed, as explained in Fig. (3.2).

➢ Meshing

The discretization of the domains is achieved by using quadrilateral components that are specifically concentrated at the borders of the computational domain. The optimal grid size is chosen by testing three grid sizes and choosing the best one, as explained in section 3.3.2; the grid arrangement is shown in Figure (3.5).

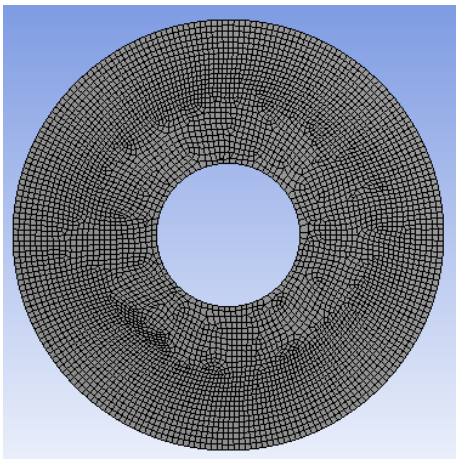

Fig. (3.5) grid arrangement

➢ Setup

The gradient is defined using the least squares cell-based method, and the pressure, momentum, and energy are defined using the second-order upwind method. The SIMPLE method employs the relationship between pressure and velocity adjustments in order to enforce mass convection and compute the pressure field. The updating of calculated

variables at every iteration is controlled by the pressure-based solver via the application of under-relaxation to the equations. In order to accelerate the process of convergence of pressure-velocity iteration algorithms, relaxation factors of 0.3, 1.1, 0.7, and 0.90 are used for the pressure, density, body force momentum, and liquid percentage, respectively. After every iteration of the solver, the amount of residuals for every one of the saved variables is calculated and then saved. The convergence criteria of 10^{-6} are used to assess the convergence of continuity, velocity, and energy.

- **Solution**

After setting the temperature of the inner tube and other parameters for the inner tube, the outer shell, and the PCM, the program is run until the melting is completely complete.

- **Results**

The results are obtained after melting is complete for temperature distribution, the advance of the melting front, the liquid fraction, etc., and for different times, and charts of the numerical results are made to be compared with the practical results as explained in Chapter Five.

3.3.1 The validation of the computational model

To establish the validity of the current model, it is necessary to conduct a comparative analysis with the experiments result or numerical findings acquired by different studies. This analysis should consider the similarity of the melting problem and the conditions of the study. The results obtained from the melting process of PCM for the state without fins and for an inner tube temperature of 70 °C were compared with the practical results obtained by Husseini et al. [8], which includes melting RT50 as a PCM in a horizontal annular chamber with an inner tube diameter of 22 mm and an outer shell diameter of 85 mm. The water circulation at a temperature of 70°C in the inner tube lead to melt the PCM. Figure (3.6) compares the theoretical and practical outcomes of this study with the practical outcomes of Husseini et al. [8]. The utmost variance between the

two outcomes is approximately 7%. The assumptions required to derive the numerical solution and experimental heat losses can both explain this variation.

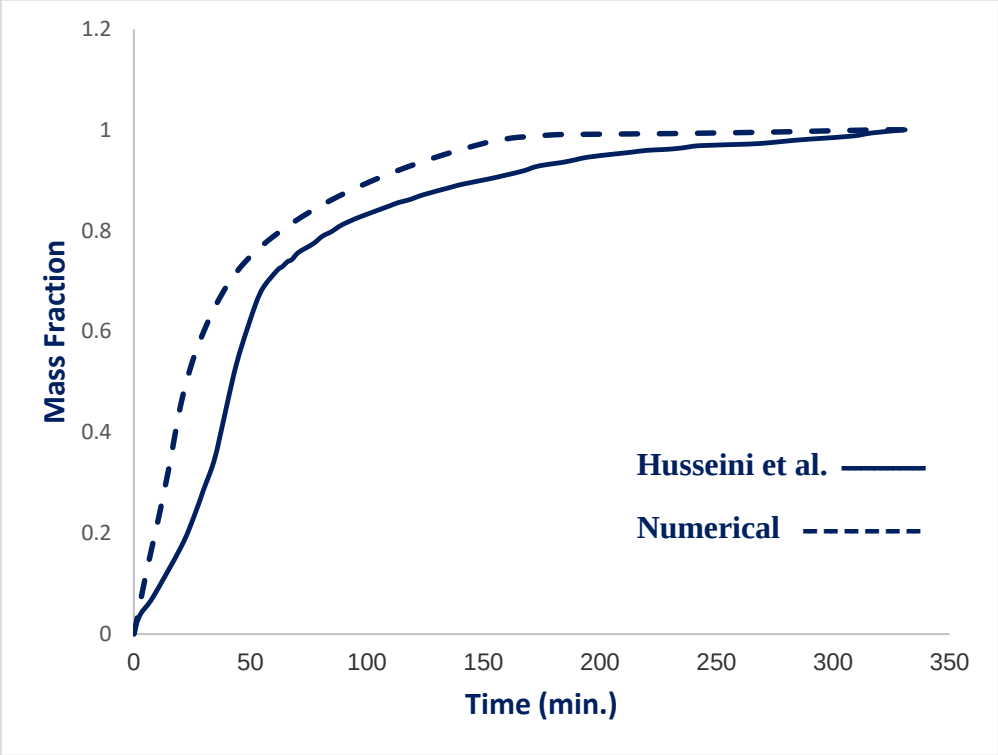

Fig. (3.6) Comparison between present numerical results and experimental result of Husseini et al. [8].

3.3.2 Mesh size- independence test

The purpose of conducting the mesh size independence test was to find the most suitable number of mesh elements that achieves a consistence between solution accuracy and the computational model's cost and implementation time. The investigation examines the impact of altering the proportion of molten material on the determination of the most favorable mesh dimension. The PCM's starting temperature is recorded as 15 °C, while the water entering the system has an input temperature of 70 °C and a discharge rate of 6 l/min. Three groups of mesh-size are examined, which are, 2221, 5001, and 7653 elements. According to the investigation of a liquid fraction, the melting times of three different amounts of elements are 180, 182, and 185 minutes. Hence, the meshing

technique 5001 is employed throughout the whole of the numerical investigation. The diagram shown in Figure (3.7) provides an explanation for the concept.

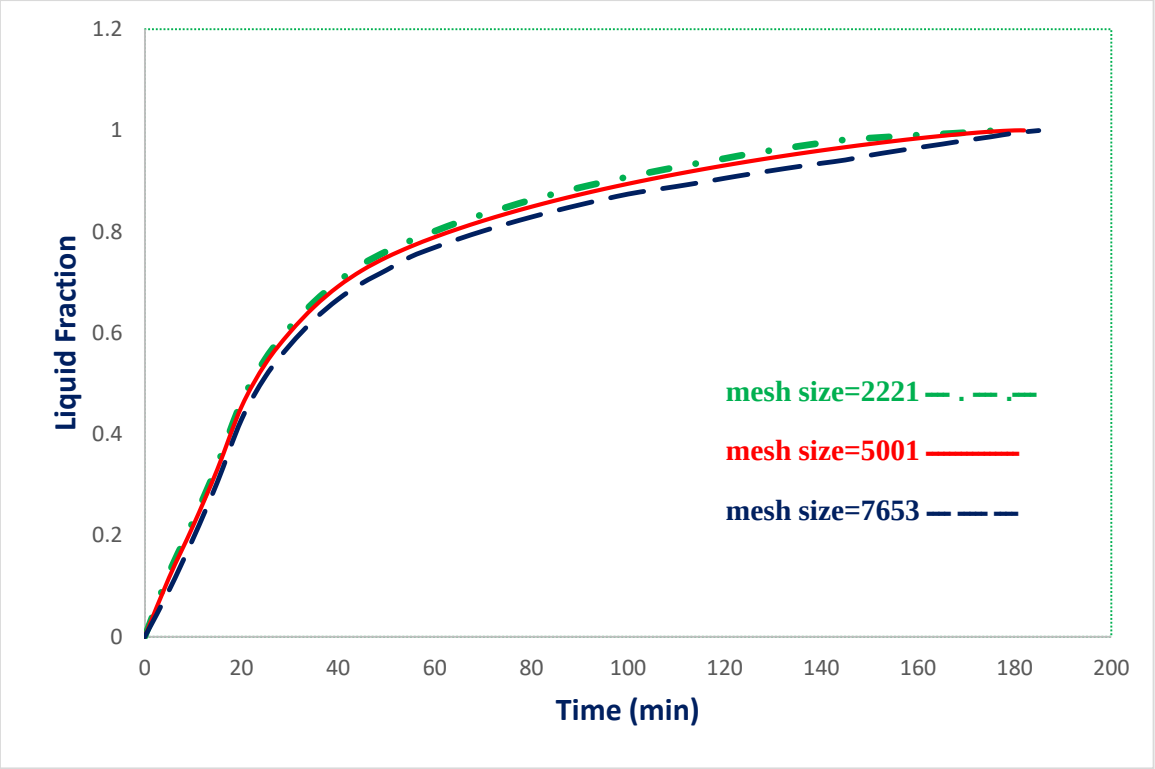

Fig. (3.7). Test of mesh size-independence

3.3.3 Time - step independence test

The test of time step is carried out to examine how every iteration's time step influences the accuracy and agreement of the numerical findings. There are three different time-step values tried out: 0.05 s, 0.1 s, and 0.5 s, as shown in Figure (3.8). The same previous initial and boundary conditions were considered.

The findings displayed that the time step had a very little impact on the melt fraction. The numerical study relied on a time step of 0.1 s to achieve the agreement between the accuracy and the time of computational investigation .

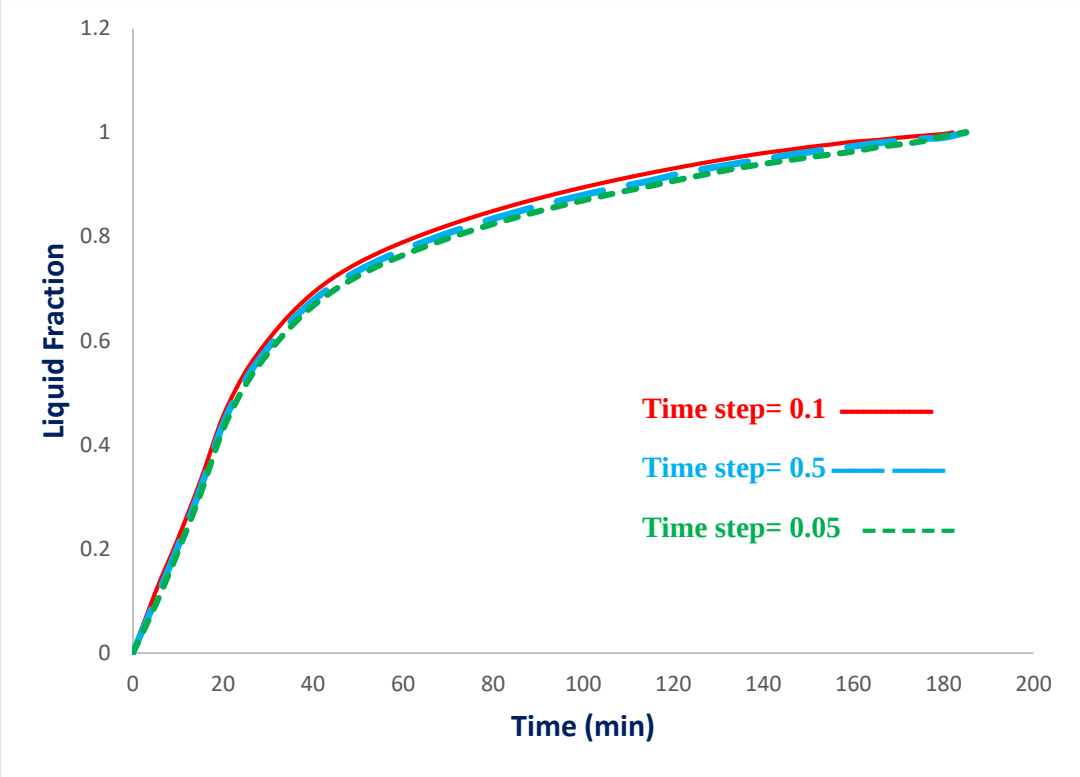

Fig. (3.8) The influence of the time step on the liquid fraction of PCM

3.3.4 The mushy zone constant independence test

Figure (3.9) shows how the constants of the mushy zone (10^5, 10^6, and 10^7) affect the liquid fraction of PCM in the horizontal heat exchanger. The same previous initial and boundary conditions were considered. The findings showed a clear correlation between the constant of the mushy zone and the time of PCM melting. Melting times increase as mushy zone constant values rise. The melting times are 182, 191, and 200 minutes for mushy zone constants of 10^5, 10^6, and 10^7, respectively. Depending on the above results, the constant for the mushy zone is set to 10^5.

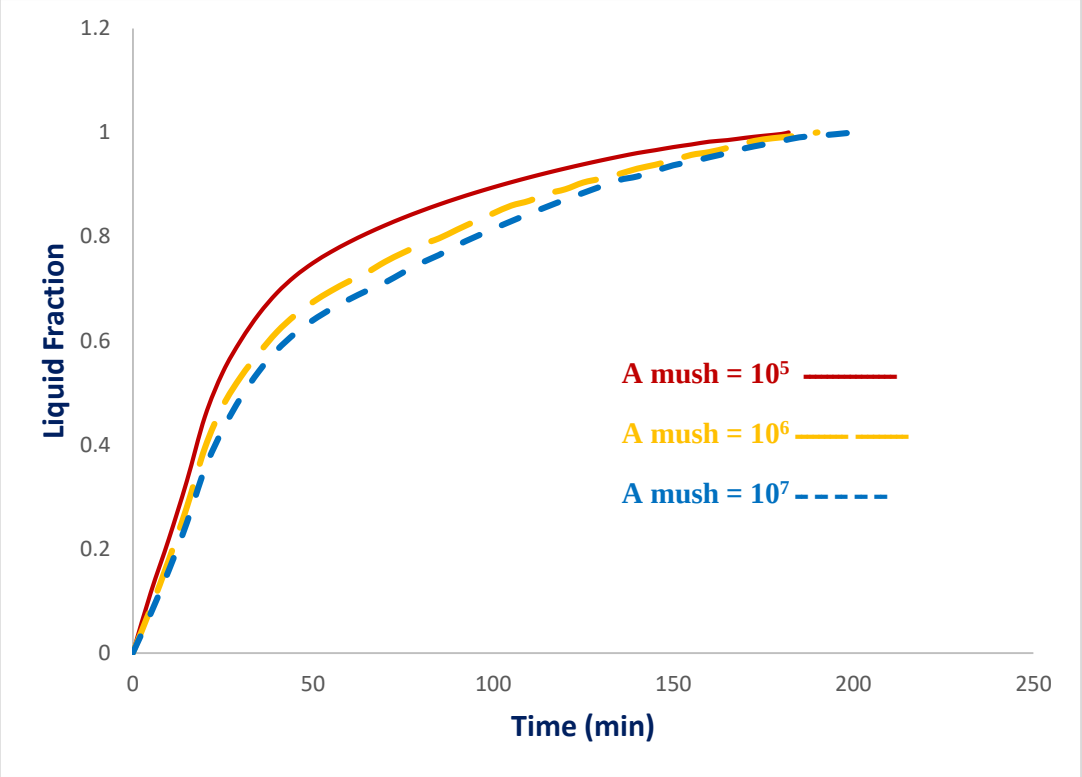

Fig. (3.9) independence test of mushy zone

CHAPTER FOUR
EXPERIMENTAL WORK

Chapter Four: Experimental Work

This chapter contains a comprehensive experimental work description performed to examine the thermal behavior of PCM melting inside circular annular cavities with different shapes of fins fixed to the interior tube of the thermal storage unit.

4.1 Experimental setup

The experimental setup includes assembling the device used to test the melting of PCM, which consists of parts whose details will be mentioned later, and recording all the practical results obtained from the test. The experimental facilities can be presented schematically and photographically in Fig. (4.1) and Fig (4.2), respectively.

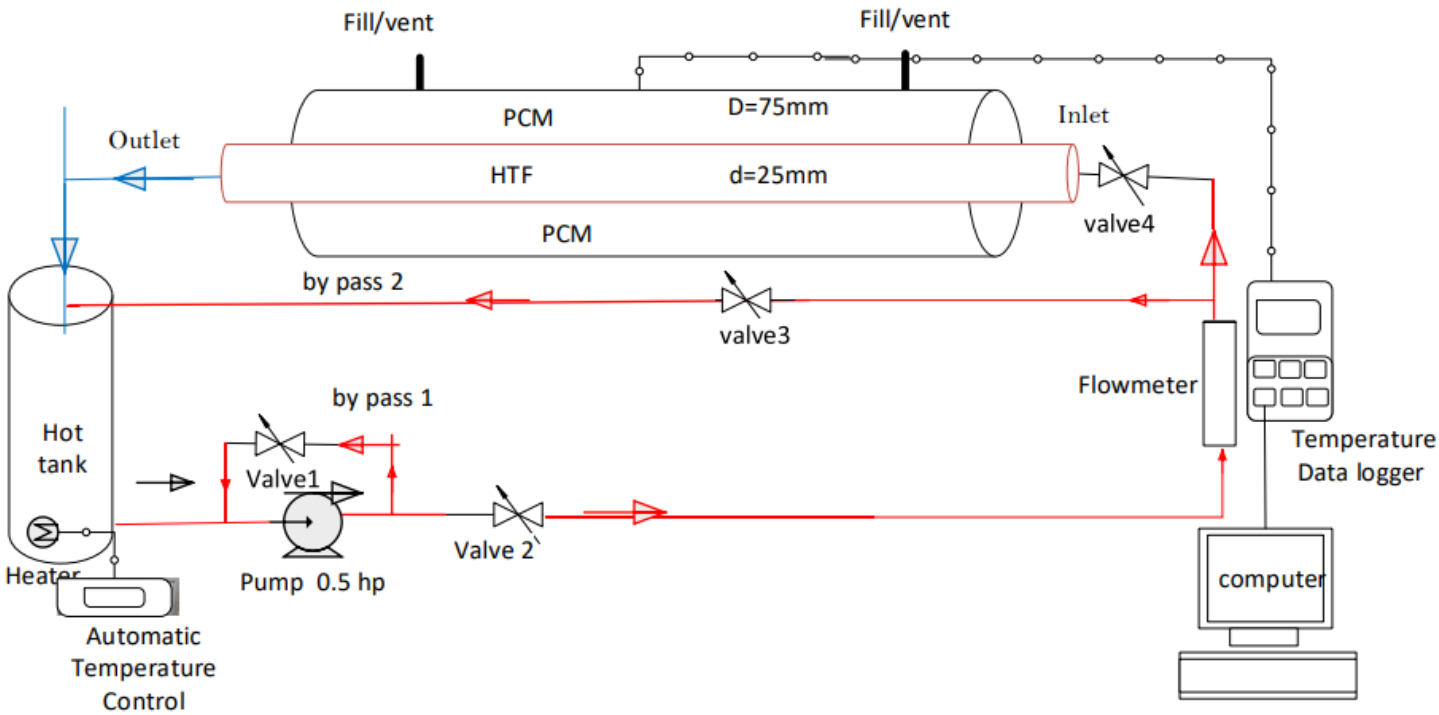

Fig. (4.1) Scheme of the experimental facilities.

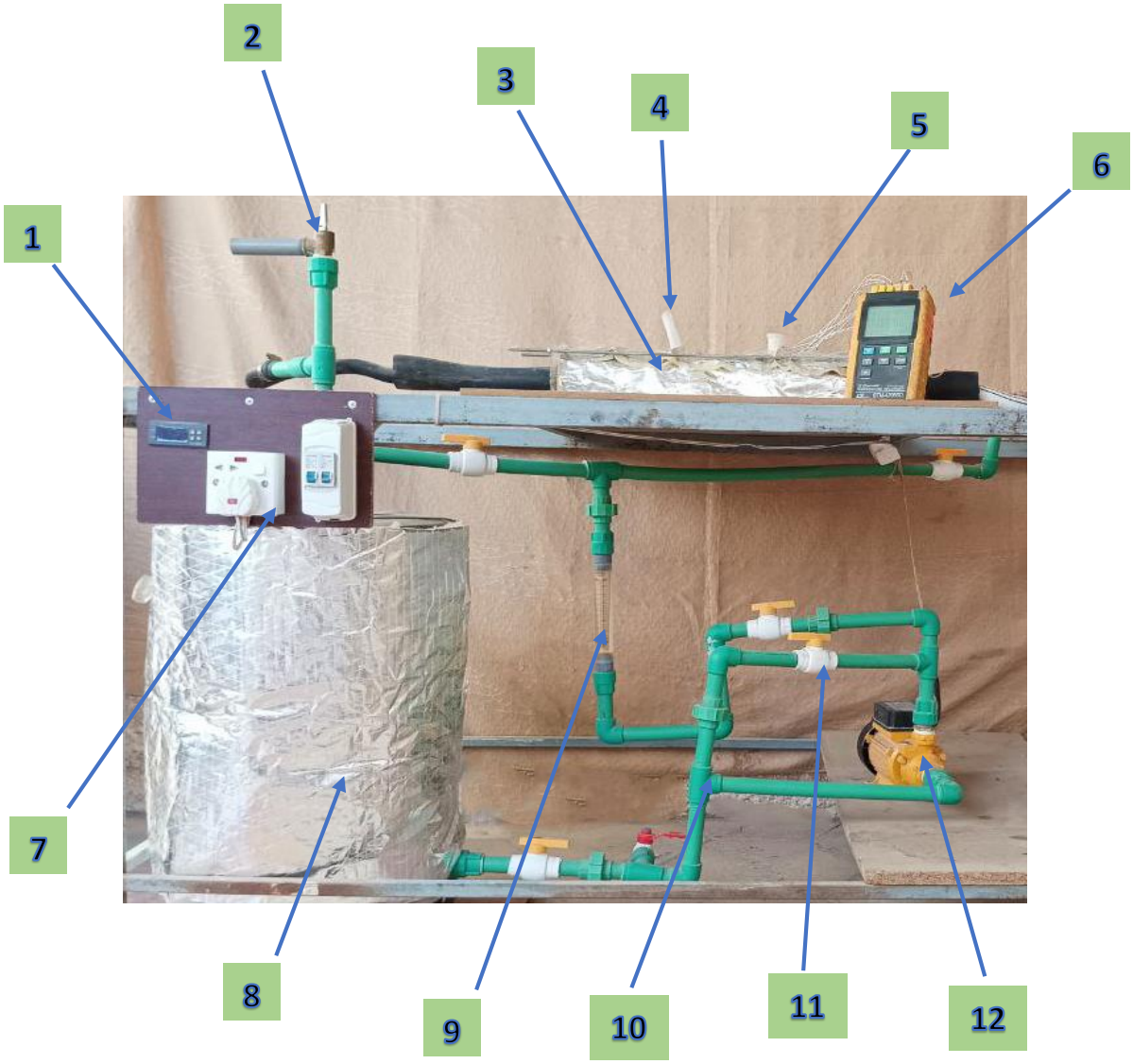

1. Automatic temperature controller; 2. Safety valve; 3. PCM-Heat exchanger; 4. Vent tube; 5. Fill tube; 6. Data logger; 7. electric control panel; 8. Water heater; 9. Flowmeter; 10. Pipes; 11. valve 12. Water pump

Fig. (4.2) Photo of the experimental facilities

4.2 The experimental apparatus's components

The experimental setup is composed of the following units:

1- Test Rig

2- Water heating unit

3- Digital thermostat

4- Heat transfer fluid pump

5- Flow meter for water

6- Data logger

7- Thermocouples

8- Valves

9- Digital camera

10- Piping system and other accessories

4.2.1 Test Rig

The test rig described in Figure (4.3), consists of the following:

1. A transparent plastic outer shell with a length of 500 mm, an inner diameter of 75 mm, and a thickness of 2.5 mm. The transparency of the plastic allows monitoring of the melting behavior of the PCM. The outer shell is wrapped with a 20 mm thick glass wool insulation layer to reduce heat leakage. The two holes are drilled to fill PCM fluid and accommodate any change in PCM volume during melting.

2. A 1000 mm long, 25 mm wide, and 0.9 mm thick copper inner tube used to transport the heat transfer fluid (water), where the thermal energy from the hot water causes the PCM to melt.

Three cases of the inner tube were used:

- Without fins

- Four longitudinal fins installed on the inner tube in the form of X- type

- Four longitudinal fins installed on the lower part of the inner tube

3- Two transparent square plastic covers with a thickness of 10 mm to seal the outer shell, equipped with rubber rings to prevent the leakage of PCM, as shown in figure (4.4).

4. The PCM material whose specifications are mentioned in Chapter 3.

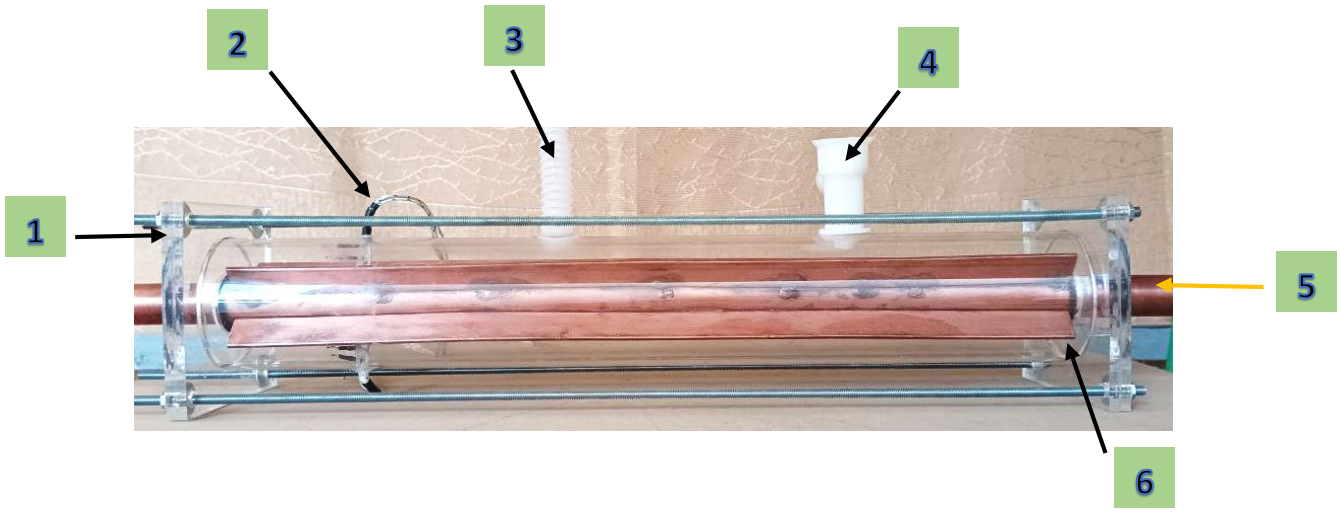

1. Square acrylic sheet; 2. Thermocouples; 3. Vent tube; 4. Fill tube; 5. Interior copper tube; 6. Outer acrylic shell

Fig. (4.3) Photo of the PCM annular cavity heat exchanger (test rig).

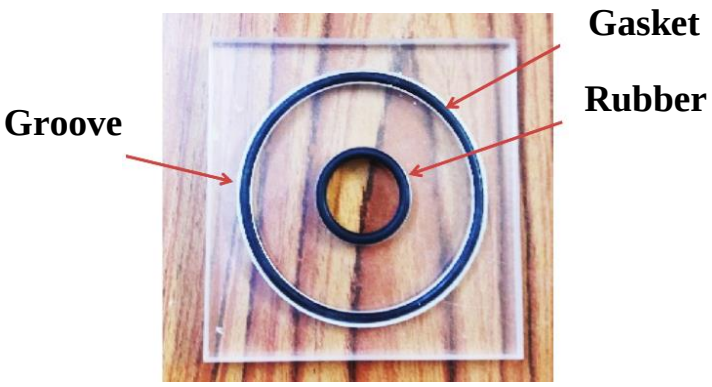

Fig. (4.4) Square acrylic sheet

4.2.2 Water heating unit

This unit is represented by a cylindrical container with capacity of 80 liters insulated with glass fiber, as shown in Figure (4.5). The tank is supplied with a 1500 -W electric heater to heat the water to the required temperature.

Fig. (4.5) Electric water heater

4.2.3 Digital thermostat

The digital thermostat includes a digital display that can be adjusted to the desired temperature (Figure (4.6)). In addition, an internal temperature sensor has been installed in the electric heater.

Fig. (4.6) Digital thermostat

4.2.4 Heat transfer fluid pump

The water pump (Figure (4.7)) is used to transfer hot water from the electric heater to the inner copper tube and then return it to the heater. It has a maximal discharge rate of 50 l/min, a head of 9 m, and an output of 0.5 horsepower.

Fig. (4.7) Water pump

4.2.5 Flowmeter

Water flow through the inner tube was measured using a flowmeter with a range of 2–18 l/min, as described in Fig. (4.8). Direct calibration of the flow meter has been done by using a scalar vessel as well as a stopwatch. The time required to fill the scalar vessel is

recorded. The process is repeated several times, and the calculated flow rates and measured values of the flow rates are shown in Fig (4.9).

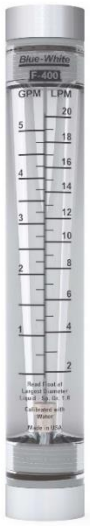

Fig. (4.8) The Flow meter

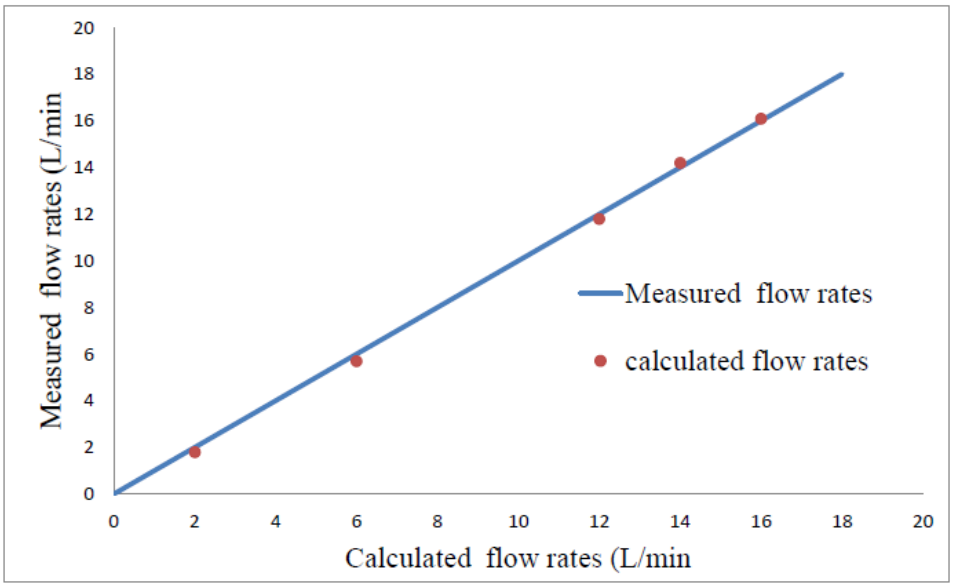

Fig. (4.9) Calibration of the Flow meter

4.2.6 Data logger

A twelve-channel temperature data recorder (Lutron BTM-42085SD) was used to record the temperatures.

4.2.7 Thermocouples

By using ten **k-type** thermocouples have a general temperature range of **(-200 to 1260°C)**, the thermal behavior of PCM melting was monitored. Two of them were used to measure both the inlet and outlet water temperatures, and the eight remaining were installed at different locations inside the test rig by means of a plastic rod to record PCM temperatures during melting at different times (Fig. (4.10)).

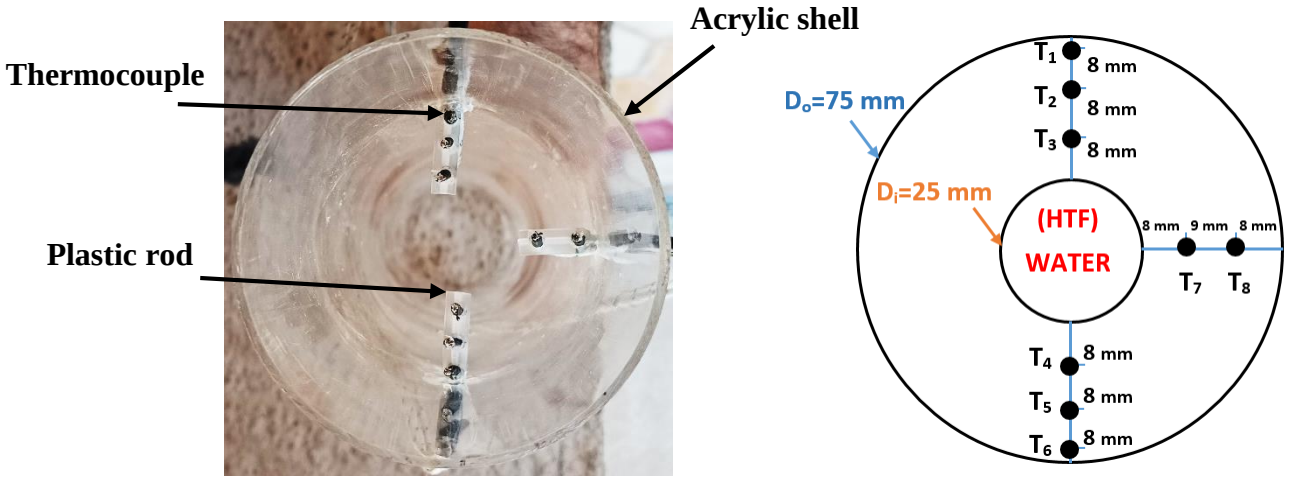

Fig. (4.10) The distribution of thermocouples

The thermocouple calibration procedure is detailed in appendix (B)

4.2.8 Valves

In order to control the direction and rate of water flow in the test device, four valves were used for this purpose.

4.2.9 Digital camera

In order to monitor the melting progress front, a digital camera was used, as represented in Fig. (4.11).

Fig. (4.11) The Digital camera

4.2.10 Piping system and other accessories

The water was transported by means of a network of PVC pipes. In addition, there is an electric control panel to control the water pump and the electric water heater.

4.3 PCM (phase change material RT-42)

Paraffin wax (RT-42) produced by the German company Rubitherm was used. The wax is white in its solid state, and it is clear in its liquid phase (Fig. (4.12)) (appendix A).

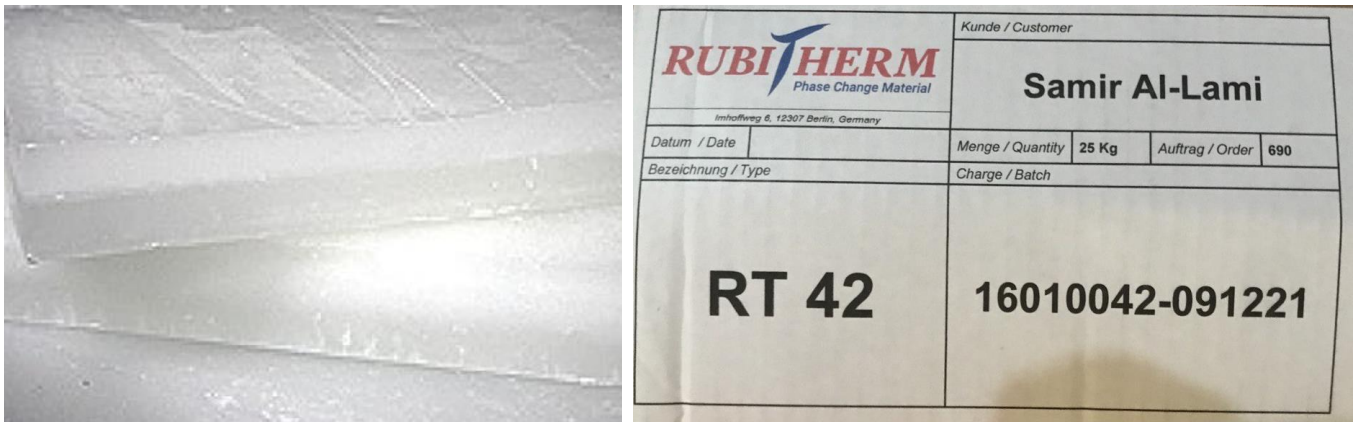

Fig. (4.12) photo of PCM

4.4 Procedure for Experimentation

In order to seal off any potential air leaks, the liquid PCM was poured in layer-by-layer via the annular vent. The filling process was completed in many steps, during which time the liquid PCM was allowed to solidify gradually. Before each test, the water supply was heated to a greater temperature than necessary to compensate for heat losses in the piping system. The bypass valve is shut off, and the intake valve to the storage unit is opened when the bypass temperature reaches the set point. All thermocouple readings were recorded, and the solid-liquid interface was photographed using a digital camera. The insulation layer was removed for a while to capture the photo of the melting interface. Three different HTF temperatures of 60, 70, and 80 ^{o}C were considered to determine their

effect on the melting process in various designs of the thermal energy storage heat exchanger.

4.5 The PCM's thermal energy storage

During the phase shift, the PCM absorbs both sensible and latent heats. The sum of these heats acts the thermal energy stored in the PCM. The following equation is used to estimate the amount of energy stored [3]:

$$Q_s = m_{pcm}\left[Cp_s\,(T_{avs} - T_i)\,(1 - f) + f\,L + f\,Cp_l\,(T_{avl} - T_i)\right] \ldots\ldots\ldots \textbf{(4.1)}$$

Where T_{avs}, T_{avl}, and T_i represent, the average solid and liquid temperatures, as well as the starting temperature, respectively. As f refers to the liquid-to-solid ratio, it may be considered as:

$$f = \frac{V_l}{V_s + V_l} \qquad \ldots \textbf{(4.2)}$$

V_s denotes the volume of solid PCM, while V_L represents the volume of molten PCM.

4.6 Uncertainty and Analysis of Errors

Uncertainties in measurement affect the accuracy of physical quantities. Repeated measurements show fluctuations in outcomes regardless of how well the environment is controlled. Maintaining variables that remain constant is unattainable. Furthermore, these devices are made with a certain level of accuracy, and the manner in which the scale is read with fractional approximations introduces additional sources of uncertainty. Therefore, methods may be used to reduce the mistake by conducting calibration procedures on the measuring instruments and minimizing the level of uncertainty. To

accurately determine the level of uncertainty, it is essential to provide appropriate references and identify the sources of uncertainty associated with each component. The assessment of mistakes has great importance in any experimental investigation. The approach outlined by Holman [50] was used to determine the uncertainty associated with each estimated variable.

Let's pretend R depends on a whole bunch of other stuff: x_1, x_2,... x_n. This leads to an uncertainty in W_R, which is:

$$w_R = \left[\left(\frac{\partial R}{\partial x_1} w_1\right)^2 + \left(\frac{\partial R}{\partial x_2} w_2\right)^2 + \cdots + \left(\frac{\partial R}{\partial x_n} w_n\right)^2\right]^{\frac{1}{2}} \quad \ldots\ldots. (4.3)$$

The uncertainty in the independent variables is denoted by w_1, w_2, ….., w_n.

For example, the uncertainty in calculating the energy stored (Eq. (4.1)) depends on the experimental errors that maybe happening in the independent parameters as given in Table (4.1).

Table (4.1) Uncertainties of independent parameters

Independent parameter	Uncertainty (w)
Temperature difference	± 0.38 °C
liquid fraction	± 0.25
The volume of solid and liquid PCM	± 0.003 m^3

4.7 Check for Repeatability

The degree to which two or more independent measurements of the same parameter provide the same or similar results is known as its repeatability or test-retest dependability. All measurements were taken within a certain period and done by the same person on the same equipment. The experiments were conducted for many days, and some were run at different times of the day. To examine the repeatability in a specific circumstance, the thermocouple readings of T5 were selected from the X-type fin heat

exchanger model with a constant inner tube temperature of 70 °C and three readings were taken (**Fig. (4.13)**). The differences between the three tests were rather small. However, there were three repetitions of each test, and the averages of the results were considered.

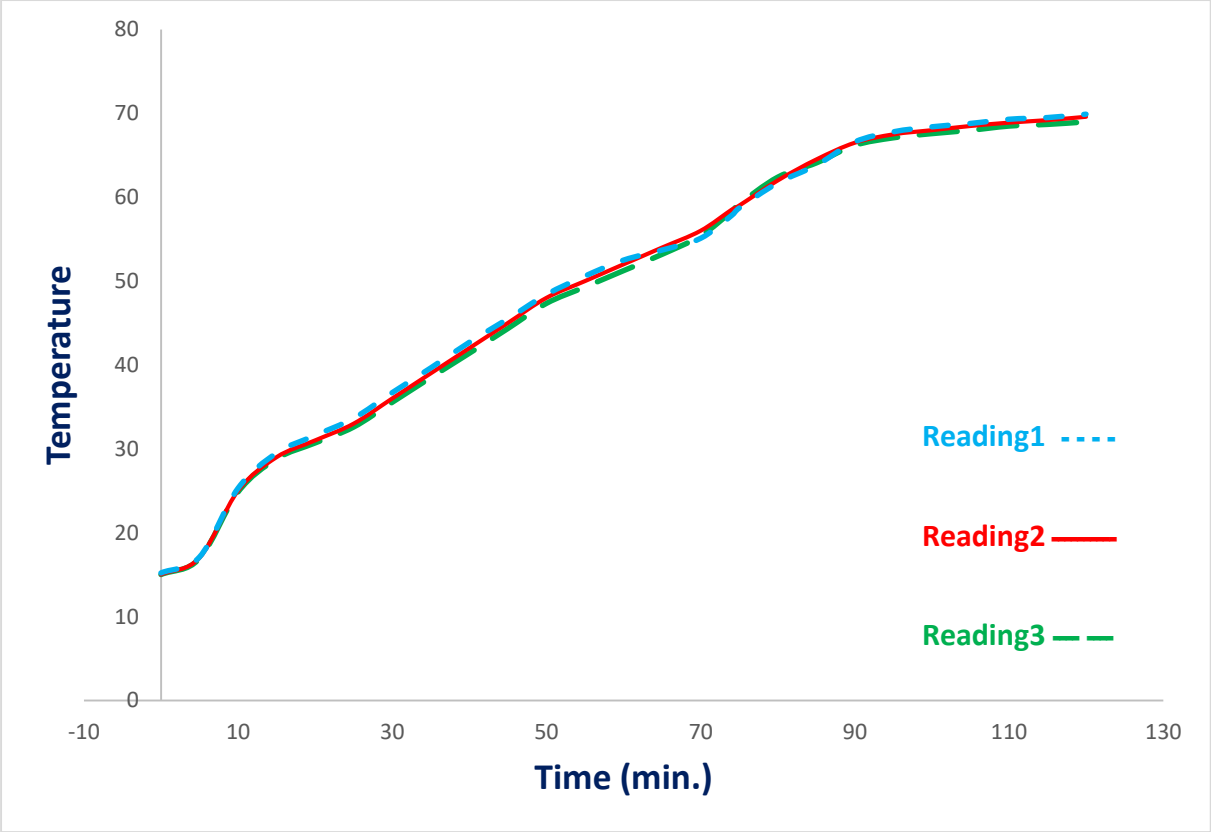

Fig. (4.13) Repeatability in temperature measurements of T_5

Chapter Five
Results and Discussion

Chapter Five: Results and Discussion

This chapter presents and discusses findings from experiments and numerical calculations related to the melting process of PCM (RT- 42) contained within an annular shell and a tube LHTES. The annular region is filled with PCM, while hot water at a required temperature is circulated through the inner tube to serve as the heat source for the melting process. There are three kinds of LHTES: without fins, four X-shape fins, and four below-type fins.

The experimental and numerical investigations were performed for three inlet HTF temperatures of 60, 70, and 80 ^{o}C. For fear of prolonging it, the results of 70 ^{o}C are exhibited because the trends of the results are similar for the three temperatures.

5.1 Temperature Distribution of PCM

The measured temperature distribution of thermocouples (TCs) within PCM of an unfinned unit is illustrated in **Fig. (5.1)** for a 70 ^{o}C as an inlet HTF temperature. It was shown that the readings of TC located in the upper part of the heat exchanger are subjected to natural convection. Therefore, high temperatures were registered, and some non-uniformity and perturbation in temperature are indicated (for example, TC3). The highest temperatures were recorded for TC1, TC2, and TC3, in the top part of the unit where natural convection dominated. In contrast, the minimum readings of temperature belonged to TC4, TC5, and TC6, in the lower part of the unit where conduction was dominant. After 250 minutes, the temperature of all TCs approached the steady-state conditions and approximated the HTF temperature.

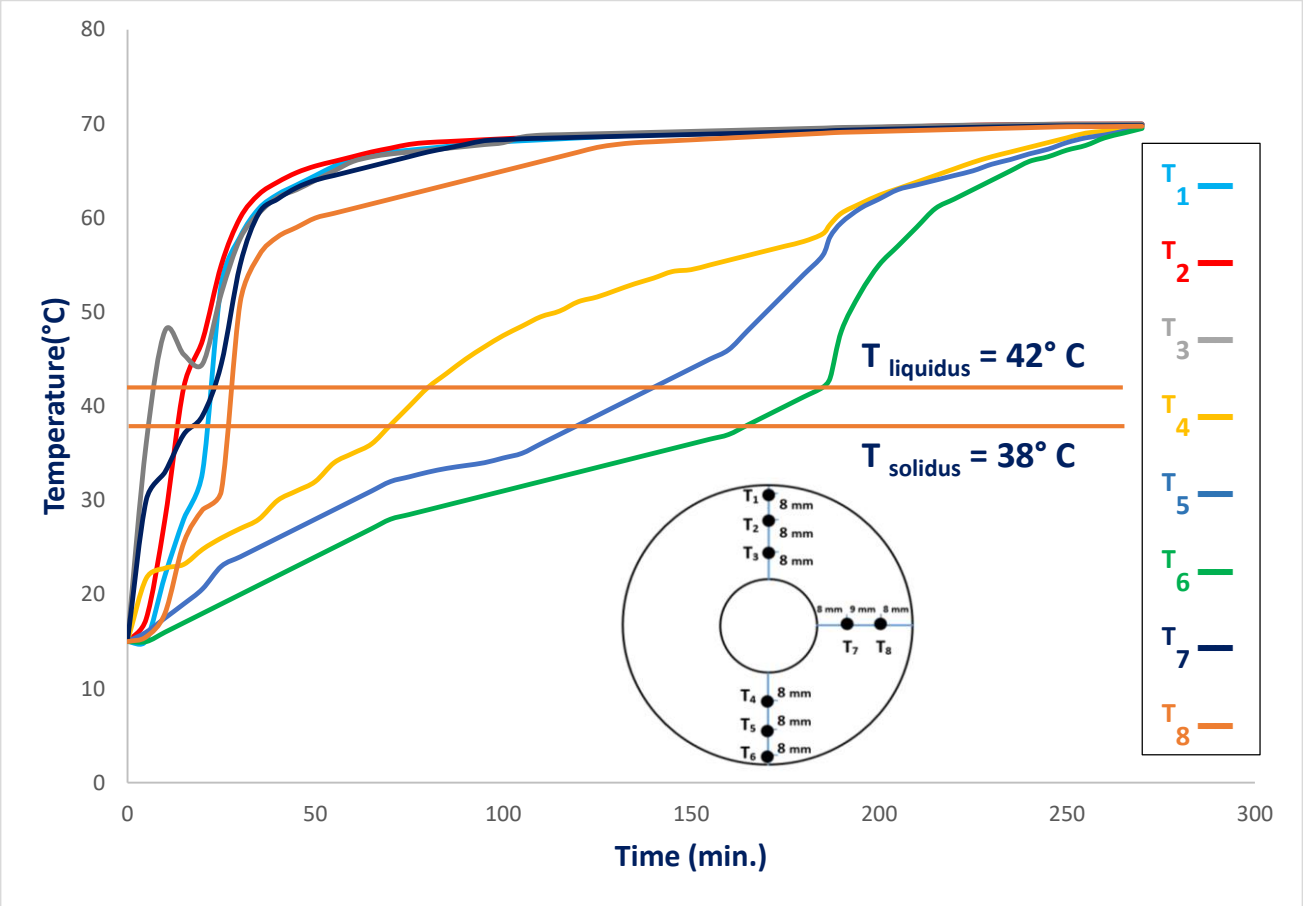

Fig. (5.1). The measured PCM temperature distribution within unfinned LHTES at 70 °C of inlet HTF temperature.

The PCM temperature readings with X-shape and below-fin distribution finned storage units at HTF inlet temperature of 70 ^{O}C are presented in **Fig. (5.2)** and **Fig. (5.3**), respectively. The results showed more uniform temperatures and no perturbation. By adding fins, the effective thermal conductivity of PCM increases, which leads to the efficient spreading of heat supplied from HTF across the entire PCM in the storage. This also reduces the time required to reach the steady-state condition. For X-distribution and below-distribution of fins, the PCM temperatures reached the steady-state values at approximately 120 min and 70 min, respectively.

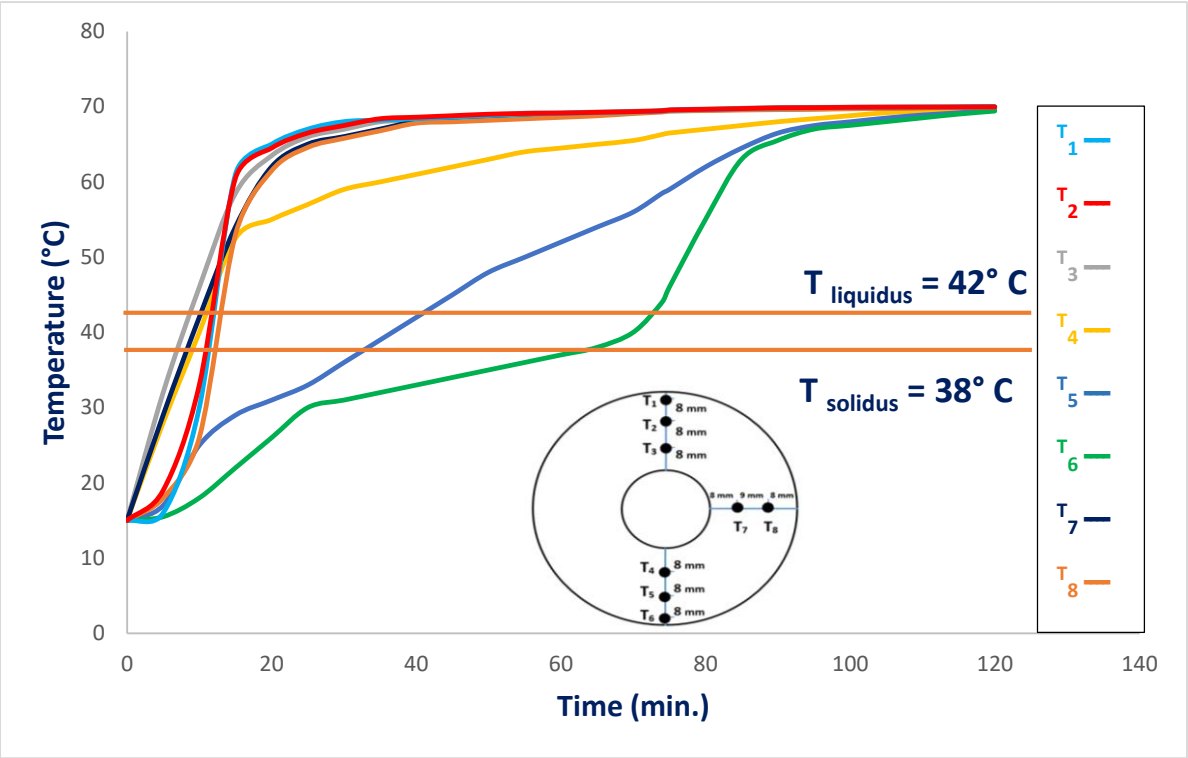

Fig. (5.2). The measured PCM temperature distribution within X-distribution finned LHTES at 70 °C of inlet HTF temperature.

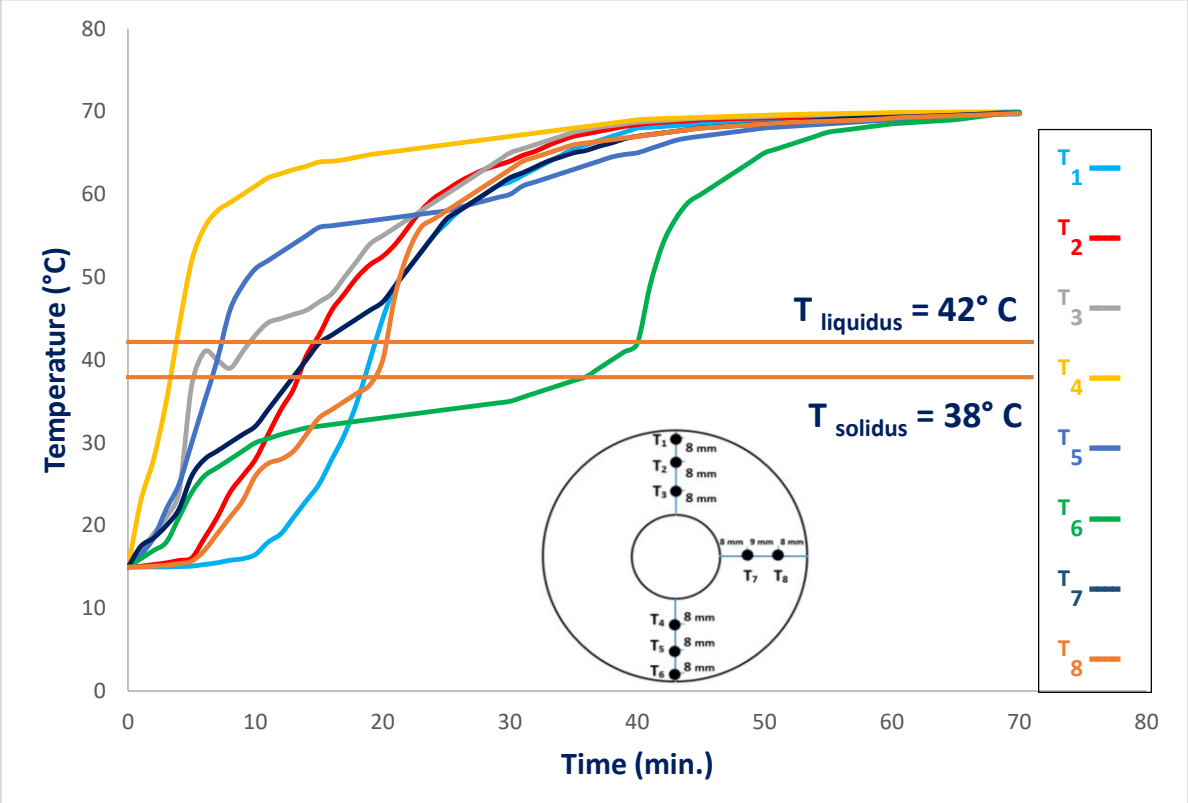

Fig. (5.3). The measured PCM temperature distribution within below-distribution finned LHTES at 70 °C of inlet HTF temperature.

The transient numerical values of PCM temperatures of unfinned, X-finned, and below-finned LHTES units are shown in **Fig. (5.4)**, **Fig. (5.5)**, and **Fig. (5.6)**, respectively. The temperature distribution exhibits the same trends as the measured temperature data. It can be shown that for the case without fins, the points located in the upper part of the heat exchanger are subject to natural convection. Therefore, the temperature distribution there is gradual and, at some points, irregular. For instance, at site T_3, temperatures rise, then fall, and then return to rise. As for the points close to the heat source (the inner tube) in the case without fins (T_3 and T_7) and the points located within the natural convection zone (T_1, T_2, T_8), the locations of the fastest melting and there is a rapid change in temperature there until the melting is complete. After that, the temperatures will be almost the same. As for the rest of the points located in the lower part, the melting is slow, and the change in temperature at the beginning of the melting is slight. As time progresses, the change is rapid as a result of the sensible heat from the liquid PCM.

In the case of using X-shaped fins, as shown in **Fig. (5.5)**, the temperature distribution will be more uniform due to the effect of the fins on the melting process, in addition to the effect of natural convection. All points quickly reach the melting point, except for the two points specified at the bottom of the heat exchanger, where melting is slow due to the weak effect of the fins and natural convection together.

When utilizing the below-fin distribution, as displayed in **Fig. (5.6)**, When utilizing the below-fin distribution, as displayed in Figure 5.6, the temperature distribution in the upper portion of the heat exchanger tends to be gradual and uneven at some points due to the unique effect of natural convection on the melting process in that area. On the other hand, in the lower half, the effect of the fins is evident, and the gradient of the points situated near the hot inner tube (T4 and T5) is steep, resulting in the PCM melting rapidly in these areas. However, the point near the bottom wall is the slowest melting point due to the significantly weakened effect of the fins and natural convection.

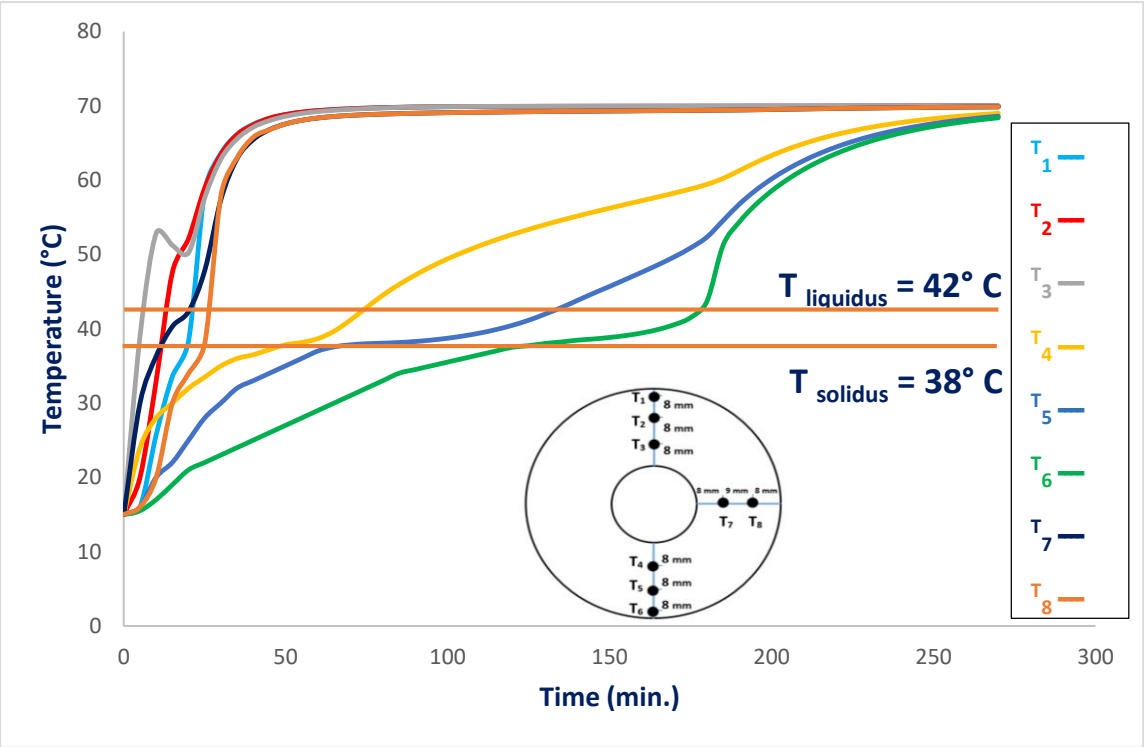

Fig. (5.4). The numerical PCM temperature distribution within unfinned LHTES at 70 °C of inlet HTF temperature.

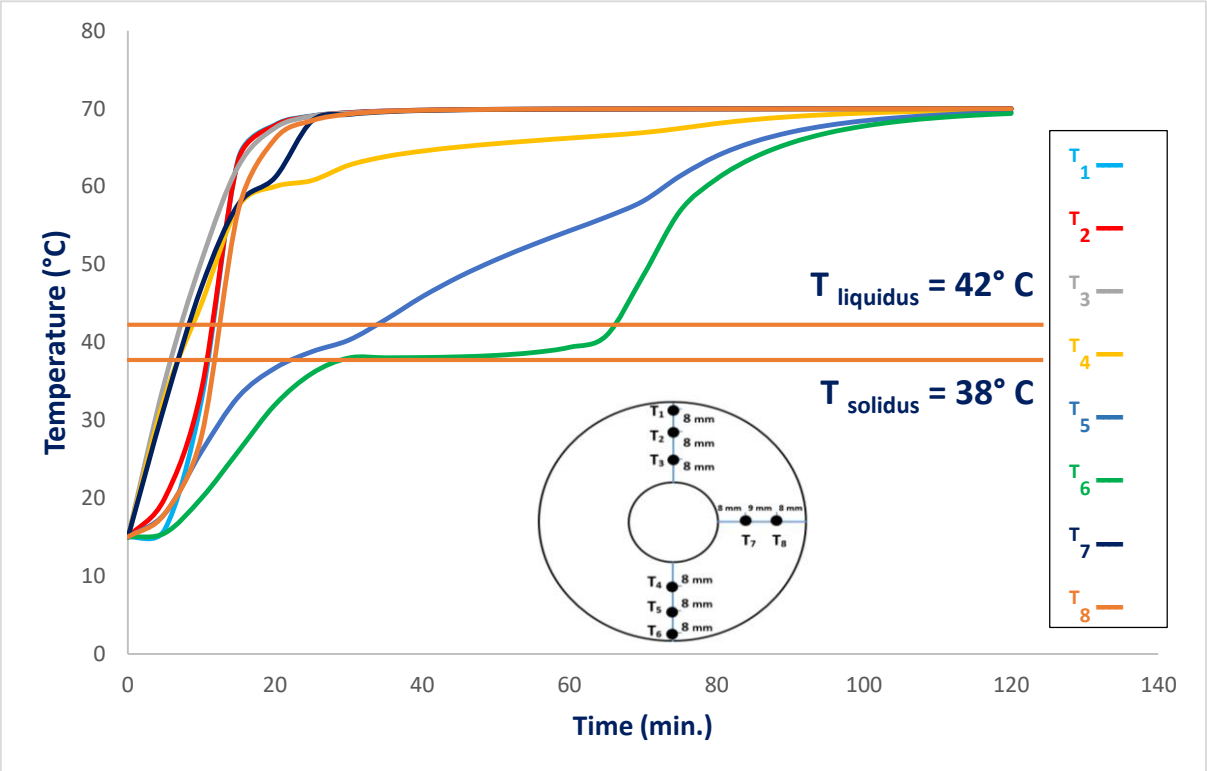

Fig. (5.5). The numerical PCM temperature distribution within X-finned LHTES at 70 °C of inlet HTF temperature.

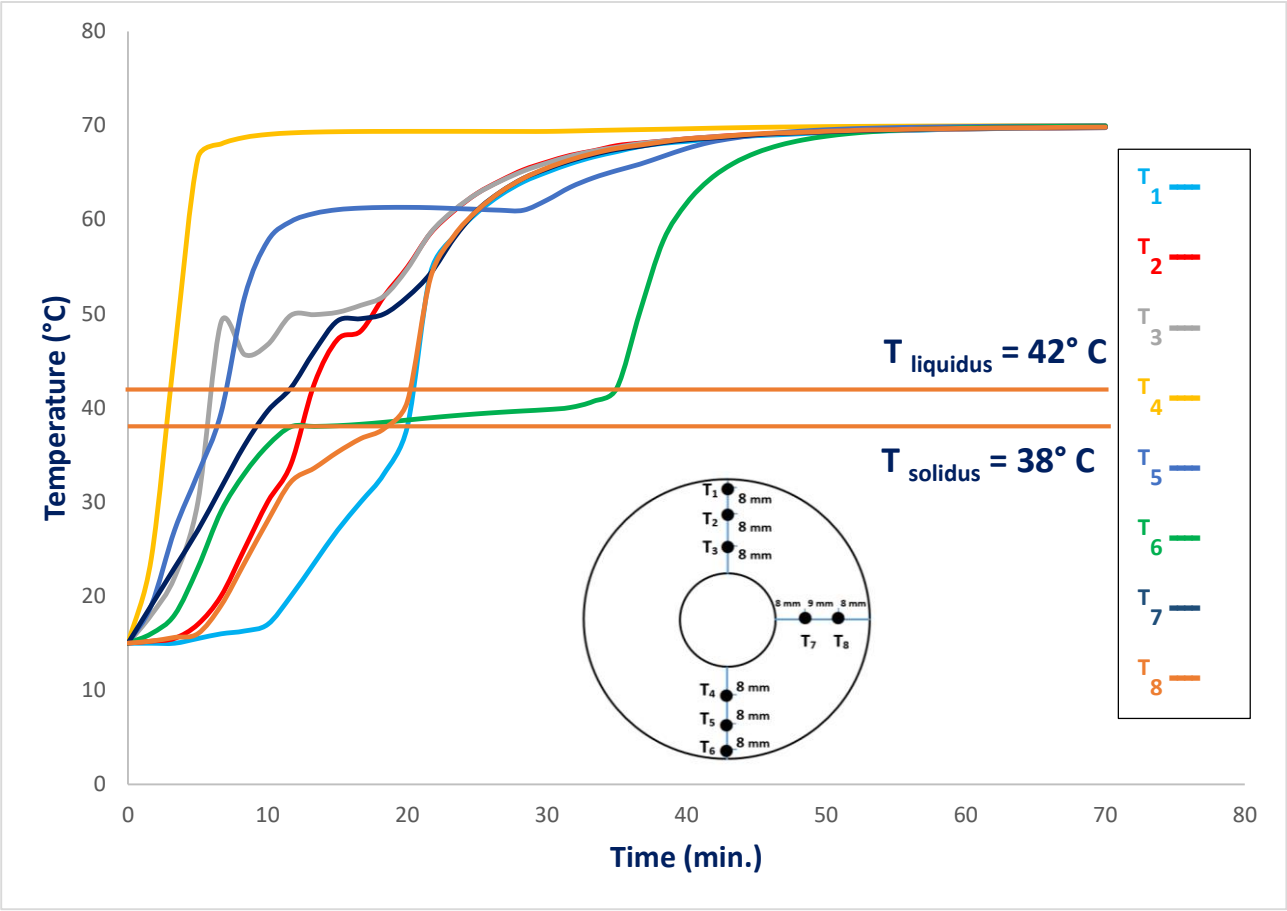

Fig. (5.6). The numerical PCM temperature distribution within below-finned LHTES at 70 °C of inlet HTF temperature.

The comparisons between the numerical values and measurements of PCM temperatures within unfinned, X-finned, and below-finned storage units are presented in **Fig. (5.7)**, **Fig. (5.8)**, and **Fig. (5.9)**, respectively. The selected temperatures are T_2, T_5 and T_8. The results indicate that the numerical findings align closely with the experimental data. However, it appears that the numerical values of temperature are slightly higher than the measured data. The possible reasons for this inconsistency in findings are:

1. Heat dissipation during the experiments must be taken into account.

2. It is necessary to consider mathematical assumptions to facilitate numerical investigation.

3. Thermophysical properties of PCM depend on temperature, but they have been ignored in the numerical model.

4. There might be a difference in the boundary conditions imposed during the experiments and the numerical investigation.

5- Measurement errors and uncertainties caused by the devices.

6- The precision of the installation of the test device units.

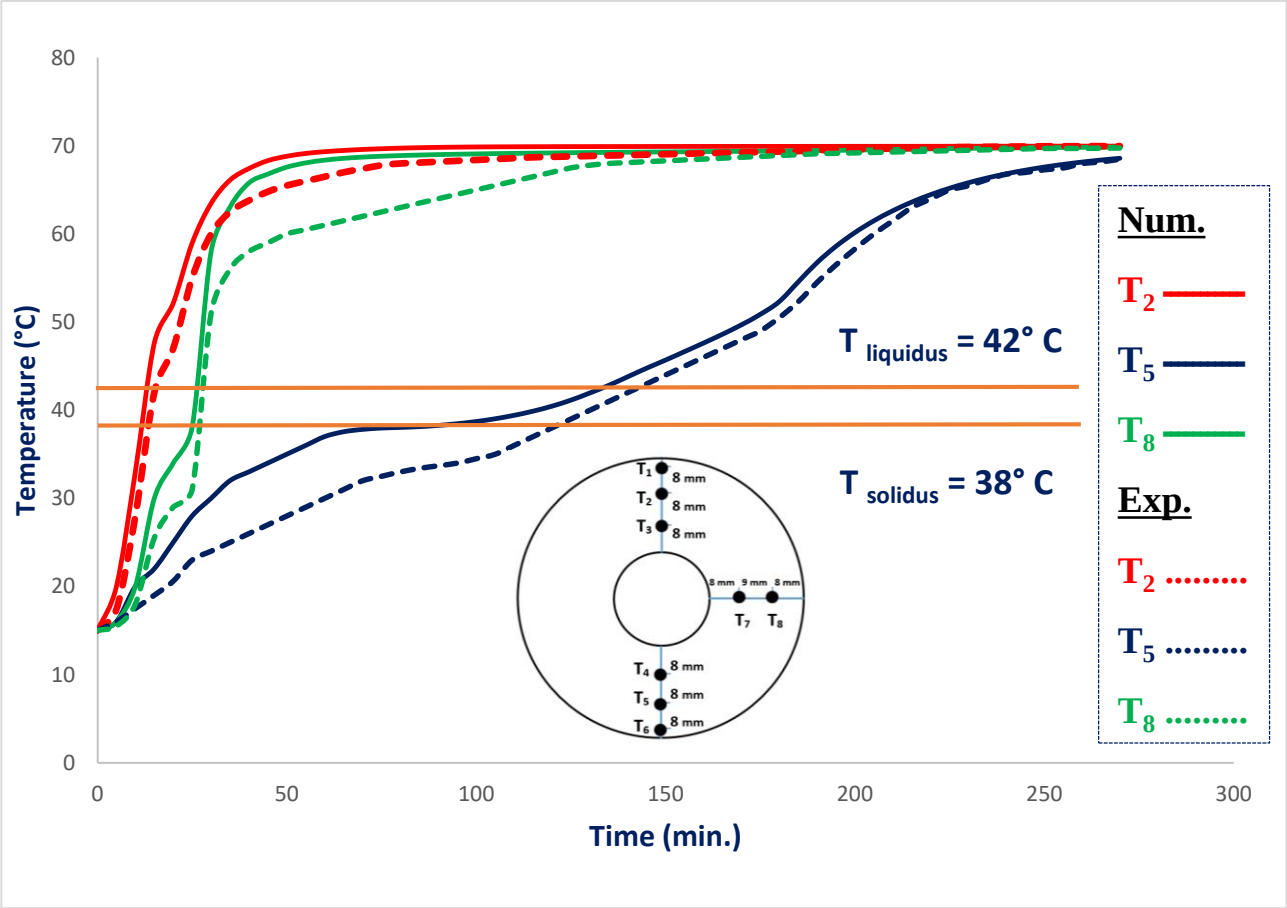

Fig. (5.7). Comparison between numerical & measured temperatures distribution for (T_2, T_5, T_8) of PCM in unfinned storage unit at 70 °C of inlet HTF temperature.

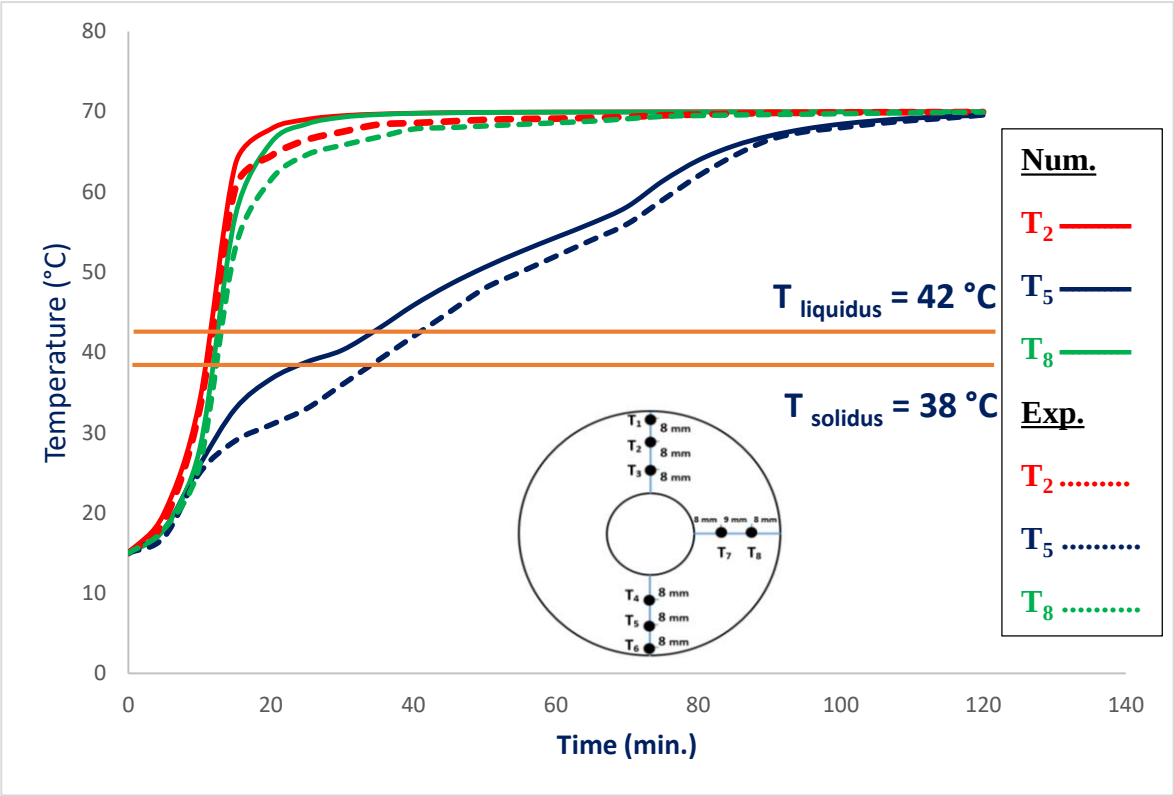

Fig. (5.8). Comparison between numerical & measured temperatures distribution for (T_2, T_5, T_8) of PCM in X-finned storage unit at 70 °C of inlet HTF temperature.

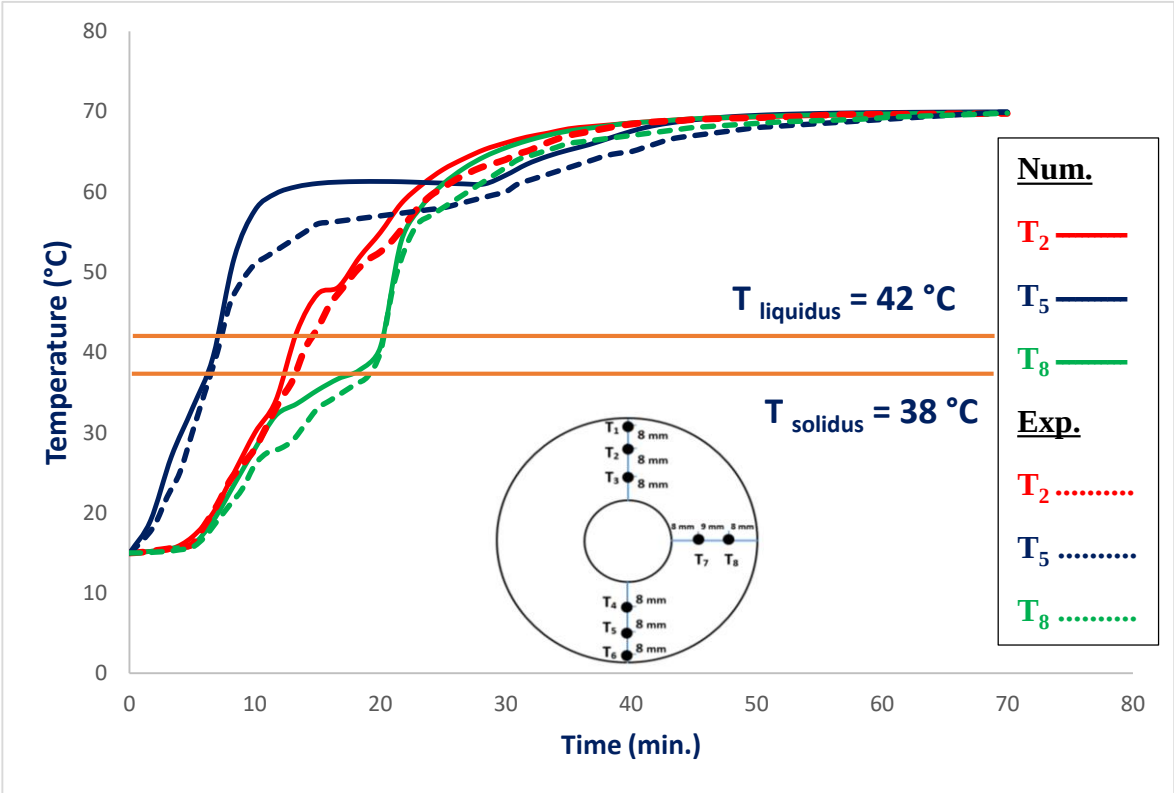

Fig. (5.9). Comparison between numerical & measured temperatures distribution (T_2, T_5, T_8) of PCM in below-finned storage unit at 70 °C of inlet HTF temperature.

In order to demonstrate the effect of adding fins on reducing the melting time of PCM in the site with the most delayed melting, which is site T_6, a comparison was made, shown in fig. (5.10), temperature distribution of site T_6 for numerical results of the three cases (Without fins, 4X-type fins, and 4 below-type fins).

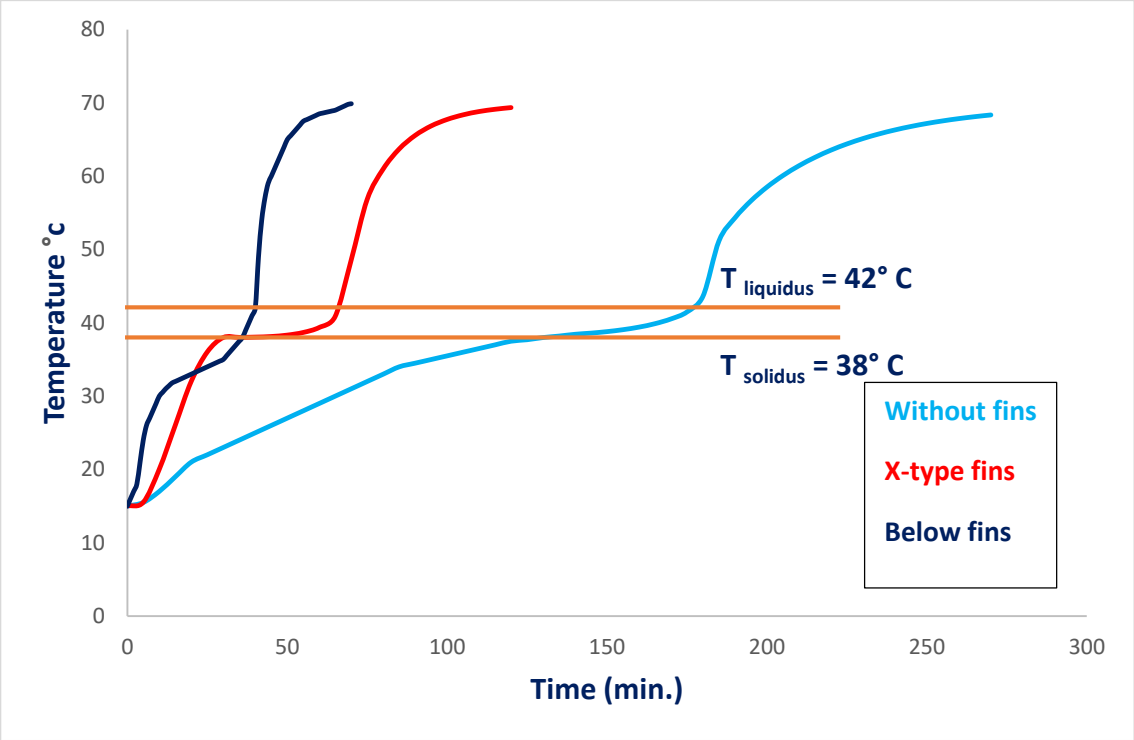

Fig. (5.10) comparison of temperature distribution of site T_6 for numerical results of the three cases (Without fins, 4X-type fins, and 4 below-type fins) at 70 °C of inlet HTF temperature

5.2 Progress of solid-liquid front

The progress of the solid-liquid interface during PCM melting is an important factor to consider. In **Fig. (5.11),** a photographic illustration of the melting process as it progresses over time is illustrated for three different types of horizontal heat exchangers (Without fins, 4X-type fins, and 4 below-type fins) at an inner wall temperature of 70 °C. The experimental findings revealed that the melting front is parallel to the heated surfaces of the inner tube in the unfinned unit and to the inner tube and fine surfaces for finned units. This behaviour is justified due to the conduction is dominated at the early periods

of the melting process. Later, the strength of the natural convection is enhanced, and the melting rate is higher in the upper part of the unit. In contrast, the lower part is dominated by conduction. Therefore, the overheating and low melting issues are observed at the upper part and lower part, respectively, of unfinned unit. However, these issues are mitigated, and the overall melting rate is enhanced by inserting fins. After 30 minutes of melting, the PCM was 58%, 90%, and 97% melted for the unfinned, X-finned, and below-finned thermal storage units, respectively.

The numerical predicted results of the PCM melting front inside unfinned and finned thermal storage units are explained in **Fig. (5.12)** at 70 °C of HTF temperature. The same trend of the experimental results is indicated. It appears from the results above that for the case without fins, the melting of the PCM begins in the first minutes in a circular form on the wall of the hot inner tube as a result of the transfer of heat from the wall to the PCM through thermal conduction. As time progresses, natural convection dominates the melting process, especially in the upper part, while in the lower part of the unit, the melting of PCM is delayed for a long time. The result of adding fins to the system is to improve heat transfer to the PCM and reduce melting time. It is observed that using four X-type fins, the natural convection, and fins control the melting of PCM, and inserting fins treated the low melting to some extent in the lower part of the heat exchanger. By adding four below-type fins, the melting process was further improved so that natural convection dominated the melting process in the upper part, while the fins played a major role in melting the PCM in the lower part and treated the poor melting in the lower area. From the first minutes, the melting of a large percentage of PCM. After 30 minutes from the start of melting, only about 60% of the PCM has melted in the case without fins, while more than 92% of the PCM has melted with the introduction of X-shaped fins. The below-type fins result in approximately 98% of the PCM melting.

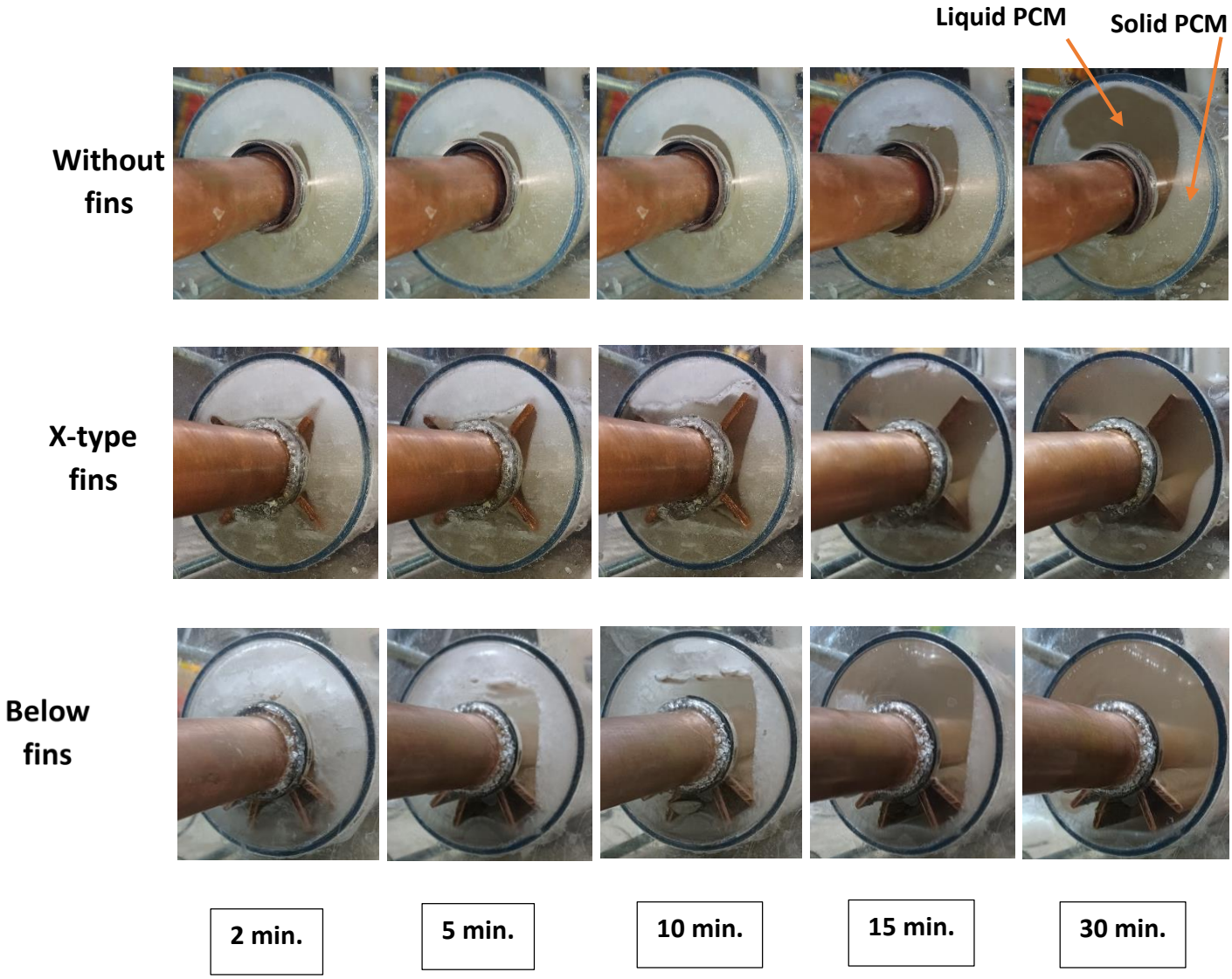

Fig. (5.11). Photographic illustration of melting front of unfinned, X-finned, and 4-blow finned storage unit at 70 °C of inlet HTF temperature.

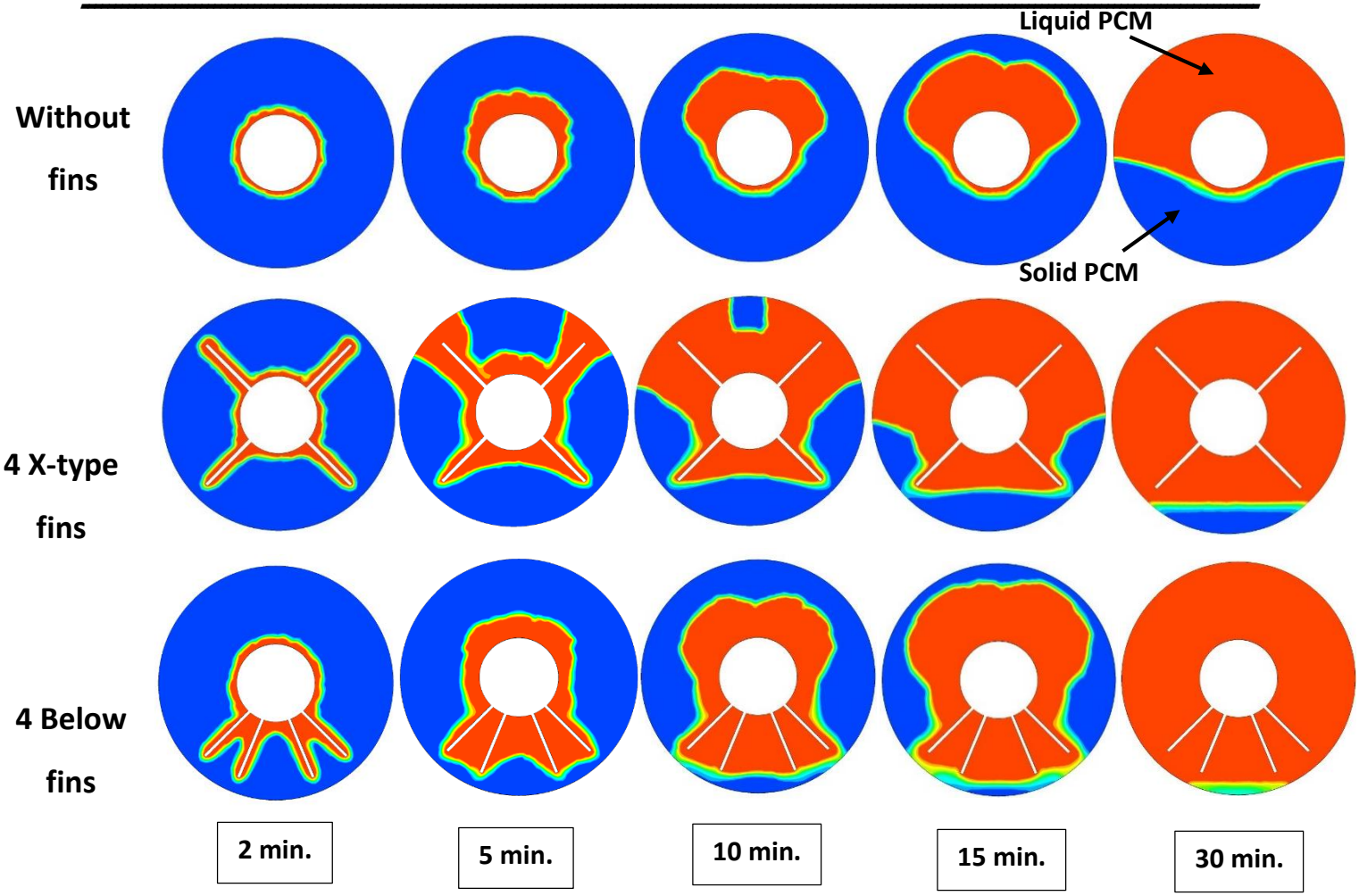

Fig. (5.12). Numerical progress of melting front of unfinned, X-finned, and 4-blow finned storage unit at 70 °C of inlet HTF temperature.

The comparisons of the experimental and numerical results of melting progress are shown in **Figures (5.13), (5.14), and (5.15)** for unfinned, X-finned, and below-finned thermal storage units, respectively. It can be observed that the computational melting interface advances at a faster rate than the experimental one. This difference can be attributed to the same reasons mentioned in section 5.1.

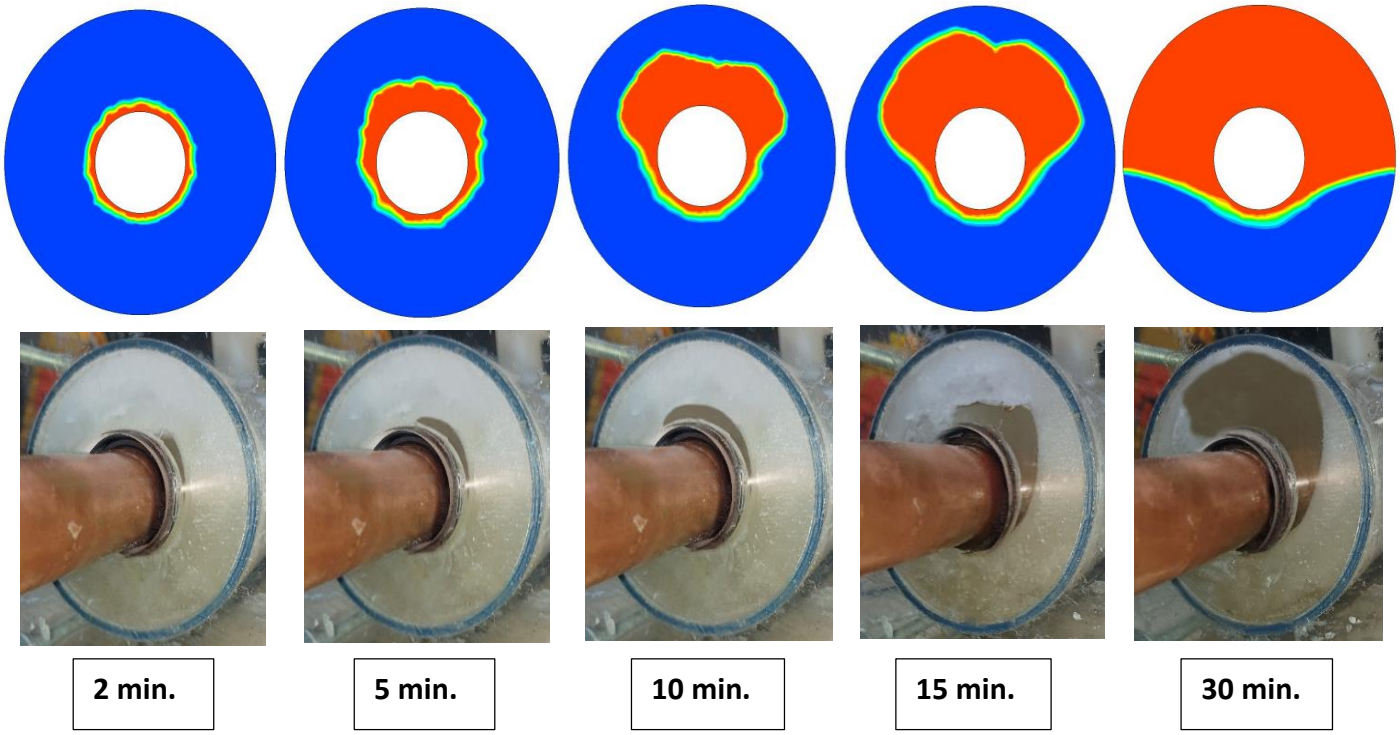

Fig. (5.13). Comparison between numerical and experimental PCM melting progress of without fins heat exchanger

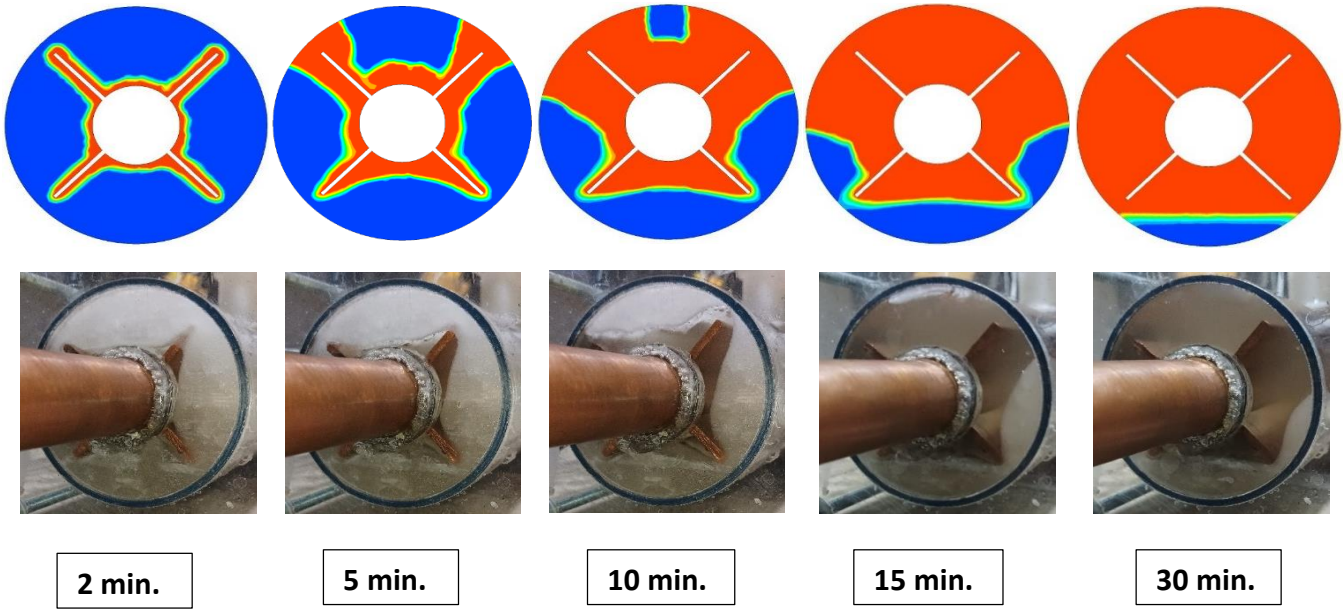

Fig. (5.14). Comparison between numerical and experimental PCM melting progress of X-type fins heat exchanger

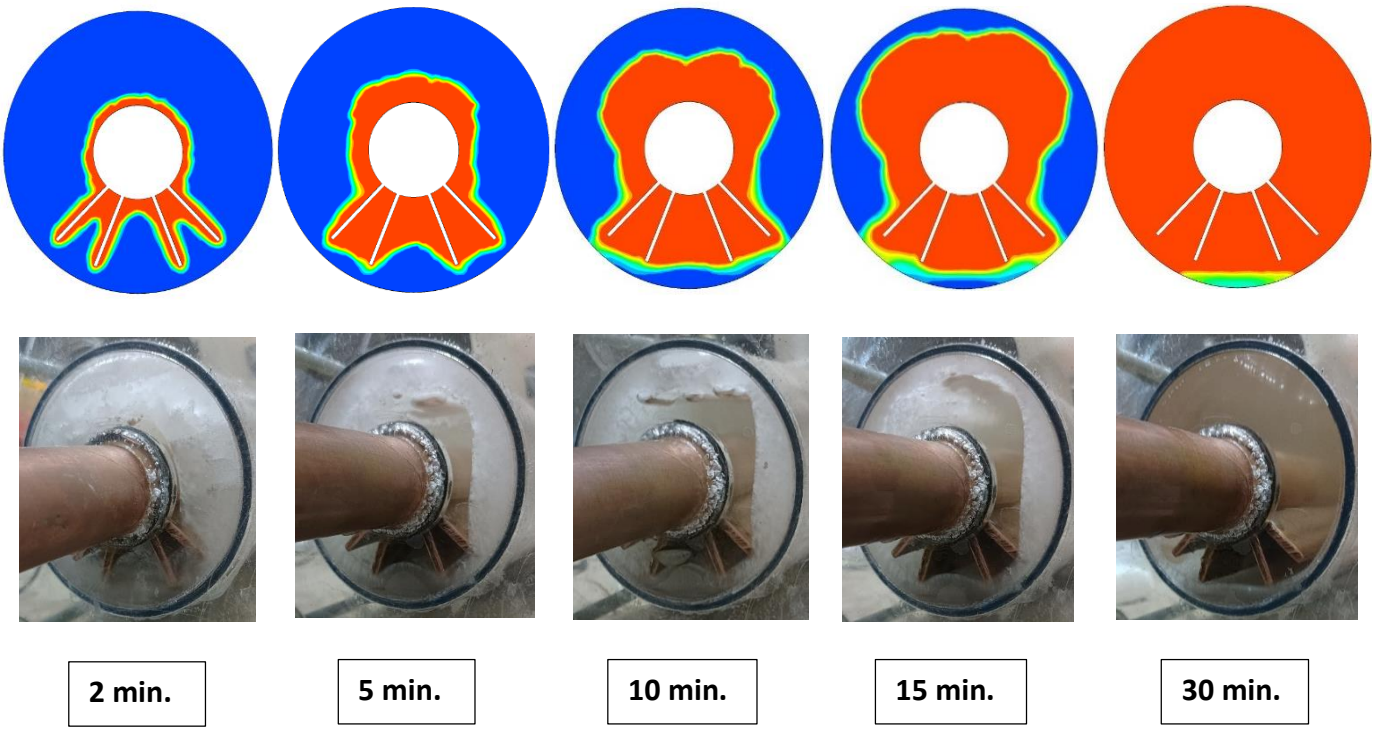

Fig. (5.15). Comparison between numerical and experimental PCM melting progress of below-fins heat exchanger.

5.3 Predicted temperature contours of PCM

The predicted results of the temperature contours for PCM inside a horizontal annular cavity of three cases of the heat exchanger at 70 °C of inlet HTF temperature are presented in Fig. (5.16). The melting begins when the PCM temperature reaches the melting point. The molten PCM formed around the hot tub due to the predominant conduction heat transfer. Then, the buoyancy-driven convection has been developed, and PCM liquid ascends upward, leading to a higher melting rate at the upper part of the cavity. The melting rate at the bottom portion of the cavity takes longer than the upper part. This problem can be addressed using fins, and the melting can be accelerated.

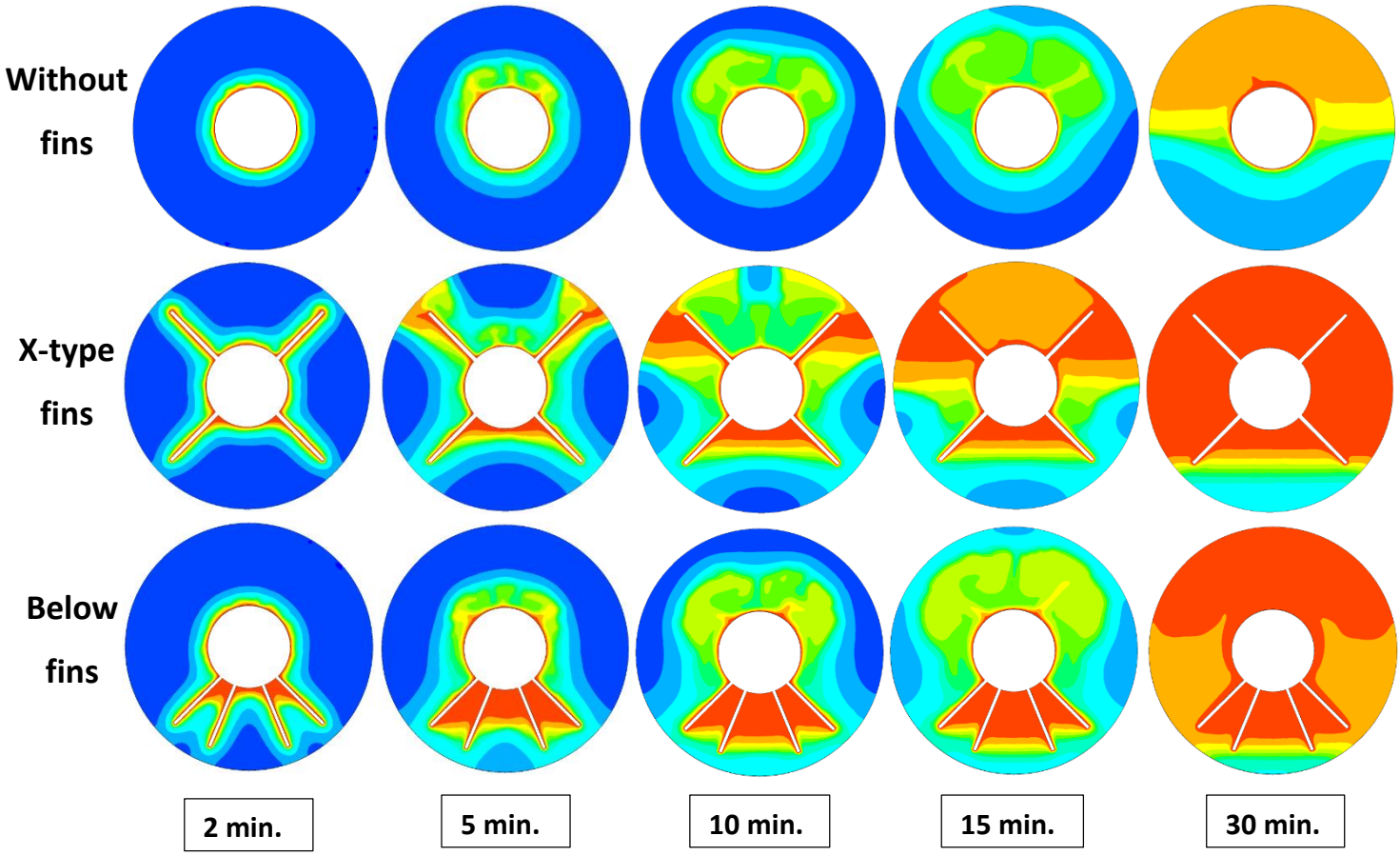

Fig. (5.16). Temperature contours of PCM of unfinned, X-finned, and 4-blow finned storage unit at 70 °C of inlet HTF temperature.

5.4 The velocity vector of the PCM melt

Fig. (5.17) presents the velocity vector for PCM inside a horizontal annular cavity of three cases of the heat exchanger at 70 °C of inlet HTF temperature. At the initial times, there was no generation or movement of PCM liquid. Later, a simple movement around the inner tube is generated at the start of the melting process, causing a layer of liquid PCM under the conduction control. After a while, the velocity vector of liquid PCM increases, and the hot, low-density liquid moves toward the top part of the cell due to the buoyancy effect. The liquid velocity is slow in the lower part, where conduction is dominant in the case of a heat exchanger without fins. The fins have a clear effect by increasing the velocity of the molten PCM at the bottom of the heat exchanger.

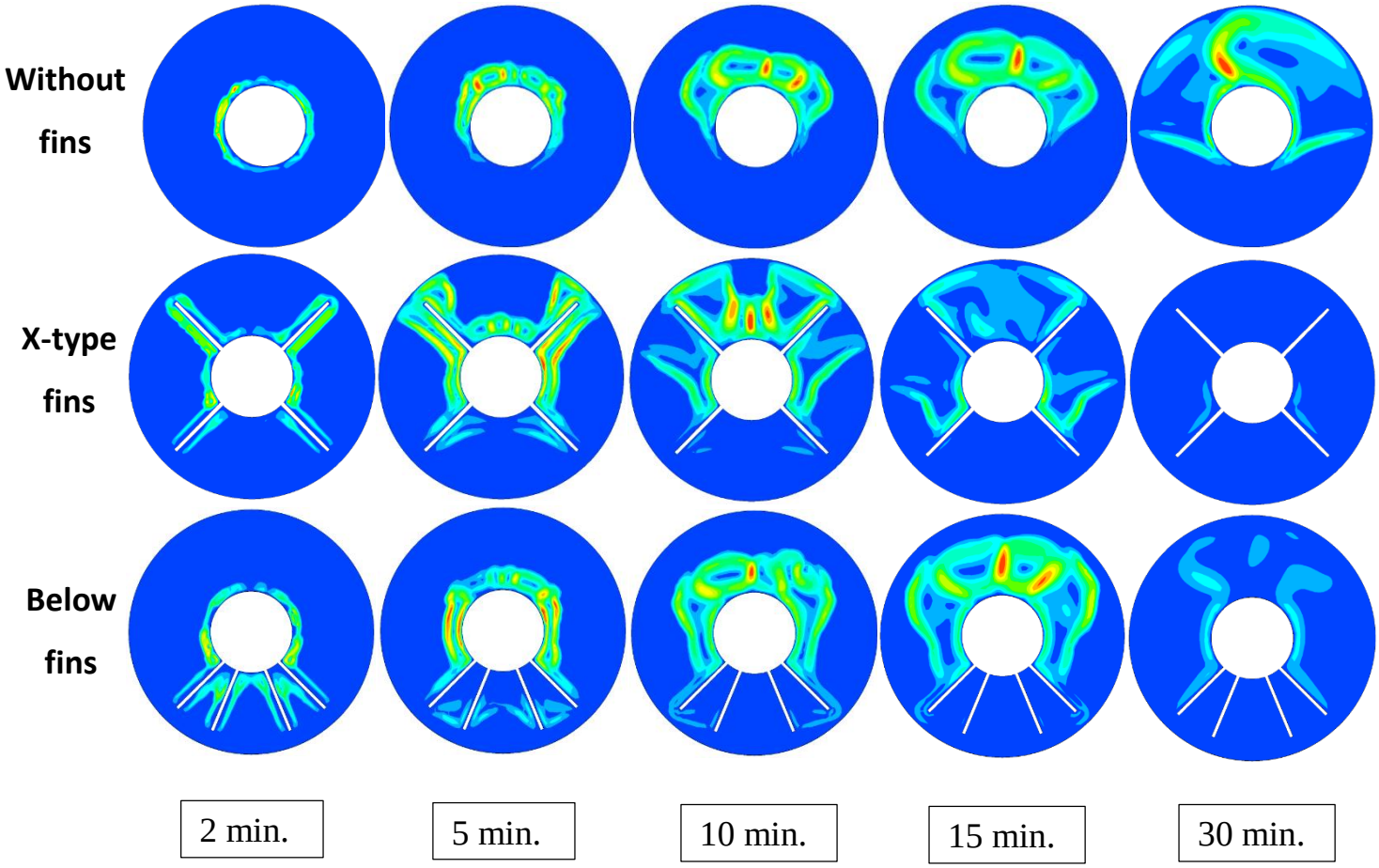

Fig. (5.17). Velocity contours of PCM of unfinned, X-finned, and 4-blow finned storage unit at 70 °C of inlet HTF temperature.

5.5 The liquid fraction

The liquid (or melt) fraction represents the amount of melted PCM divided by the total amount of the PCM. The experimental findings and numerical results of the liquid fraction for unfinned, X-finned, and below-finned thermal storage units are explained in **Fig. (5.18)** and **Fig. (5.19)**, respectively, for an inlet HTF temperature of 70 ^{o}C. It is noted that the rate of melt fraction is high initially due to the conduction dominating the charging process. Then, the rate of melting is decreased due to the thermal resistance of the liquid layer that impedes the exchange of heat between the HTF and PCM.

Inserting the fins enhances the effective thermal conductivity of PCM and accelerates the charging process. It is clear that the experimental melting time is reduced

by 78% and 60% by using a thermal storage unit with 4 below-type fins and 4 X-type fins, respectively, compared to the heat exchanger without fins. The numerical results indicate that the melting time is reduced by 79.6 % and 62.56 % by using a below-finned unit type and X-finned unit, respectively, compared to the unfinned unit.

The comparison of experimental and numerical melt fractions for unfinned and finned thermal storage units is presented in **Fig. (5.20)**. It is worth noting that the difference between experimental and numerical liquid fractions is 92.68%, 94.6%, and 97.32% for the three cases (4 below-type fins, 4 X-type fins, and without fins), respectively.

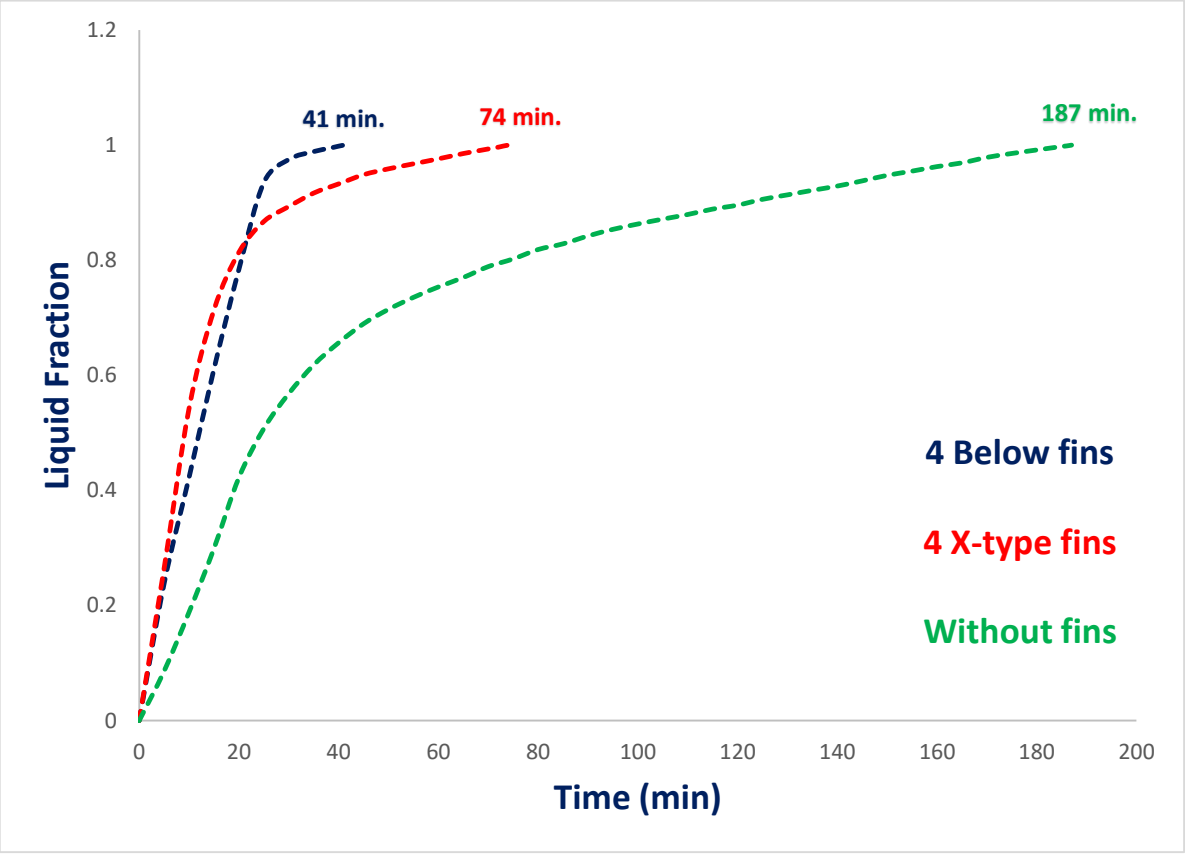

Fig. (5.18). Experimental temporal liquid fraction for unfinned and finned thermal storage unit at 70 °C of inlet HTF temperature.

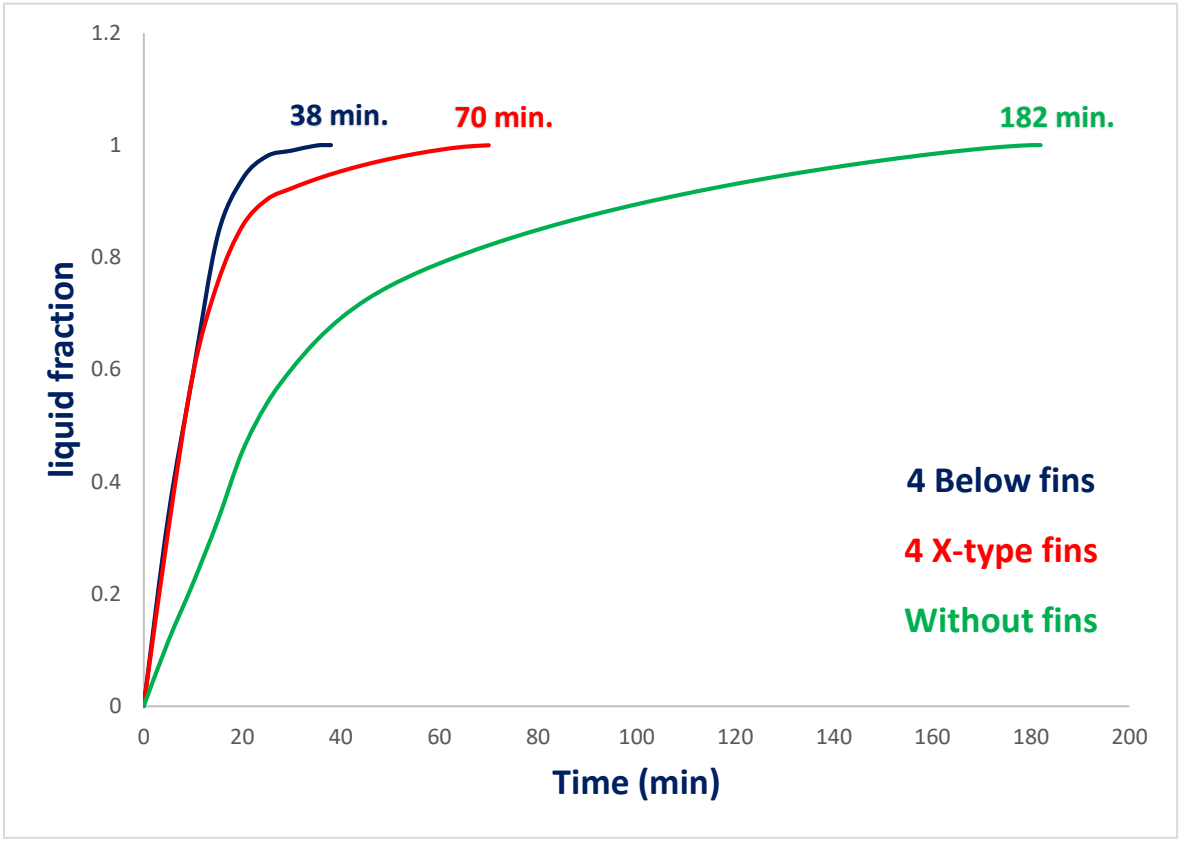

Fig. (5.19). Numerical temporal liquid fraction for unfinned and finned thermal storage unit at 70 °C of inlet HTF temperature.

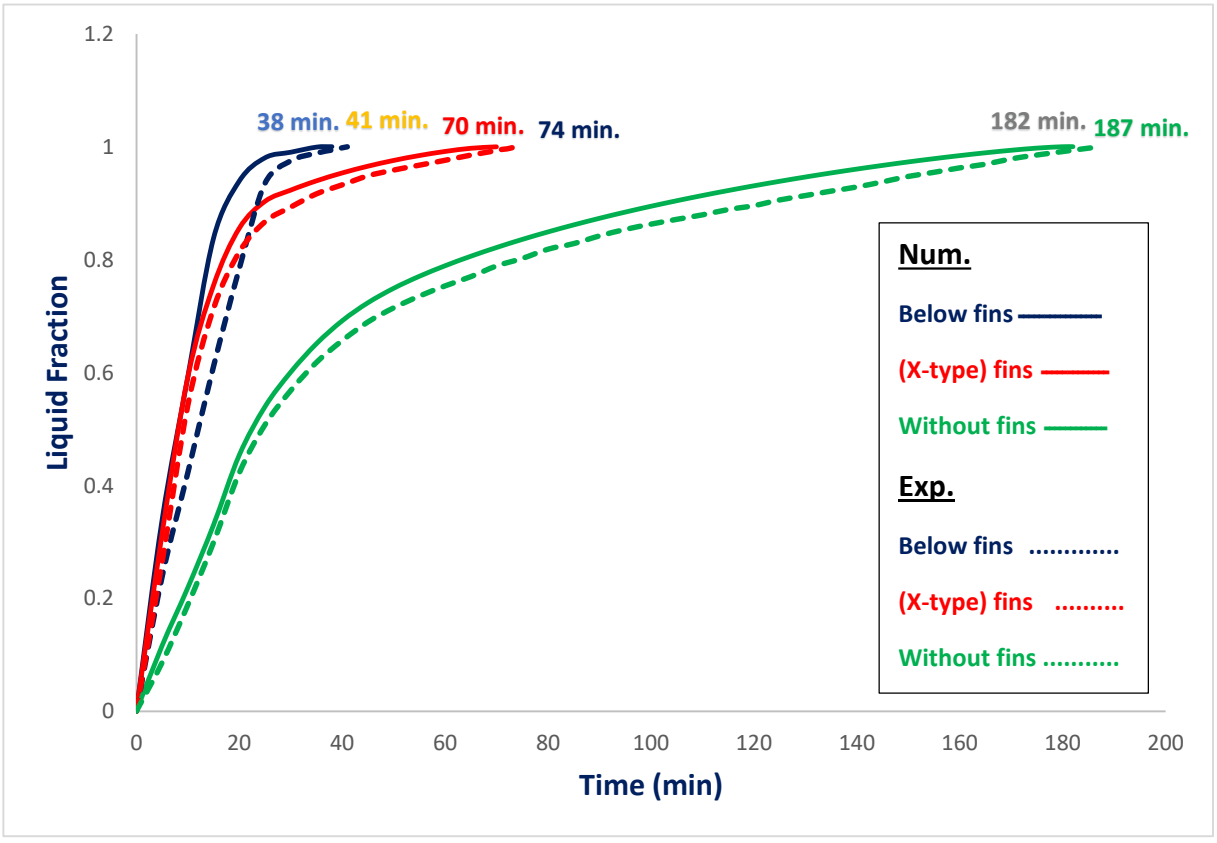

Fig. (5.20). Comparison between numerical and experimental liquid fractions for unfinned and finned thermal storage unit at 70 °C of inlet HTF temperature.

The influence of the temperature of inlet HTF on the numerical values of melt fraction of unfinned, X-finned, and below-finned LHTES units is explained in **Fig. (5.21), Fig. (5.22),** and **Fig. (5.23)**, respectively. It is shown that there is a significant effect of the water inlet temperature on the melting time. By increasing the water inlet temperature in all three cases, the amount of heat transferred from the inner tube, the source of heat supply, to the PCM increases, which leads to a reduction in the melting time.

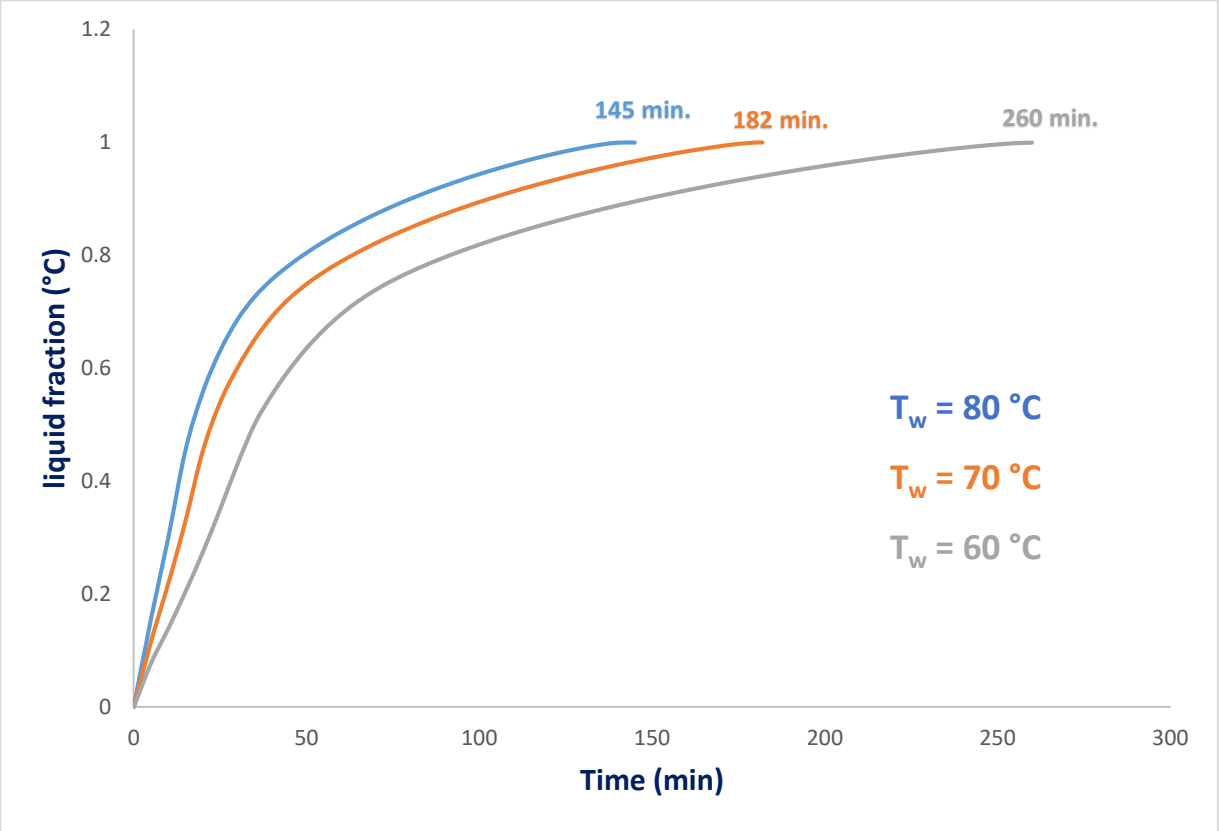

Fig. (5.21). Effect of inlet HTF temperatures on the numerical liquid fractions for unfinned thermal storage unit.

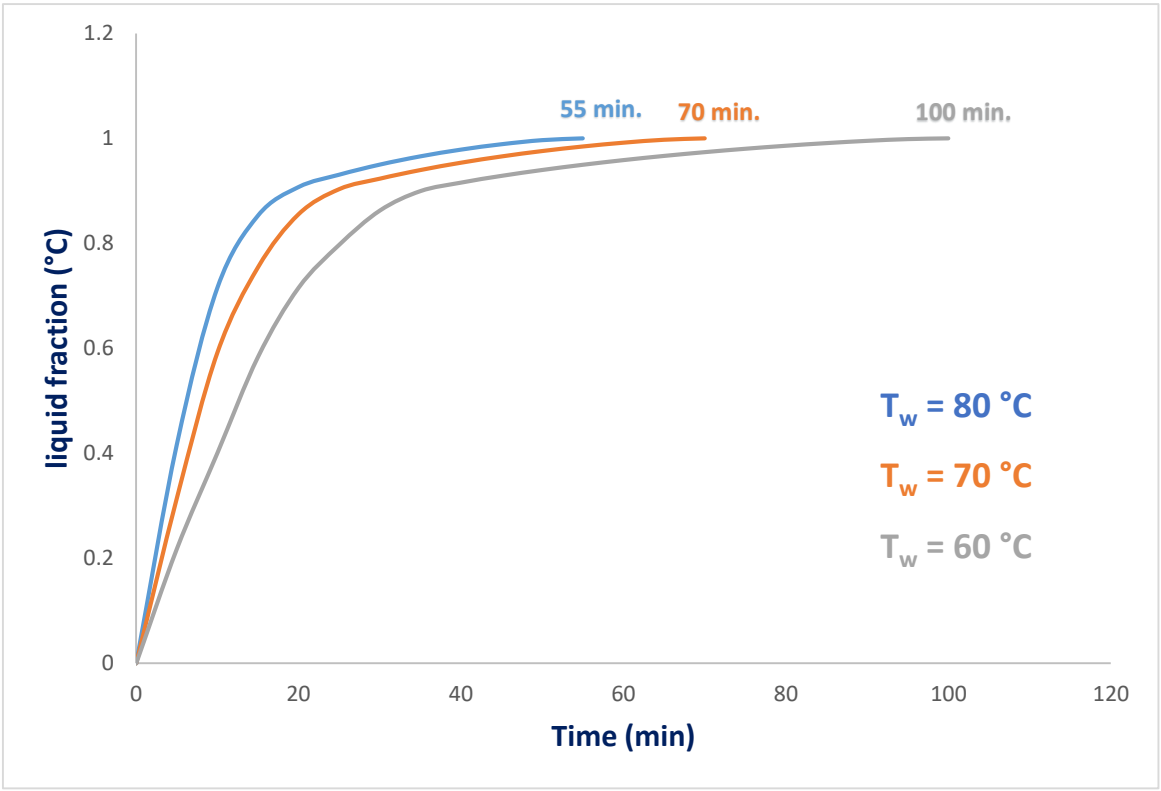

Fig. (5.22). Effect of inlet HTF temperatures on the numerical liquid fractions for X-finned thermal storage unit.

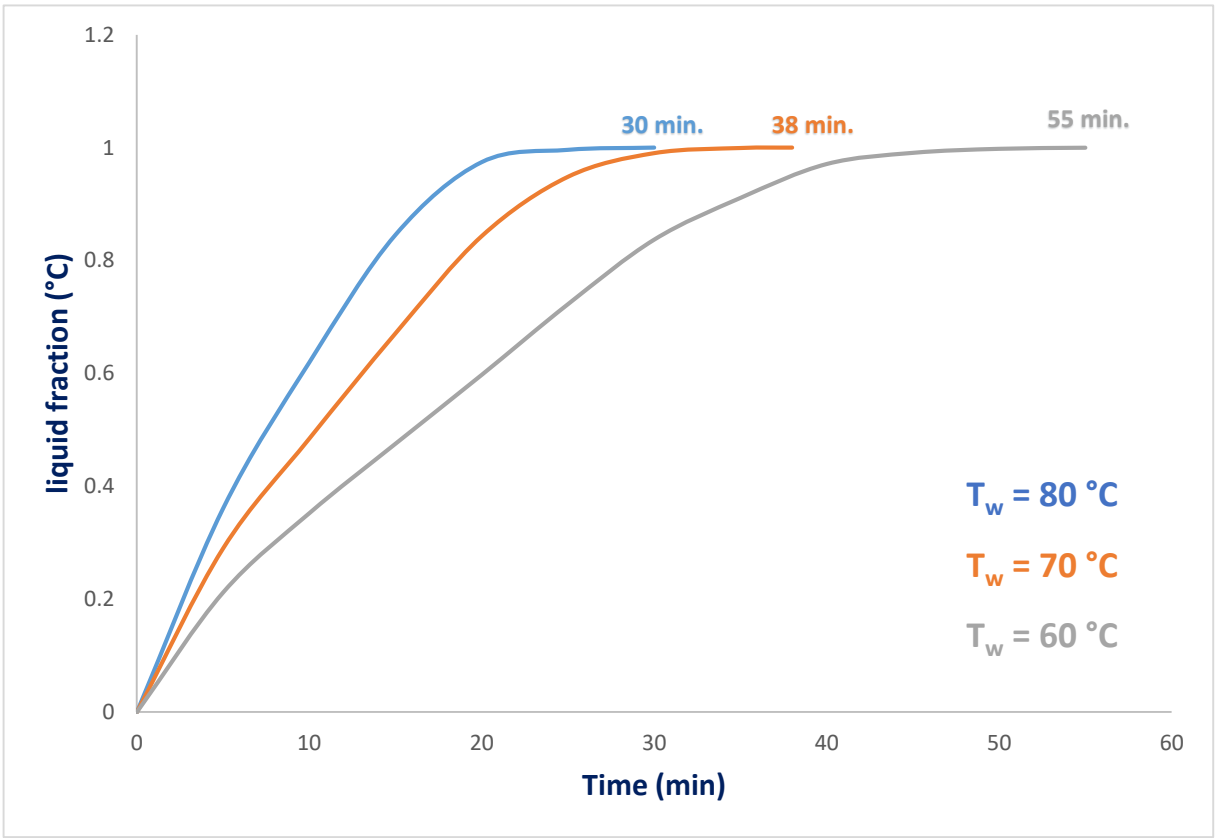

Fig. (5.23). Effect of inlet HTF temperatures on the numerical liquid fractions for below-finned thermal storage unit.

5.6 Stored energy by PCM

The experimental and numerical results of the change in the amount of thermal energy stored in PCM over time for unfinned and finned thermal storage units are shown in **Fig. (5.24)**. At the same time, the numerical values of stored energy are indicated in **Fig. (5.25)**. Both the solid and liquid states of PCM store energy sensibly and latently throughout the phase shift process. Solid PCM absorbs the conveyed energy from the heated water sensibly in the first stage. The solid-to-liquid phase shift during PCM melting consumes a substantial amount of the transmitted energy. Furthermore, the PCM liquid melt starts absorbing energy rationally. At all HTF temperatures, observations show that the total stored thermal energy rises with time. The increase in thermal energy storage is dampened when all solid PCM melts because all transmitted energy is effectively absorbed by liquid PCM. The amount of thermal energy stored in PCM also varies depending on the heat exchanger that was used, and it increases as the water temperature inlet rises. The PCM's stored energy is immediately retrieved upon activation of the solidification (discharge) mode.

The numerical values of stored energy indicated that there is a slight difference between the three cases in the amount of stored thermal energy, but there is a big difference in the time to reach the maximum amount of stored energy, as this depends on the time of melting. The percentages of reducing the time to reach the upper value of the stored energy were 66.66 % and 55.55 % for the two cases with four below-type fins and 4 X-type fins, respectively, relative to the case of without fins. Therefore, the state (4below-type fins), in addition to having the shortest melting time, is the best by reaching the maximum stored energy in the shortest time.

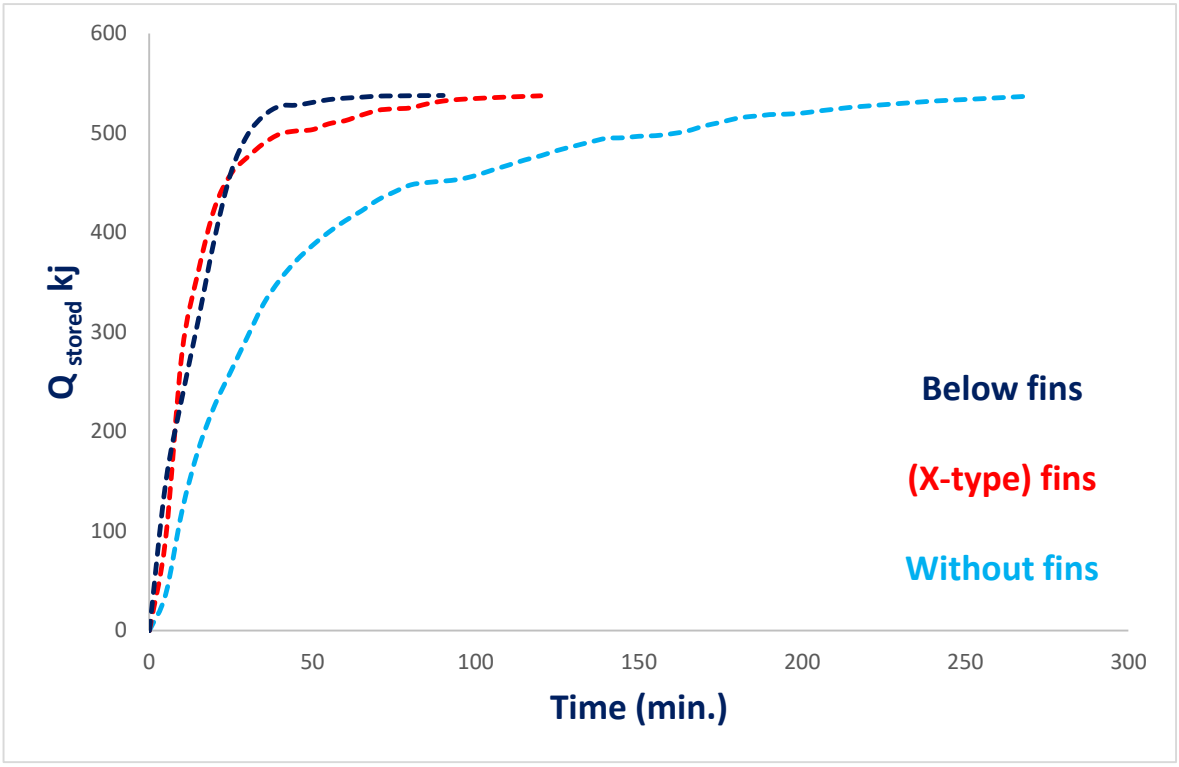

Fig. (5.24). Experimental stored energy unfinned and finned thermal storage units at 70 °C of inlet HTF temperature.

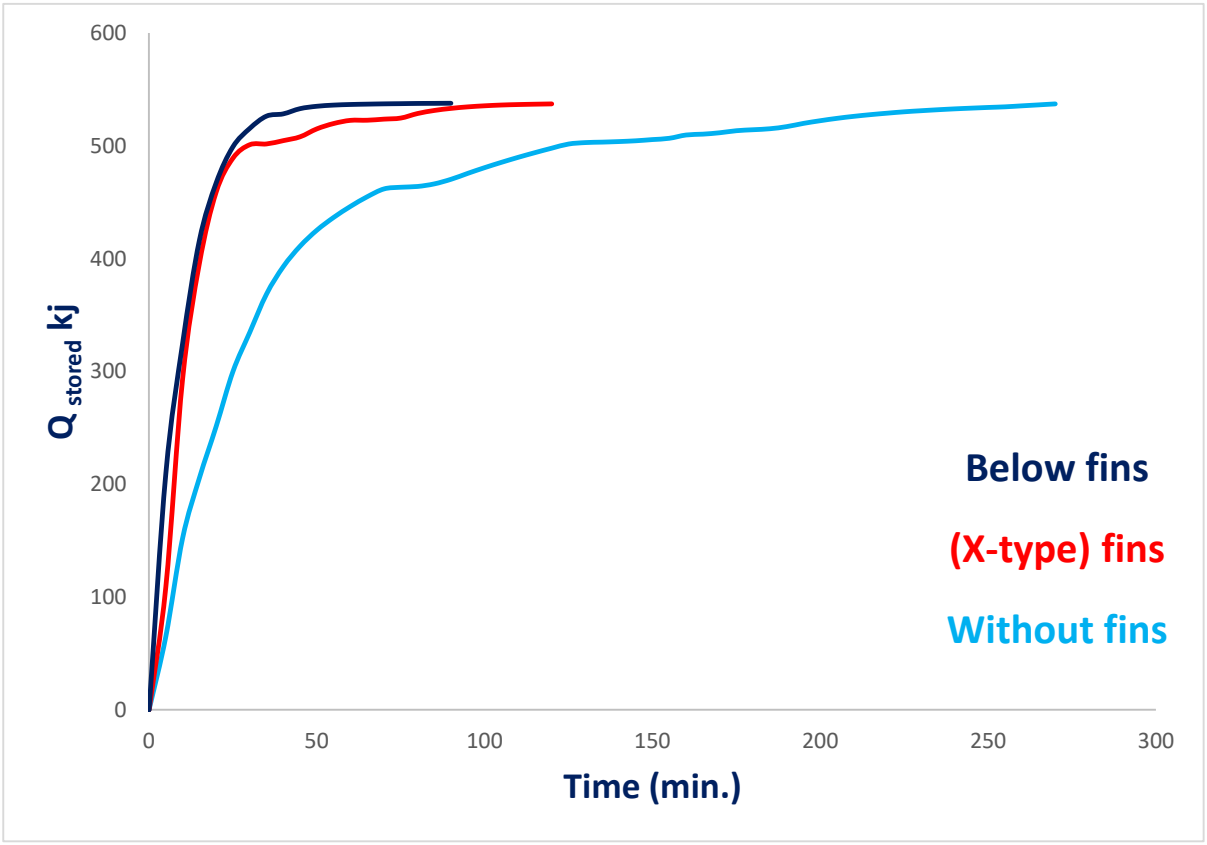

Fig. (5.25). Numerical stored energy unfinned and finned thermal storage units at 70 °C of inlet HTF temperature.

The comparisons between the numerical and experimental energy stored of PCM within the horizontal cavity with a 70 °C inlet HTF temperature for three cases (without fins, 4 X-type fins, and four below-type fins) are shown in **Fig. (5.26)**. The results indicate that there is little difference between the numerical and experimental outcomes for all three cases. Although the highest energy stored in PCM was achieved at different times for the three cases, the scenario with four below-type fins demonstrated the lowest time.

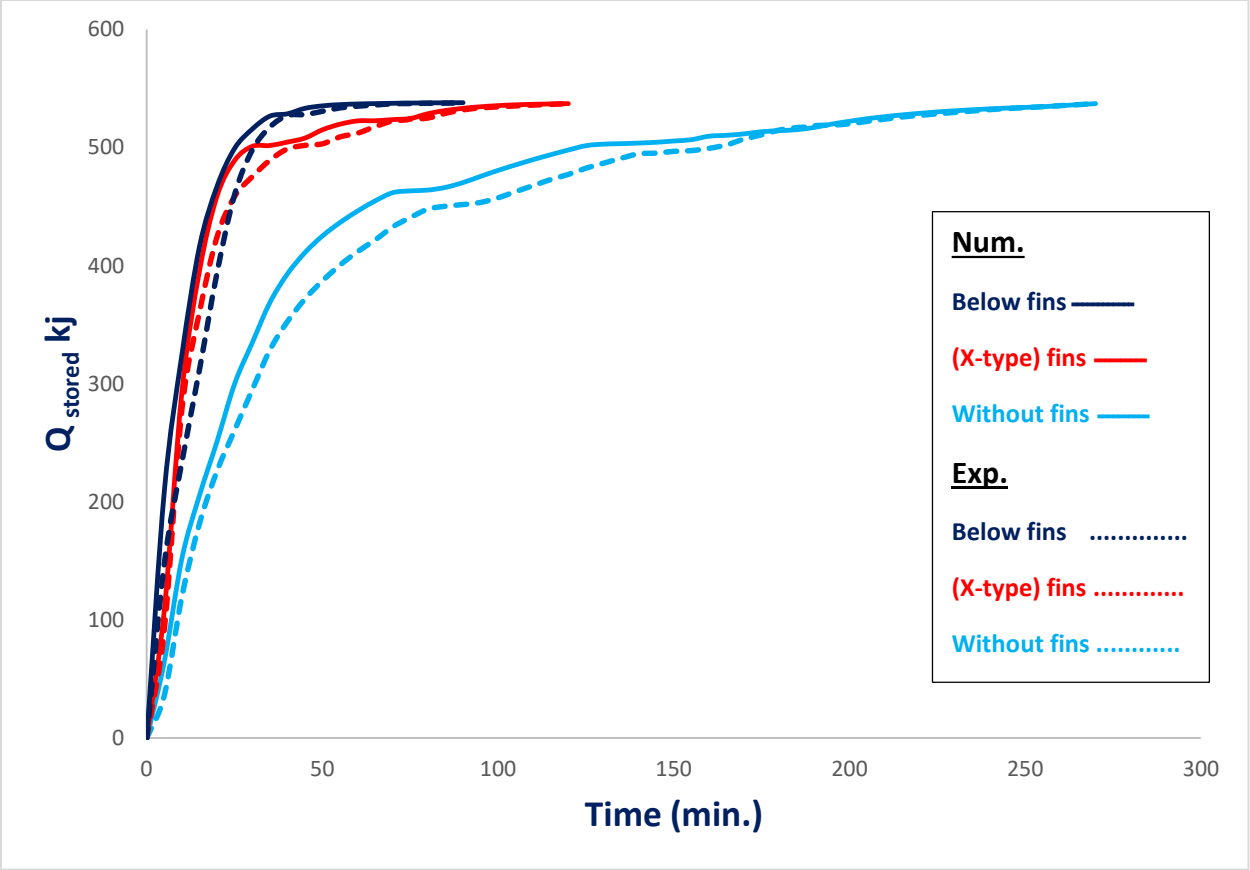

Fig. (5.26). Comparisons between the numerical and experimental energy stored of PCM within finned and finned thermal storage units at 70 °C of inlet HTF temperature.

CHAPTER SIX

CONCLUSIONS AND RECOMMENDATIONS

Chapter Six: Conclusions and Recommendations

6.1 Conclusions

The PCM charging in finned and unfinned LHTES is investigated experimentally and computationally. The following conclusions can be obtained.

1- Natural convection and overheating dominate the melting at the top part of the unfinned storage unit, while thermal conduction controls the bottom part.

2- Inserting fin suppresses overheating in the top part and increases the melting rate at the bottom part of the thermal storage unit.

3- The greatest numerical and experimental reductions in charging time due to using a below-fin distribution storage unit compared to an unfinned unit instead are 79.31% and 77.75 %, respectively, at a water inlet temperature of 80 °C. At the same time, the numerical and experimental reductions in charging times are 79% and 78, respectively, at a water inlet temperature of 70 °C.

4- Increasing the HTF (water) inlet temperature has a significant effect on reducing the melting time. By increasing the water inlet temperature for below-fin distribution storage unit from 60 to 70 and from 60 to 80, respectively, resulted in reducing the charging time by 31 % and 45.5 %.

6.2 Recommendations for future studies

The following recommendations can be suggested for future studies in the field of thermal energy storage:

1- Investigating the PCM solidification in the X-shape and below-distribution fins and comparing the performance with that of unfinned latent heat storage units.

2- Examining the effect of geometrical parameters of the fins, such as length and thickness, on the thermal characteristics of PCM melting in latent heat storage units.

3- Studying the effect of different fins' configurations, such as T-shaped fins, dendritic fins, tree-shaped fins, and bifurcated fins instead of traditional longitudinal fins in the lower part of the LHTES.

4- Investigating the effect of the combined heat transfer enhancement techniques, such as fin-nanoparticles, fin-porous media, and porous media-nanoparticles, on the thermal features of latent heat storage units.

References

References

1- Zalba, B., Marin, J. M., Cabeza, L. F., Mehling, H., Review on thermal energy storage with phase change: materials, heat transfer analysis and applications, Applied Thermal Engineering, 23, 2003: pp. 251–283.

2- Gasia, J., Steven, N.H., Belusko, M., Luisa, F., Cabeza, Bruno F., Experimental investigation of the effect of dynamic melting in a cylindrical shell-and-tube heat exchanger using water as PCM, Applied Thermal Energy,185, 2017: pp.136–145.

3- Tabassum. T., A Numerical Study of a Double Pipe Latent Heat Thermal Energy Storage System, Master Thesis, 2009, McGill University.

4- Gao, D., Deng, T., Energy storage: Preparations and physicochemical properties of solid- liquid Phase change materials for thermal energy storage, 2013: pp. 32–44

5- R. Dutta, A. Atta, and T. K. Dutta, "Experimental and Numerical Study of Heat Transfer in Horizontal Concentric Annulus Containing Phase Change Material," vol. 86, no. August, pp. 700–710, 2008.

6- Hamid Ait Adine, Hamid El Qarnia, "Numerical analysis of the thermal behavior of a shell-and-tube heat storage unit using phase change materials," Appl. Math. Model., vol. 33, no. 4, pp. 2132–2144, 2009.

7- Ahmad Ali Rabienataj Darzi, Mousa Farhadi , Kurosh Sedighi "Numerical study of melting inside concentric and eccentric horizontal annulus," Appl. Math. Model., vol. 36, no. 9, pp. 4080–4086, 2012.

8- M. J. Hosseini, A. A. Ranjbar, K. Sedighi, and M. Rahimi, "A combined experimental and computational study on the melting behavior of a medium temperature phase change storage material inside shell and tube heat exchanger" Int. Commun. Heat Mass Transf., vol. 39, no. 9, pp. 1416–1424, 2012.

9- W. Wang, K. Zhang, L. Wang, and Y. He, "Numerical study of the heat charging and discharging characteristics of a shell-and-tube phase change heat storage unit," Appl. Therm. Eng., vol. 58, no. 1–2, pp. 542–553, 2013.

10- M. Avci and M. Y. Yazici, "Experimental study of thermal energy storage characteristics of a paraffin in a horizontal tube-in-shell storage unit," Energy Convers. Manag., vol. 73, pp. 271–277, 2013.

11- M. Akgu and K. Kaygusuz, "Experimental study on melting / solidification characteristics of a paraffin as PCM," vol. 48, pp. 669–678, 2007.

12- H. Shmueli, G. Ziskind, and R. Letan, "International Journal of Heat and Mass Transfer Melting in a vertical cylindrical tube: Numerical investigation and comparison with experiments," Int. J. Heat Mass Transf., vol. 53, no. 19–20, pp. 4082–4091, 2010.

13- M. Longeon, A. Soupart, J. Fourmigué, A. Bruch, and P. Marty, "Experimental and numerical study of annular PCM storage in the presence of natural convection," Appl. Energy, vol. 112, pp. 175–184, 2013.

14- Yifei Wang, Liang Wang, Ningning Xie, Xipeng Lin, Haisheng Chen "International Journal of Heat and Mass Transfer Experimental study on the melting and solidification behavior of erythritol in a vertical shell-and-tube latent heat thermal storage unit," HEAT 42/85WSMASS Transf., vol. 99, pp. 770–781, 2016.

15- Saeid Seddegha, Mahmood Mastani Joybarib, Xiaolin Wanga, Fariborz Haghighatb "Experimental and numerical characterization of natural convection in a vertical shell-and-tube latent thermal energy storage system," Sustain. Cities Soc., vol. 35, no. March, pp. 13–24, 2017.

16- F. Agyenim and N. Hewitt, "The development of a finned phase change material (PCM) storage system to take advantage of off-peak electricity tariff for improvement in cost of heat pump operation," Energy Build., vol. 42, no. 9, pp. 1552–1560, 2010.

17- S. Mat, A. A. Al-abidi, K. Sopian, M. Y. Sulaiman, and A. Th, "Enhance heat transfer for PCM melting in triplex tube with internal – external fins," ENERGY Convers. Manag., vol. 74, pp. 223–236, 2013.

18- A. A. Al-abidi, S. Mat, K. Sopian, M. Y. Sulaiman, and A. Th, "Experimental study of melting and solidification of PCM in a triplex tube heat exchanger with fins," Energy Build., vol. 68, pp. 33–41, 2014.

19- Z. Li and Z. Wu, "Analysis of HTFs , PCMs and fins effects on the thermal performance of shell – tube thermal energy storage units," Sol. ENERGY, vol. 122, pp. 382–395, 2015.

20- Peilun Wang, Hua Yao, Zhipeng Lan, Zhijian Peng, Yun Huang, Yulong Ding "Numerical investigation of PCM melting process in sleeve tube with internal fins," Energy Convers. Manag., vol. 110, pp. 428–435, 2016.

21- Yanping Yuan, Xiaoling Cao, Bo Xiang, Yanxia Du "Effect of installation angle of fins on melting characteristics of annular unit for latent heat thermal energy storage," Sol. Energy, vol. 136, pp. 365–378, 2016.

22- A. A. Rabienataj. Darzi, M. Jourabian, and M. Farhadi, "Melting and solidification of PCM enhanced by radial conductive fins and nanoparticles in cylindrical annulus," ENERGY Convers. Manag., vol. 118, pp. 253–263, 2016.

23- W. Wang, L. Wang, and Y. He, "Parameter effect of a phase change thermal energy storage unit with one shell and one finned tube on its energy efficiency ratio and heat storage rate," Appl. Therm. Eng., vol. 93, pp. 50–60, 2016.

24- X. Cao, Y. Yuan, B. Xiang, L. Sun, and Z. Xingxing, "Numerical investigation on optimal number of longitudinal fins in horizontal annular phase change unit at different wall temperatures," Energy Build., 2017.

25- Jasim M. Mahdi, Sina Lohrasbi, Davood D. Ganji, Emmanuel C. Nsofor "Accelerated melting of PCM in energy storage systems via novel configuration of fins in the triplex-tube heat exchanger," Int. J. Heat Mass Transf., vol. 124, pp. 663–676, 2018.

26- S. Deng, C. Nie, G. Wei, and W. Ye, "Improving the melting performance of a horizontal shell-tube latent-heat thermal energy storage unit using local enhanced finned tube," Energy Build., vol. 183, pp. 161–173, 2019.

27- A. M. Abdulateef, J. Abdulateef, K. Sopian, and S. Mat, "Case Studies in Thermal Engineering Optimal fin parameters used for enhancing the melting and solidification of phase-change material in a heat exchanger unite," Case Stud. Therm. Eng., vol. 14, no. June, p. 100487, 2019.

28- L. A. Khan and M. M. Khan, "Role of orientation of fins in performance enhancement of a latent thermal energy storage unit," Appl. Therm. Eng., p. 115408, 2020.

29- Cheng Yu, Xuan Zhang, Xi Chen, Chengbin Zhang, Yongping Chen "Melting performance enhancement of a latent heat storage unit using gradient fins," Int. J. Heat Mass Transf., vol. 150, p. 119330, 2020.

30- Hongyang Li, Chengzhi Hu, Yichuan He, Dawei Tang, Kuiming Wang "Influence of fin parameters on the melting behavior in a horizontal shell-and-tube latent heat storage unit with longitudinal fins," J. Energy Storage, vol. 34, no. January, p. 102230, 2021.

31- Ahmed H.N. Al-Mudhafara, Andrzej F. Nowakowskib, Franck C.G.A. Nicolleaub "Enhancing the thermal performance of PCM in a shell and tube latent heat energy storage system by utilizing innovative fins," Energy Reports, vol. 7, pp. 120–126, 2021.

32- T. Zhang, G. Lu, and X. Zhai, "Design and experimental investigation of a novel thermal energy storage unit with phase change material," Energy Reports, vol. 7, pp. 1818–1827, 2021.

33- Manish K. Rathod, Jyotirmay Banerjee "Thermal performance enhancement of shell and tube Latent Heat Storage Unit using longitudinal fins," Appl. Therm. Eng., vol. 75, pp. 1084–1092, 2015.

34- A. Sciacovelli, F. Gagliardi, and V. Verda, "Maximization of performance of a PCM latent heat storage system with innovative fins," Appl. Energy, vol. 137, pp. 707–715, 2015.

35- Xiaohu Yang, Zhao Lu, Qingsong Bai, Qunli Zhang, Liwen Jin, Jinyue Yan "Thermal performance of a shell-and-tube latent heat thermal energy storage unit: Role of annular fins," Appl. Energy, vol. 202, pp. 558–570, 2017.

36- A. Rozenfeld, Y. Kozak, T. Rozenfeld, G. Ziskind "Experimental demonstration, modeling and analysis of a novel latent-heat thermal energy storage unit with a helical fin," Int. J. Heat Mass Transf., vol. 110, pp. 692–709, 2017.

37- Zakir Khan, Zulfiqar Ahmad Khan "Experimental investigations of charging/melting cycles of paraffin in a novel shell and tube with longitudinal fins based heat storage design solution for domestic and industrial applications," Appl. Energy, vol. 206, no. June, pp. 1158–1168, 2017.

38- Liang Pu, Shengqi Zhang, Lingling Xu, Yanzhong Li "Thermal performance optimization and evaluation of a radial finned shell-and-tube latent heat thermal energy storage unit," Appl. Therm. Eng., vol. 166, p. 114753, 2020.

39- O. K. Yagci, M. Avci, and O. Aydin, "Melting and solidification of PCM in a tube-in-shell unit: Effect of fin edge lengths' ratio," J. Energy Storage, vol. 24, no. May, p. 100802, 2019.

40- Xiaohu Yang, Junfei Guo, Bo Yang, Haonan Cheng, Pan Wei, Ya-Ling He "Design of non-uniformly distributed annular fins for a shell-and-tube thermal energy storage unit," Appl. Energy, vol. 279, no. August, p. 115772, 2020.

41- Z. Elmaazouzi, M. El Alami, H. Agalit, and E. G. Bennouna, "Performance evaluation of latent heat TES system-case study: Dimensions improvements of annular fins exchanger," Energy Reports, vol. 6, pp. 294–301, 2020.

42- Z. Elmaazouzi, M. El Alami, A. Gounni, and E. G. Bennouna, "Thermal energy storage with phase change materials: Application on coaxial heat exchanger with fins," Mater. Today Proc., vol. 27, no. xxxx, pp. 3095–3100, 2020.

43- Mert Gürtürk, Besir Kok "A new approach in the design of heat transfer fin for melting and solidification of PCM," Int. J. Heat Mass Transf., vol. 153, p. 119671, 2020.

44- D. S. Mehta, B. Vaghela, M. K. Rathod, and J. Banerjee, "Thermal performance augmentation in latent heat storage unit using spiral fin: An experimental analysis," J. Energy Storage, vol. 31, no. April, p. 101776, 2020.

45- S. Tiari, A. Hockins, and M. Mahdavi, "Numerical study of a latent heat thermal energy storage system enhanced by varying fin configurations," Case Stud. Therm. Eng., vol. 25, no. November 2020, p. 100999, 2021.

46- Y. Zhu, Y. Yu, and Y. Qiu, "Effect of fins with unequal length on the performance of cylindrical latent heat storage system," J. Energy Storage, vol. 35, no. January, p. 102224, 2021.

47- B. Lu, Y. Zhang, D. Sun, Z. Yuan, and S. Yang, "Experimental investigation on thermal behavior of paraffin in a vertical shell and spiral fin tube latent heat thermal energy storage unit," Appl. Therm. Eng., vol. 187, no. January, p. 116575, 2021.

48- F. He, S. Li, Y. Zuo, Y. Gao, and F. Pang, "Influence of heat transfer fluid on thermal performance improvement of latent heat storage unit with helical fins," Case Stud. Therm. Eng., vol. 49, no. May, p. 103356, 2023.

49- www.rubitherm.com

50- Holman JP. Analysis of experimental data. Experimental methods for engineers. 2001:48-143.

Appendix

Appendix (A) Physical and thermal properties of the PCM

Data sheet

RUBITHERM

RT42

RUBITHERM® RT is a pure PCM, this heat storage material utilising the processes of phase change between solid and liquid (melting and congealing) to store and release large quantities of thermal energy at nearly constant temperature.
The RUBITHERM® phase change materials (PCM's) provide a very effective means for storing heat and cold, even when limited volumes and low differences in operating temperature are applicable.

Properties for RT-line:
- high thermal energy storage capacity
- heat storage and release take place at relatively constant temperatures
- no supercooling effect, chemically inert
- long life product, with stable performance through the phase change cycles
- melting temperature range between -9 °C and 100 °C available

The most important data:	Typical Values	
Melting area	38-43 main peak: 41	[°C]
Congealing area	43-37 main peak: 42	[°C]
Heat storage capacity ± 7,5% Combination of latent and sensible heat in a temperatur range of 35°C to 50°C.	165	[kJ/kg]*
	48	[Wh/kg]*
Specific heat capacity	2	[kJ/kg·K]
Density solid at 15°C	0,88	[kg/l]
Density liquid at 80°C	0,76	[kg/l]
Heat conductivity (both phases)	0,2	[W/(m·K)]
Volume expansion	12,5	[%]
Flash point	186	[°C]
Max. operation temperature	72	[°C]

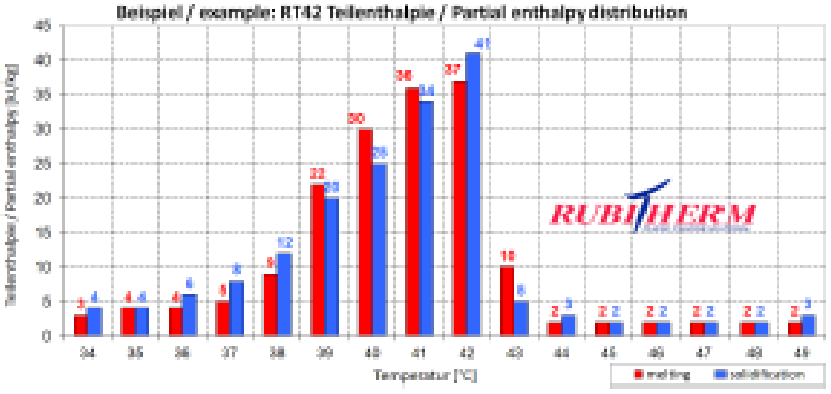

Rubitherm Technologies GmbH
Imhoffweg 6
D-12307 Berlin
phone: +49 (30) 7109622-0
E-Mail: info@rubitherm.com
Web: www.rubitherm.com

The product information given is a non-binding planning aid, subject to technical changes without notice.
Version 09.10.2020

*Measured with 3-layer-calorimeter.

RUBITHERM
Phase Change Material

Rubitherm Technologies GmbH
Imhoffweg 6
12307 Berlin
www.rubitherm.com
Tel: +49 30 71 09 622-0
Fax: +49 30 71 09 622-22

Rubitherm Technologies GmbH . Imhoffweg 6 . D-12307 Berlin

Imam Abbas Holy Shrine
Bain Al-Harmain Department
Eng. Alaa Hamzah Salman

56001 Karbala
IRAK

LIEFERSCHEIN
KOPIE 2

Nummer	:	20220000703
Datum	:	17.11.2022
Kunde	:	90000
Auftrag	:	20220000690
Bestellung vom	:	E-Mail 06.11.2022

Pos.	Artikelnummer Bezeichnung	LO	ME	Liefermenge

Anfrage durch: Al-lami Samir, allami1963@icloud.com

Purchaser: Al-lami Samir, allami1963@icloud.com
your purchase order no.: E-Mail
our offer no.: 20220000498

Dear Customer,
We thank you for your purchase order and confirm as follows:

1	16010042 RUBITHERM RT 42 HS-code: 27129099 Ch: 16010042-091221	0001	kg	30
2	96020104 Verpackung	0001		1
3	96020100 Versandkosten	0000		1

PREIS-UND LIEFERBEDINGUNGEN
Mit einer Bestellung erklären Sie sich mit unseren nachfolgenden Bedingungen einverstanden.

Zahlungskondition: Neukunden bezahlen die 1.Lieferung per Vorkasse; später 10 Tage netto nach Datum der Rechnung per Überweisung. Kreditkarten werden nicht akzeptiert.

Lieferbedingungen: DAP Karbala
Nach vorheriger Absprache, beauftragt Rubitherm einen Spediteur für den Transport.
(*)Wir weisen Sie daraufhin, dass der angebotene Transportpreis von dem Transportpreis zum Lieferzeitpunkt abweichen kann. Grund hierfür sind im Transportpreis enthaltene Zuschläge die marktabhängig sind und ständigen Schwankungen unterliegen. Rubitherm behält sich vor, Ihnen die Preisdifferenz in Rechnung zu stellen. Der Kunde verpflichtet sich zu

Rubitherm Technologies GmbH
Imhoffweg 6
12307 Berlin
Germany

Warenannahme: Mo-Fr. 08:00-14:30 Uhr
Entladung über Rampe (Höhe 1,10m). Keine seitliche Entladung möglich!

Kennzeichen | Datum | Ware erhalten / Name

RUBITHERM

Rubitherm Technologies GmbH
Imhoffweg 6
12307 Berlin
www.rubitherm.com
Tel: +49 30 71 09 622-0
Fax: +49 30 71 09 622-22

Lieferschein - Nummer 20220000703 vom 17.11.2022 LIEFERSCHEIN Seite 2

Pos.	Artikelnummer Bezeichnung	ME	Liefermenge

Zahlung dieser Differenz.

Die Lieferung erfolgt innerhalb von 4 Wochen, störungsfreie Produktion vorausgesetzt.

Rubitherm Technologies GmbH
Imhoffweg 6
12307 Berlin
Germany

Warenannahme: Mo-Fr. 08:00-14:30 Uhr
Entladung über Rampe (Höhe 1,10m). Keine seitliche Entladung möglich!

Kennzeichen Datum Ware erhalten / Name

Appendix (B) thermocouple calibration

C.O.S.Q.C IRAQ

PHT 522/2021 تاريخ المعايره ٢٠٢١/٦/٢٠ قسم المقاييس

Calibration Certificate

Central Organization for Standardization and Quality Control (COSQC)

Metrology Department - Physics Section (FOR TC - 012)

P.O. Box13032 Algaderia street, Baghdad , Tel:7785180 - E-Mail : cosqc@cosqc.gov.iq

Certificate No.: PHT 522/2021

Date of issue 20/06/2021

Customer		
Name:	جامعة كربلاء /كلية الهندسة /الدراسات العليا /قسم الهندسة الميكانيكية / طالب الماجستير زاهر عباس رحيم	
Address:	العراق - كربلاء المقدسة	
Item under calibration		
Description:	Digital Thermometer	
Manufacturer:	TBT	
Model:	ST - 1A	
Serial number:	———	
Range :	(-50 ------- 80) ° C	Res.: 0.1 °C
Date of reception:	Order no. : (215) , Date of Reception : 13/06/2021	
Condition of reception:	AS FOUND	

Standard(s) used in the calibration		
Description:	digit nano volt / micro ohm meter	PT100
Manufacturer:	Agilent / Malaysia	———
Model:	34420A	———
Serial number:	MY42000734	(1)
Other identification:	ID:PHT-01-17	ID:PHT-01-84

Calibration information	
Date of calibration:	17/06/2021 Due To : 17/06/2022
Place of calibration:	PH LAB. 1
Method(s) of calibration:	Calibration method using - PROC-TC-012 (A)
Calibrated quantity:	Temperature ° C
Results of calibration:	Attached a complete result in Annex 1 of this certificate
Measurement uncertainty:	The reported expanded uncertainty is based on UKAS M3003 Standard and the standard Uncertainty multiplied by coverage factor k=2 to give confidence level of 95%
Metrological traceability:	The traceability of measurement results to the SI units is assured by the National standard maintained at Central Organization for standardization and Quality Control through calibration at :-UME/ (certificate No. G1KS-127)
Environmental conditions of calibration:	Temp. 30.05 °C RH 19.3%
Observations, opinions or recommendations:	The Results in Annex 1 should be taken into consideration

Approved by:

Eng.
Moyasser Ali Taher
Head Of Physics Section
20/06/2021

Ref. PROC -TC-012

Calibration Certificate

Central Organization for Standardization and Quality Control (COSQC)

Metrology Department - Physics Section (FOR TC - 012)

P.O. Box13032 Algaderia street, Baghdad , Tel:7785180 - E-Mail : cosqc@cosqc.gov.iq

Certificate No.: PHT 522/2021

Date of issue 20/06/2021

Annex 1

Results

The results of the measurements are given on table below.

Set. Value °C	Ref. (R) °C	UUC (M) °C	Error (M - R) °C	Uncertainty ± °C
60	60.03	59.9	-0.13	0.11

Calibrated by :
Khalid Naser
20/06/2021

Revised by :
Hanaa Mohammed
20/06/2021

Approved by :
Moyasser Ali Taher
20/06/2021

Appendix (C) Published research

Kerbala Journal for Engineering Sciences
Refereed Scholarly Journal
ISSN: 2709-6718

Manuscript Acceptance Letter

Dear Authors, Hayder A. Al-Salami, Nabeel S. Dhaidan, and Fadhel N. Al-Mousawi,

I am pleased to inform you that based on the recommendations of the reviewers and the editorial board members, your manuscript entitled:

Review of PCM charging in tabular latent heat thermal energy storage systems

has been accepted for publication in the (Kerbela Journal of Engineering Sciences). The manuscript will be published in Vol. (04), Issue (01), on 03/ 2024.

Thanks for submitting your manuscript to our journal. Please do not hesitate to contact us if you have any questions regarding the publication process.

Best wishes,

Prof. Dr. Basim K. Nile
Editor-in-Chief
Kerbala Journal of Engineering Sciences (KJES)
Date: 5/02/2024

Published by College of Engineering, University of Kerbala, Iraq
Email: kjes@uokerbala.edu.iq

Kerbala Journal for Engineering Sciences

https://kjes.uokerbala.edu.iq

Review of PCM charging in tabular latent heat thermal energy storage systems

Hayder A. Al-Salami*, Nabeel S. Dhaidan**, Fadhel N. Al-Mousawi***

* Department of Mechanical Engineering, College of Engineering, University of Kerbala

E-mail:- e.hayder81@gmail.com

** Department of Mechanical Engineering, College of Engineering ,University of Kerbala

E-mail:- nabeel.sh@uokerbala.edu.iq

*** Department of Mechanical Engineering, College of Engineering ,University of Kerbala

E-mail:- fadhelnor@gmail.com

Received: 21 September 2023; Revised: 29 September 2023; Accepted: 22 February 2024

Abstract

This paper includes a review of several previous studies associated with the charging behavior of phase-change materials (PCM) in horizontal and vertical tabular (annular) Latent Heat Thermal Energy Storage (LHTES) units. The effects of various factors on charging, such as heat transfer fluid (HTF) inlet temperature, the eccentricity of the inner tube, the inclination angle of the storage unit (−90◦, −60◦, −30◦, 0◦, 30◦, 60◦, 90◦), and the mass flow rate of HTF are investigated. Natural convection controls the charging process in the upper part of the thermal storage unit, while thermal diffusion dominates the melting in the lower part. Also, the HTF inlet temperature has a clear and significant effect on reducing the melting time of PCM. In addition, increasing the inner tube eccentricity results in a reduction in the charging time.

Keywords: PCM, Melting, LHTES, Concentric, Eccentric

1. Introduction

The main challenges of exploiting renewable energy resources are the availability and interruption of these sources. For instance, solar energy exists during the day and is interrupted by the absence of sunlight [1]. Also, there are wind turbines that operate only when the wind blows, etc. A gap or time lag

KJES
Kerbala Journal for Engineering Sciences
Refereed Scholarly Journal
ISSN: 2709-6718

Manuscript Acceptance Letter

Dear Authors, Hayder A. Al-Salami, Nabeel S. Dhaidan, and Fadhel N. Al-Mousawi,

I am pleased to inform you that based on the recommendations of the reviewers and the editorial board members, your manuscript entitled:

Computational study of the PCM charging in the latent heat thermal energy storage system

has been accepted for publication in the (Kerbela Journal of Engineering Sciences). The manuscript will be published in Vol. (04), Issue (01), on 03/ 2024.

Thanks for submitting your manuscript to our journal. Please do not hesitate to contact us if you have any questions regarding the publication process.

Best wishes,

Prof. Dr. Basim K. Nile
Editor-in-Chief
Kerbala Journal of Engineering Sciences (KJES)
Date: 28/03/2024

Published by College of Engineering, University of Kerbala, Iraq
Email: kjes@uokerbala.edu.iq

Kerbala Journal for Engineering Sciences
https://kjes.uokerbala.edu.iq

Computational study of the PCM charging in the latent heat thermal energy storage system

Hayder A. Al-Salami*, Nabeel S. Dhaidan**, Fadhel N. Al-Mousawi***
* Department of Mechanical Engineering, College of Engineering, University of Kerbala
E-mail:- e.hayder81@gmail.com
** Department of Mechanical Engineering, College of Engineering ,University of Kerbala
E-mail:- nabeel.sh@uokerbala.edu.iq
*** Department of Mechanical Engineering, College of Engineering ,University of Kerbala
E-mail:- fadhelnor@gmail.com

Received: 14 February 2024; Revised: 11 March 2024; Accepted: 28 March 2024

Abstract

This paper presents the computational investigation of the charging characteristics of PCM inside a latent heat thermal energy storage (LHTES) unit that consists of a horizontal heat exchanger type of the inner tube and outer shell using ANSYS/FLUENT software. The melting process numerically tested for the heat transfer fluid HTF (water) inlet temperature (60, 70, and 80 ℃), and the PCM's initial temperature is 15 ℃. Also, this study examined the effect of the mushy zone constant. Extensive measures show that charging time decreases with increased water inlet temperature. The melting of PCM completes in a time of 260 minutes when using a water inlet temperature of 60 ℃, while the melting time reaches 182 minutes when the water inlet temperature is 70 ℃, and the melting completes in a time of 145 minutes by using the hot water entry temperature of 80 ℃. When the water inlet temperature increased from 60 ℃ to 70 ℃ and 80 ℃, respectively, the melting time was saved by about 30% and 44%. The best melting time reduction is achieved at an HTF inlet temperature of 80 ℃. In addition, the melting time increased as constant values rose in the mushy zone. The melting times are 182, 191, and 200 minutes for mushy zone constants 10^5, 10^6, and 10^7, respectively. So, the mushy zone constant of 105 leads to the best reduction in melting time.

Keywords: PCM, Charging, LHTES, Natural convection, Mushy zone constant, Melting time.

Thermal Science and Engineering Progress 51 (2024) 102640

Contents lists available at ScienceDirect

Thermal Science and Engineering Progress

journal homepage: www.sciencedirect.com/journal/thermal-science-and-engineering-progress

Review of PCM charging in latent heat thermal energy storage systems with fins

Hayder A. Al-Salami [b], Nabeel S. Dhaidan [b,*], Hawraa H. Abbas [a,b], Fadhel N. Al-Mousawi [b,c,d], Raad Z. Homod [e]

[a] College of Information Technology Engineering, Al-Zahraa University for Women, Karbala, Iraq
[b] College of Engineering, University of Karbala, Karbala, Iraq
[c] Centre for Research on Environment and Renewable Energy (CRERE), University of Karbala, Iraq
[d] University of Birmingham, UK
[e] Department of Oil and Gas Engineering, Basrah University for Oil and Gas, Basrah, Iraq

ARTICLE INFO

Keywords:
PCM
Melting
Fins
LHTES
Heat transfer enhancement

ABSTRACT

Phase change materials (PCM) are considered promising tools for storing a high density of thermal energy in heat storage systems. The inherent low thermal conductivity of PCM can be remedied by using several thermal conductivity enhancers, especially fins. The effect of one or several thermal conductivity enhancers on the PCM melting was discussed in previous review articles. However, the impact of fin only on the PCM melting was rarely reported. The present article provides a comprehensive review of studies related to the thermal performance of PCM charging in finned annular heat exchangers as LHTES systems. The studies are classified according to the orientations of the LHTES systems (horizontal or vertical). This review includes a survey of several previous studies associated with the charging behaviour of PCM in horizontal and vertical annular thermal storage units equipped with fins. The effects of various factors on charging, such as geometrical factors of different fins, configuration, arrangement installation angle, pitch, number, thickness, and height, are reviewed. It was inferred that inserting the fin suppresses overheating in the top part of the thermal storage unit and improves the melting rate at the bottom part of the thermal storage. Therefore, the overall heat transfer rate is improved, and melting time is reduced. Also, the increasing the number, length, and thickness of fins indicated a pronounced enhancement in the melting process. At the same time, employing the non-uniform distribution of fins and/or using different fin dimensions (length and thickness) between the lower and upper parts of the storage unit improves the charging process. Decreasing the fin number and fin dimensions at the upper part and increasing them at the lower part result in an improvement of the thermal performance of the charging process. Also, decreasing the fin's pitch and installation angle improves the melting rate. Furthermore, using the topology-optimized structure for fins improves the thermal performance.

1. Introduction

The main challenge faced by the development of the exploitation of renewable energy resources is the time lag between energy sources and energy demand. The energy storage systems represent an effective tool for storing excess energy at a specified time and releasing this energy when needed. The thermal can be stored sensibly and latently. The phase change materials (PCM) are considered a promising tool for storing large amounts of latent thermal energy at approximately constant temperature. Therefore, PCM is applied in many latent heat thermal energy storage systems (LHTESS) applications [1–5]. However, the PCM suffers from a big challenge as its low thermal conductivity suppresses the rate of heat transfer through the melting and solidification process. However, the PCM must overcome a big challenge as its low thermal conductivity suppresses the heat transfer rate through the melting and solidification process. However, some techniques are applied to increase the effective thermal conductivity of PCM, like inserting fins [6–8], dispersing nanoparticles [9–13], and embedding porous media [14,15]. Among these thermal conductivity enhancers, the fins were more effective due to their simplicity, easy manufacturing,

* Corresponding author.
E-mail address: nabeel.s@uokerbala.edu.iq (N.S. Dhaidan).

https://doi.org/10.1016/j.tsep.2024.102640
Received 9 January 2024; Received in revised form 11 May 2024; Accepted 16 May 2024
Available online 18 May 2024

الخلاصة

تتضمن الدراسة الحالية التحقق العددي والتجريبي من الخواص الحرارية لمواد متغيرة الطور الموضوعة في وحدة تخزين الطاقة الحرارية الكامنة الحلقية الأفقية مع إضافة الزعانف الداخلية. جهاز تخزين الطاقة بطول 500 ملم يتكون من غلاف خارجي معزول حرارياً مصنوع من البلاستيك الشفاف بقطر 75 ملم وأنبوب داخلي من النحاس يستخدم لنقل مائع نقل الحرارة (الماء) بقطر 25 ملم. يتم ملأ المساحة بين الأنبوب الداخلي والغلاف الخارجي بمادة متغيرة الطور من نوع شمع البارافين RT 42.

تم اختبار ثلاثة نماذج من وحدة تخزين الطاقة الحرارية الكامنة وهي : بدون زعانف، ذات زعانف على شكل X، وذات زعانف سفلية ، تكون نسبة كتلة الزعانف إلى المادة متغيرة الطور ثابتة لوحدتي التخزين ذات الزعانف، يبلغ طول الزعنفة الطولية 500 ملم وارتفاعها 20 ملم وهي متصلة بالأنبوب الداخلي لوحدة التخزين ، تم استخدام طريقة المسامية والمحتوى الحراري لحل النموذج العددي ثنائي الأبعاد لمشكلة ذوبان المواد متغيرة الطور ودراسة تأثير درجات حرارة دخول الماء الساخن المختلفة (60، 70، 80 درجة مئوية) على زمن الذوبان عملياً وعددياً.

ومن خلال مراقبة عملية الذوبان أظهرت النتائج تقارباً كبيراً بين النتائج العددية والعملية، يسيطر الحمل الحراري الطبيعي والسخونة الزائدة على الذوبان في الجزء العلوي من وحدة التخزين التي لا تحتوي على الزعانف، بينما يتحكم التوصيل الحراري بمعدل ذوبان منخفض في الجزء السفلي، يؤدي إدخال الزعانف إلى منع ارتفاع درجة الحرارة في الجزء العلوي وزيادة معدل الذوبان في الجزء السفلي من وحدة التخزين الحراري. كما أن زيادة درجة حرارة مدخل (الماء) له تأثير كبير على تقليل زمن الذوبان، فقد انخفض زمن الذوبان بنسبة 31% و45.5% بزيادة درجة حرارة مدخل الماء من 60 إلى 70 درجة مئوية، ومن 60 إلى 80 درجة مئوية، على التوالى.

أعلى التخفيضات العددية والتجريبية في وقت الشحن تم الحصول عليها باستخدام وحدة التخزين ذات الزعانف السفلية مقارنة بوحدة لا تحتوي على زعانف وهي بمقدار 79.31% و77.75%، على التوالي، عند درجة حرارة مدخل الماء تبلغ 80 درجة مئوية. وفي الوقت نفسه تبلغ التخفيضات العددية والتجريبية في أوقات الشحن 79% و78 على التوالي، عند درجة حرارة مدخل الماء 70 درجة مئوية.

جمهورية العراق

وزارة التعليم العالي و البحث العلمي

جامعة كربلاء

كلية الهندسة

قسم الهندسة الميكانيكية

تحري السمات الحرارية لتخزين الطاقة الحرارية الكامنة مع الزعانف الداخلية

رسالة مقدمة الى كلية الهندسة / جامعة كربلاء كجزء من متطلبات نيل درجة الماجستير في علوم الهندسة الميكانيكية

الباحث:

حيدر عبد الخالق عزيز

باشراف :

أ.د. نبيل شهيد ضيدان

أ.م.د. فاضل نور الدين الموسوي

1444هـ **2023 م**